Design and Optimization of Microstrip Antenna by Bandwidth Enhancement Techniques

A thesis submitted to the
Department of Electrical & Electronic Engineering
in partial fulfillment of the requirements for the degree of
Master of Science in Electrical & Electronic Engineering.

By

Khondaker Refai Arafat

Roll No. 0710105

Department of Electrical & Electronic Engineering
Faculty of Electrical & Computer Engineering
RAJSHAHI UNIVERISTY OF ENGINEERING &TECHNOLOGY
Rajshahi-6204, Bangladesh

March, 2010

ABSTRACT

Antenna design has grown more stringent and difficult over the years as the world becomes strictly a wireless environment. The inherent tradeoffs that exist between gain, radiation pattern, bandwidth, and physical size and the multiple parameters that must be considered make antenna design a lengthy and tedious process. Methods have been devised which automate this complex process of antenna optimization through the use of genetic algorithms, particle swarm optimization, and simulated annealing. Genetic algorithms are capable of handling a large number of design parameters and work for optimization problems that have discontinuous or non-differentiable multi-dimensional solution spaces, making them ideal for antenna optimization. In the present work, a genetic algorithm has been used for size reduction in microstrip patch antennas operating at 2.4GHz. The designs are obtained by interfacing the genetic algorithm and Ansoft High Frequency System Simulator (HFSS 9.2) and validated through design, construction, and testing. SuperNEC 2.9 is used, and a method of communication between MATLAB 7.5 and SuperNEC 2.9 has been developed to make the genetic algorithm optimization possible.

In order to overcome the limitations of microstrip antennas such as narrow bandwidth (< 5%), lower gain (-6 dB), excitation of surface waves etc, a new solution method; using Photonic Bandgap (PBG) materials, as substrates has attracted increasing attention. Unlike other methods, this new method utilizes the inherent properties of dielectric materials to enhance microstrip antenna performance. These periodic structures have the unique property of preventing the propagation of electromagnetic waves for specific frequencies and directions which are defined by the shape, size, symmetry, and the material used in their construction. Some PBG structures include drilled holes in dielectrics, patterns etched in the ground plane, and metallic patches placed around microstrip structures. The aim of this project are to design, simulate and fabricate the new EBG structure operating at 7.5GHz frequency and study the performance of the rectangular microstrip antenna with and without PBG structure. Those designs were simulated with HFSS 9.2 and photonic crystal structures are calculated by Translight 3.01b. Both, simulated and measured data were compared and contrasted.

CONTENTS

CHAPTER 1

INTRODUCTION

1.1 Motivation:

The widespread use of miniature wireless devices has drawn the renewed attention of the antenna community to explore the possibilities of designing antennas with optimal geometry and performance for such devices. In this regard, microstrip antennas are considered as the promising candidates. A microstrip antenna consists of a conducting patch of any planner or non-planner geometry on one side of a dielectric substrate with a ground plane on the other side. In spite of their various attractive figures like low profile, light weights, low cost, easy fabrication and so on, the microstrip elements suffer from an inherent limitation of narrow impedance bandwidth and low gain in the order of 6dB [1]. So, widening the bandwidth of microstrip elements has become a major branch of activities in this field. The simplest way of improving the impedance bandwidth performance of the patch antenna is the tunning of substrate parameters and feeding techniques. For example, a 20-25% increase of bandwidth is possible by an optimally designed aperture coupled microstrip antenna [2-10]. Many works have been done to improve the impedance bandwidth of microstrip antennas [4-12]. A very brief survey of the related works is presented below.

A proximity-fed triangular patch in a circular slot is reported in [4] which shows more than 90% of SWR<2 bandwidth. Genetic Algorithm (GA) is being successfully applied to electromagnetic optimization problems recently [2]. It has been successfully applied by a number of researchers to improve the impedance bandwidth [4]. The principle of introducing low Q-factor of the cavity below the patch can be achieved by lowering the dielectric constant of the substrate or by increasing the substrate thickness. Use of the photonic band gap (PBG) structures as antenna substrates is one promising solution to this problem and thus it attracts a large fraction of antenna people to work with PBG [6].

1.2 Microstrip Patch Antennas:

Due to the huge demand for smaller cell phones and other mobile communication devices, it is becoming increasingly important to reduce the size of antennas. Due to the mass production nature of the cell phone market, it is also important for the antennas to be inexpensive and easy to produce.

Many techniques have been used to attempt to achieve this reduction in size with varying success. It has been shown that increasing the effective dielectric constant of the substrate will lead to decreased dimensions [13], [14]. While this approach is straight-forward, the materials used to produce this high permittivity are generally lossy in nature, expensive, and can increase the sensitivity of the design to small changes in antenna dimensions. A superstrate can be added to achieve a higher dielectric constant [15], however, the required thickness of the superstrate adds to the fabrication process and can lead to a large patch profile.

Shorting pins can be used to reduce the size of a patch antenna to about half of the original dimensions [16]. When placed in the middle of the antenna, the shorting strips make use of image theory to act as a mirror and thus cause the antenna to behave as if it was double its actual length [17]. Shorting pins however often produce antennas with a narrow bandwidth and a low gain [18]. Decreasing the dimensions of a patch antenna results in a strong reactive input impedance. This reactance can be equalized through capacitive loading, allowing size reduction. However, this loading reduces the efficiency of the antenna and shrinks the antenna bandwidth [17].

Altering the geometry of the patch antenna can cause a size reduction. Cutting slots into the patch force the surface currents to meander thus effectively creating a longer electrical length and reducing the size of the antenna. It had been shown that the gain of the antenna suffers when employing this method however, due to the ohmic loss from the increased surface current [17]. Cutting slots into the ground plane can also cause a size reduction [19].

Recently, evolutionary algorithms, such as a genetic algorithm (GA) and particle swarm optimization (PSO) have been used to optimize patch antennas [20], [21], [22], [23].

In the 1990s, researches suggested the introduction of a photonic band gap (PBG)

structure into the printed antenna substrate, which saw the capability of removing unwanted substrate modes. This PBG substrate has two commonly employed configurations namely the perforated and metallodielectric structures. The former consists of the periodic arrangement of air-columns. The effectiveness of the perforated structure relies on the high refractive index contrast between the air-columns and the relative permittivity of the dielectric material and the type of the lattice to use. For broadband and small volume mobile communication applications, the honeycomb-lattice was shown to be of good potential.

1.3 Genetic Algorithm:

In recent years, the use of evolutionary algorithms to optimize antenna designs has shown tremendous growth. Genetic algorithms (GA) [1] are global optimization techniques that are based on the Darwinian theory of natural selection and evolution. Genetic algorithms offer many advantages over traditional numerical optimization techniques including the ability to use both continuous and discrete parameters, search across a wide sampling of the solution space, and handle a large number of variables. Derivative information of the performance surface is not needed by the GA, which eliminates many of the difficulties associated with traditional gradient-based algorithms. For these reasons, and the overall simplicity to both understand and implement, genetic algorithms have become a popular and powerful optimization technique.

Holland first introduced GA's in 1975 [1], but they were not applied to practical problems till Goldberg in the late 80s and early 90s [1]. In the 90s, GA's used within electromagnetics have been most often applied to antenna array design for array thinning, beamforming, and sidelobe minimization [1]. In the past few years, the use of genetic algorithms have spread to the design of single antennas in order to optimize parameters such as size, bandwidth, efficiency, radiation pattern, and gain [1].

The genetic algorithm searches the performance surface by randomly combining different values of each variable together to create a set of possible solutions. A fitness function is used to assign a fitness value to each possible solution within the set. Two solutions that receive higher fitness values are then combined together to produce another possible solution that exhibit characteristics of both. This process of fitness ranking and

recombining is repeated many times until an optimal solution is reached.

1.4 Genetic Algorithm and Microstrip Antenna

The use of genetic algorithms in optimizing microstrip patch antennas is relatively recent, with the majority of research occurring in the past few years. The objective is to create novel, non-intuitive shapes that fulfill the optimization criteria, such as a broad bandwidth, dual frequency, or small physical dimension.

A genetic algorithm was used to determine the patch length and width and feeding point in the design of a coaxially fed circularly polarized rectangular patch antenna. The fitness function was derived from the cavity model and evaluated such antenna characteristics as input impedance, effective loss tangent, and axial ratio. A stacked patch antenna that exhibited broadband operation was designed using a GA. The GA controlled numerous variables including the size of each patch, the thickness and permittivity of each dielectric slab, and the feed location. Method of moments software was used to analyze the fitness of each antenna based on broadside gain and input impedance [2]. The bandwidth of a microstrip patch antenna was also broadened by using a GA to optimize the feed network [24]. A dual-band microstrip patch antenna was designed using genetic algorithms to control the position of multiple slots or shorting pins between the patch and ground. Multiport analysis was used to determine the effects of the slots or pins on the input impedance, and thus assign fitness values to each of the antennas [25].

Genetic algorithms can also be used to change the shape of the patch itself and thus optimize the antenna. By dividing a regular square microstrip patch antenna into a grid of symmetrical squares, and using genetic algorithms to selectively remove the smaller metallic grid squares from the patch, novel non-intuitive shapes can be produced. This method has been employed to create dual-band antennas [26]. An example is presented in [27] where a microstrip patch antenna's resonant frequency is reduced from 3 GHz to 1.8 GHz by dividing the patch into 9 by 9 cells and selectively eliminating certain cells from the metallic patch. The resonant frequency of the antenna was found using the software tool PATCH. This shift in resonant frequency creates a size reduction of 42% when the GA-optimized patch is compared to the standard square microstrip patch that would resonant at 1.8 GHz.

1.5 Photonic Band Gap (PBG) structure and Photonic Crystals:

In the past decade, a new technology has emerged which may be the key to developing ultra-wideband microstrip antennas. This technology manipulates the substrate in such a way that surface waves are completely forbidden from forming, resulting in improvements in antenna efficiency and bandwidth, while reducing sidelobes and electromagnetic interference levels. These substrates contain so-called Photonic Crystals.

Photonic crystals are a class of periodic metallic, dielectric, or composite structures that exhibit a forbidden band, or bandgap, of frequencies in which waves incident at various directions destructively interfere and thus are unable to propagate [28,29]. Based on the dimensional periodicity of the crystal structure, the bandgaps can be in one, two, or three-dimensional planes, with the level of complexity increasing as the dimensions increase.

The first photonic-crystal structure conceptualized and manufactured was in 1991 by Eli Yablonovitch, then at Bell Communications Research in New Jersey. Yablonovitch fabricated the crystal structure by mechanically drilling holes a millimeter in diameter into a high dielectric constant material. This patterned material, which became known as "Yablonovite" prevented incident microwave signals from propagating in any direction along a unit sphere – in other words, it exhibited 3-D Bandgap. This structure has become the cornerstone for much of the research in this area with applications still in use today.

In most communication applications, however, the use of Yablonovite is not practical. The three dimensional nature of the bandgap rejects incident energy from all directions around a unit sphere, making it better suited as a high efficiency reflector or mirror. Instead, in a 2-D photonic crystal, the bandgap exists only within a plane, thereby allowing propagation along one axis of the crystal. This is the ideal scenario for microstrip antenna designs, since the "rejection plane" could be in the plane of the patch to prevent surface wave formation. In the past decade, a new technology has emerged which may be the key to developing ultra-wideband microstrip antennas.

1.6 Thesis Objective

The objective of this thesis work is to enhance the bandwidth of MSA by following the broadband design principle by lowering Q factor of the magnetic cavity under the patch, matching impedance of the feed, optimizing the patch geometry by applying Genetic Algorithm and suppressing the surface waves by drilling PBG materials.

1.7 Thesis Organization

This thesis work is divided into 10 chapters.

Chapter 1: This chapter is an introduction and gives the motivation for the work being presented. A summary of previous techniques used to reduce the size of patch antennas is presented, along with the work that has been done with patch antennas specific to genetic algorithms. A brief overview of the work done with wire antennas using genetic algorithms is also presented.

Chapter 2: This chapter gives an overview of fundamental antenna parameters including polarization, radiation pattern, Bandwidth, Q factor, Gain and Directivity.

Chapter 3: This chapter gives detail description of Microstrip patch antenna specially emphasis on Rectangular Microstrip Antenna. Here we discuss mainly on its application, advantage-disadvantage, different feeding technique, bandwidth calculation and method of its analysis.

Chapter 4: This chapter gives a detailed description of genetic algorithms.

Chapter 5: This chapter progresses with our own parametric study, design simulation using HFSS and result analysis of RMSA at 2.5 GHz frequency.

Chapter 6: This chapter is a discussion on SuperNEC GA solver and its reliability and the detailed explanations of how the genetic algorithm is applied to the optimization problems in MSA geometry. An explanation of how HFSS and SuperNEC are used to evaluate the antennas is presented along with the methods used to encode chromosomes and calculate the fitness of each individual. The results of the genetic algorithm optimization are presented which is applied on the RMSA configuration mentioned in chapter 5's parametric study. The simulated results for GA optimized RMSA also analyzed.

Chapter 7: This chapter progresses with our own parametric study, design

simulation using HFSS and result analysis of RMSA at 7.5 GHz frequency.

Chapter 8: This chapter introduces PBG and Photonic crystal concepts, Translight 3.01b as a crystal lattice solver and the design, simulation and results of PBG structured MSA in HFSS simulation.

Chapter 9: This chapter gives result comparison between an unoptimized RMSA and a GA optimized RMSA and the conventional and PBG structured MSA.

Chapter 10: This chapter is a conclusion of the achievement of the thesis work's objective and proposes the future work target.

CHAPTER 2

FUNDAMENTAL ANTENNA PARAMETERS

To describe the performance of an antenna, definitions of various parameters are necessary. Some of the parameters are interrelated and not at all of them need to be specified for complete description of the antenna performance.

2.1 Polarization

Polarization of an antenna in a given direction is defined as the polarization of the wave transmitted (radiated) by the antenna. Polarization of the radiated wave is defined as property of an electromagnetic wave describing the time varying direction and relative magnitude of the electric field vector. Polarization may be classified as linear, circular, or elliptical as shown in Figure 2.2.

Polarization also can be defined as the orientation of the electric field vector component of the electromagnetic field. In line-of-sight communications it is important that transmitting and receiving antennas have the same polarization (horizontal, vertical or circular). In non-line-of-sight the received signal undergoes multiple reflections which change the wave polarization randomly.

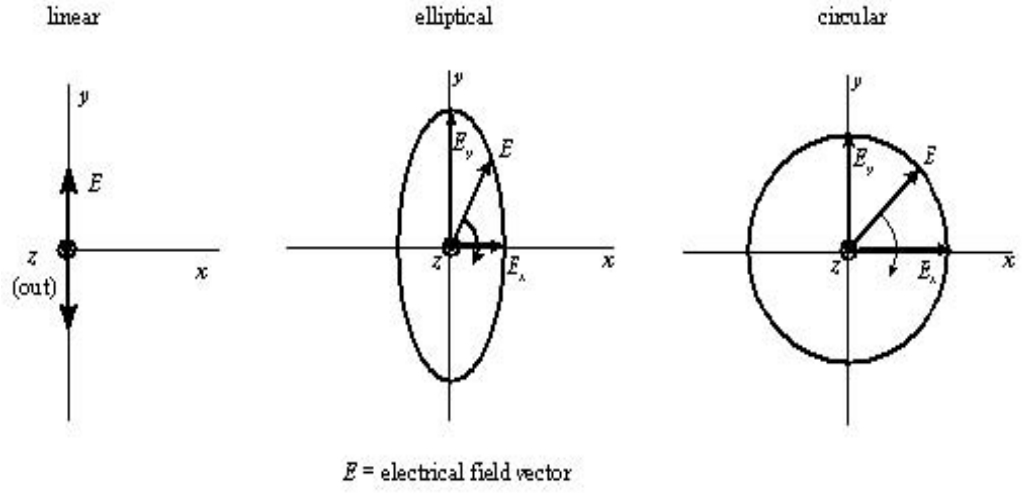

Figure 2.1 Linear, elliptical and circular polarization

2.2 Radiation Pattern

An antenna radiation pattern or antenna pattern is defined as "a mathematical function or a graphical representation of the radiation properties of the antenna as a function of space coordinates. In most cases, the radiation pattern is determined in the far-field region and is represented as a function of the directional coordinates. Radiation properties include power flux density, radiation intensity, field strength, directivity phase or polarization. The radiation pattern could be divided into:

Main lobes: This is the radiation lobe containing the direction of maximum radiation.

Minor and Side lobes: These are the minor lobes adjacent to the main lobe and are separated by various nulls. Side lobes are generally the largest among the minor lobes.

Back Lobes: This is the minor lobe diametrically opposite the main lobe.

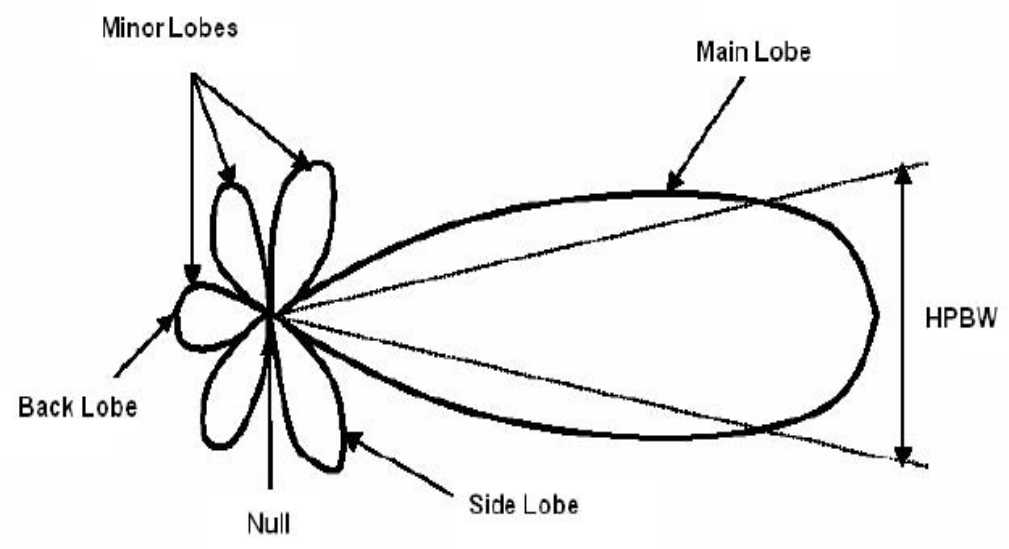

Figure 2.2 Radiation patteren, Lobes and HPBW

2.3 Half Power Beamwidth (HPBW)

The half power beamwidth is defined as: "In a plane containing the direction of the maximum of a beam, the angle between the two directions in which the radiation

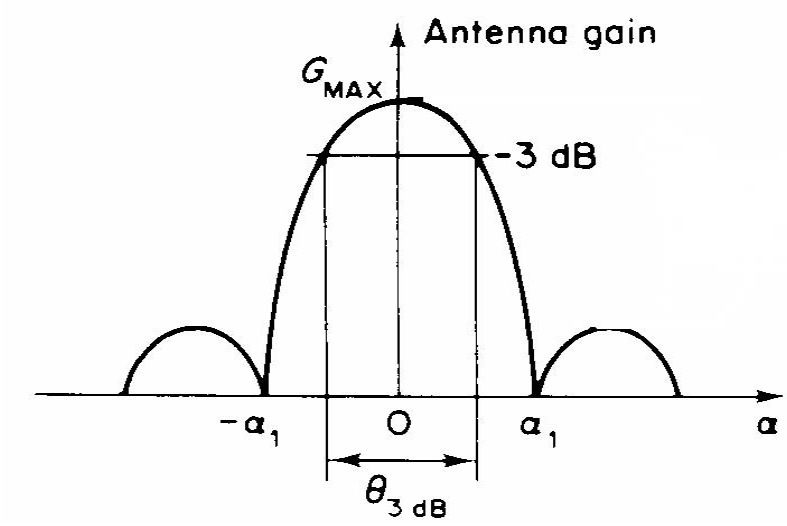

Figure 2.3 HPBW and Gain relation

intensity is one half the maximum value of the beam." Often the term beamwidth is used to describe the angle between any two points on the pattern, such as the angle between the 10dB points. In this case the specific points on the pattern must be described to avoid confusion. However the term beamwidth by itself is usually reversed to describe the 3dB beamwidth as shown in Figure 2.3.

The beamwidth of the antenna is a very important figure-of-merit, and it often used to as a tradeoff between it and the sidelobe level. In addition, the beamwidth of the antenna is also used to describe the resolution capabilities of the antenna to distinguish between two adjacent radiating sources or radar targets.

2.4 Gain and Directivity:

Antenna gain is a measure of directivity properties and the efficiency of the antenna. It is defined as the ratio of the radiation intensity in the peak intensity direction to the intensity that would be obtained if the power accepted by the antenna were radiated isotropically. The difference between the antenna gain and the directivity is that the antenna efficiency is taken into account in the former parameter. Antenna gain is measured in dBi, i.e. decibels relative to isotropic antenna.

2.5 Voltage Standing Wave Ratio (VSWR)

Voltage Standing Wave Ratio is the ratio of the maximum to minimum voltage on the antenna feeding line. Standing wave pattern is created on the feeding line when the impedance match is not perfect and a fraction of the power put into antenna is reflected

back and not radiated. For perfectly impedance matched antenna the VSWR is 1:1.

VWSR causes return loss or loss of forward energy through a system. Typical value of VSWR would be 1.5:1, where the two first numbers relate the ratio of impedance mismatch against a perfect impedance match and the second number is always 1, representing the perfect match. This impedance mismatch will reduce system efficiency.

2.6 Q factor

A truly good antenna must have low Q (Quality) factor. Antenna with high Q factor with narrow bandwidth is very sensitive to outside environment factors like rain, snow etc. To preserve antennas performance like high antenna gain, radiation diagram, VSWR, BW, proper impedance matching, proper power distribution and phasing are strongly depends on low Q factor.

CHAPTER 3

MICROSTRIP PATCH ANTENNA (MSA)

3.1 Introduction

Deschamps first proposed the concept of the MSA in 1953. However, practical antennas were developed by Munson and Howell in the 1970s. The numerous advantages of MSA, such as its low weight, small volume, and ease of fabrication using printed-circuit technology, led to the design of several configurations for various applications. With increasing requirements for personal and mobile communications, the demand for smaller and low-profile antennas has brought the MSA to the forefront.

An MSA in its simplest form consists of a radiating patch on one side of a dielectric substrate and a ground plane on the other side. The top and side views of a rectangular MSA (RMSA) are shown in Figure 3.1. However, other shapes, such as the square, circular, triangular, semicircular, sectoral and annular ring shapes are also used.

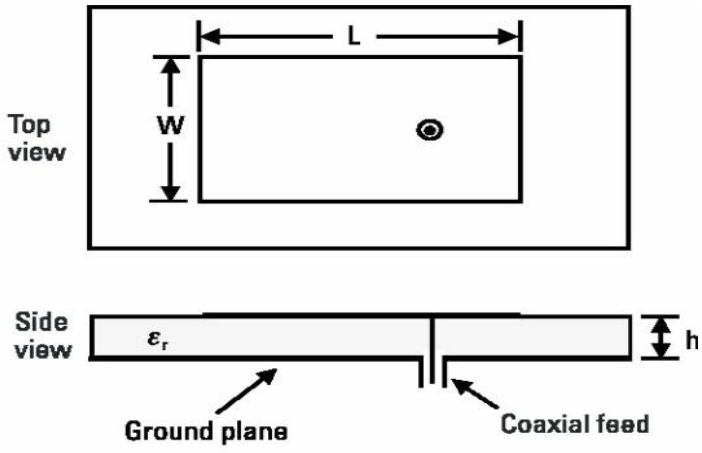

Figure 3.1 Top and Side view of MSA configuration

Radiation from the MSA can occur from the fringing fields between the periphery of the patch and the ground plane. The length L of the rectangular patch for the fundamental TM_{10} mode excitation is slightly smaller than $\lambda/2$, where λ is the wavelength in the dielectric medium, which in terms of free-space wavelength λ_0 is given as $\lambda_0/\sqrt{\varepsilon_e}$,

where ε_e is the effective dielectric constant of a microstrip line of width W. The value of ε_e is slightly less than the dielectric constant ε_r of the substrate because the fringing fields from the patch to the ground plane are not confined in the dielectric only, but are also spread in the air. To enhance the fringing fields from the patch, which account for the radiation, the width W of the patch is increased. The fringing fields are also enhanced by decreasing ε_r or by increasing the substrate thickness h. For MSA applications in the microwave frequency band, generally h is taken greater than or equal to 1/16th of an inch (0.159 cm).

3.2 Characteristics of MSAs

The MSA has proved to be an excellent radiator for many applications because of its several advantages, but it also has some disadvantages.

3.2.1 Advantages

MSAs have several advantages compared to the conventional microwave antennas. The main advantages of MSAs are listed as follows:

- They are lightweight and have a small volume and a low-profile planar configuration.
- They can be made conformal to the host surface.
- Their ease of mass production using printed-circuit technology leads to a low fabrication cost.
- They are easier to integrate with other MICs on the same substrate.
- They allow both linear and circular polarization.
- They can be made compact for use in personal mobile communication.
- They allow for dual-and triple-frequency operations.

3.2.2 Disadvantages

MSAs suffer from some disadvantages as compared to conventional microwave antennas. They are the following:

- Narrow BW;
- Lower gain;
- Low power-handling capability.

MSAs have narrow BW, typically 1–5%, which is the major limiting factor for the widespread application of these antennas. Increasing the BW of MSAs has been the major thrust of research in this field, and broad BW up to 70% has been achieved.

3.2.3 Applications of MSAs

The advantages of MSAs make them suitable for numerous applications. The telemetry and communications antennas on missiles need to be thin and conformal and are often MSAs. Radar altimeters use small arrays of microstrip radiators. Other aircraft-related applications include antennas for telephone and satellite communications. Microstrip arrays have been used for satellite imaging systems. Patch antennas have been used on communication links between ships or buoys and satellites. Smart weapon systems use MSAs because of their thin profile. Pagers, the global system for mobile communication (GSM), and the global positioning system (GPS) are major users of MSAs.

3.3 Feeding Techniques

The MSA can be excited directly either by a coaxial probe or by a microstrip line. It can also be excited indirectly using electromagnetic coupling or aperture coupling and a coplanar waveguide feed, in which case there is no direct metallic contact between the feed line and the patch. Feeding technique influences the input impedance and characteristics of the antenna, and is an important design parameter.

The coaxial or probe feed arrangement is shown in Figure 3.1. The center conductor of the coaxial connector is soldered to the patch. The main advantage of this feed is that it can be placed at any desired location inside the patch to match with its input impedance.

A patch excited by microstrip line feed is shown in Figure 3.2(a). This feed arrangement has the advantage that it can be etched on the same substrate, so the total structure remains planar. The drawback is the radiation from the feed line, which leads to an increase in the cross-polar level.

For thick substrates, which are generally employed to achieve broad BW, both the above methods of direct feeding the MSA have problems. In the case of a coaxial feed,

increased probe length makes the input impedance more inductive, leading to the matching problem. For the microstrip feed, an increase in the substrate thickness increases its width, which in turn increases the undesired feed radiation. The indirect feed solves these problems. An electromagnetically coupled RMSA is shown in Figure 3.2(b). The electromagnetic coupling is also known as proximity coupling. The feed line is placed between the patch and the ground plane, which is separated by two dielectric media. The advantages of this feed configuration include the elimination of spurious feed-network radiation; the choice between two different dielectric media, one for the patch and the other for the feed line to optimize the individual performances; and an increase in the BW due to the increase in the overall substrate thickness of the MSA.

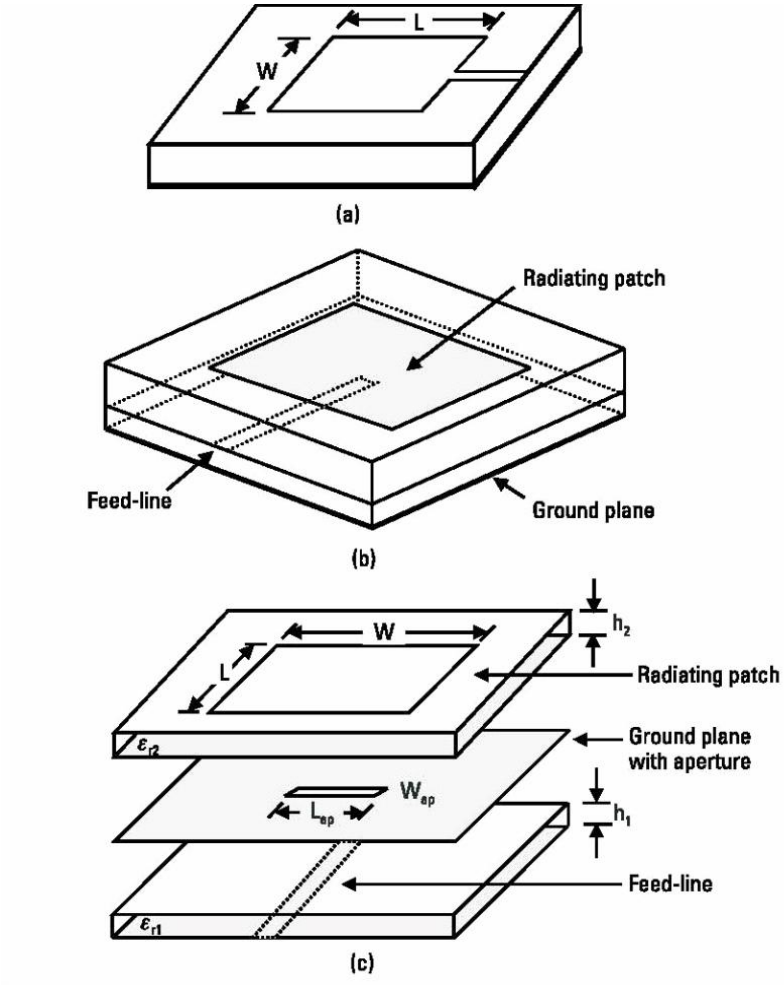

Figure 3.2 Different feeding MSA configuration: (a) Microstrip line, (b) Electromagnetic-coupling, (c) Aperture-coupled MSA

Another method for indirectly exciting a patch employs aperture coupling. In the aperture-coupled MSA configuration, the field is coupled from the microstrip line feed to the radiating patch through an electrically small aperture or slot cut in the ground plane, as shown in Figure 3.2(c). The coupling aperture is usually centered under the patch, leading to lower cross-polarization due to symmetry of the configuration. The shape, size, and location of the aperture decide the amount of coupling from the feed line to the patch. The slot aperture can be either resonant or nonresonant. The resonant slot provides another resonance in addition to the patch resonance thereby increasing the BW at the expense of an increase in back radiation. As a result, a nonresonant aperture is normally used. The performance is relatively insensitive to small errors in the alignment of the different layers. Similar to the electromagnetic coupling method, the substrate parameters of the two layers can be chosen separately for optimum antenna performance.

3.4 Methods of Analysis

The MSA generally has a two-dimensional radiating patch on a thin dielectric substrate and therefore may be categorized as a two-dimensional planar component for analysis purposes. The analysis methods for MSAs can be broadly divided into two groups.

In the first group, the methods are based on equivalent magnetic current distribution around the patch edges (similar to slot antennas). There are two popular analytical techniques:

- The transmission line model;
- The cavity model;

In the second group, the methods are based on the electric current distribution on the patch conductor and the ground plane (similar to dipole antennas, used in conjunction with full-wave simulation/numerical analysis methods). Some of the numerical methods for analyzing MSAs are listed as follows:

- The method of moments (MoM);
- The finite-element method (FEM);
- The finite-difference time domain (FDTD) method.

3.4.1 Transmission Line Model

The transmission line model is very simple and helpful in understanding the basic performance of a MSA. The microstrip radiator element is viewed as a transmission line resonator with no transverse field variations (the field only varies along the length), and the radiation occurs mainly from the fringing fields at the open circuited ends. The patch is represented by two slots that are spaced by the length of the resonator. This model was originally developed for rectangular patches but has been extended for generalized patch shapes. Many variations of this method have been used to analyze the MSA.

Although the transmission line model is easy to use, all types of configurations can not be analyzed using this model since it does not take care of variation of field in the orthogonal direction to the direction of propagation.

3.4.2 Cavity Model

In the cavity model, the region between the patch and the ground plane is treated as a cavity that is surrounded by magnetic walls around the periphery and by electric walls from the top and bottom sides. Since thin substrates are used, the field inside the cavity is uniform along the thickness of the substrate. The fields underneath the patch for regular shapes such as rectangular, circular, triangular, and sectoral shapes can be expressed as a summation of the various resonant modes of the two-dimensional resonator.

The fringing fields around the periphery are taken care of by extending the patch boundary outward so that the effective dimensions are larger than the physical dimensions of the patch. The effect of the radiation from the antenna and the conductor loss are accounted for by adding these losses to the loss tangent of the dielectric substrate. The far field and radiated power are computed from the equivalent magnetic current around the periphery.

An alternate way of incorporating the radiation effect in the cavity model is by introducing an impedance boundary condition at the walls of the cavity. The fringing fields and the radiated power are not included inside the cavity but are localized at the edges of the cavity. However, the solution for the far field, with admittance walls is difficult to evaluate.

3.4.3 MoM

In the MoM, the surface currents are used to model the microstrip patch, and volume polarization currents in the dielectric slab are used to model the fields in the dielectric slab. An integral equation is formulated for the unknown currents on the microstrip patches and the feed lines and their images in the ground plane. The integral equations are transformed into algebraic equations that can be easily solved using a computer. This method takes into account the fringing fields outside the physical boundary of the two-dimensional patch, thus providing a more exact solution.

3.4.4 FEM

The FEM, unlike the MoM, is suitable for volumetric configurations. In this method, the region of interest is divided into any number of finite surfaces or volume elements depending upon the planar or volumetric structures to be analyzed. These discretized units, generally referred to as finite elements, can be any well-defined geometrical shapes such as triangular elements for planar configurations and tetrahedral and prismatic elements for three-dimensional configurations, which are suitable even for curved geometry. It involves the integration of certain basis functions over the entire conducting patch, which is divided into a number of subsections. The problem of solving wave equations with inhomogeneous boundary conditions is tackled by decomposing it into two boundary value problems, one with Laplace's equation with an inhomogeneous boundary and the other corresponding to an inhomogeneous wave equation with a homogeneous boundary condition.

3.4.5 FDTD Method

The FDTD method is well-suited for MSAs, as it can conveniently model numerous structural inhomogenities encountered in these configurations. It can also predict the response of the MSA over the wide BW with a single simulation. In this technique, spatial as well as time grid for the electric and magnetic fields are generated over which the solution is required. The spatial discretizations along three Cartesian coordinates are taken to be same. The E cell edges are aligned with the boundary of the configuration and H-fields are assumed to be located at the center of each E cell. Each cell contains information about material characteristics. The cells containing the sources

are excited with a suitable excitation function, which propagates along the structure. The discretized time variations of the fields are determined at desired locations. Using a line integral of the electric field, the voltage across the two locations can be obtained. The current is computed by a loop integral of the magnetic field surrounding the conductor, where the Fourier transform yields a frequency response.

The above numerical techniques, which are based on the electric current distribution on the patch conductor and the ground plane, give results for any arbitrarily shaped antenna with good accuracy.

3.5 Definition of BW in terms of MSA

As mentioned earlier, the most serious limitation of the MSA is its narrow BW. The BW could be defined in terms of its VSWR or input impedance variation with frequency or in terms of radiation parameters. The VSWR or impedance BW of the MSA is defined as the frequency range over which it is matched with that of the feed line within specified limits. The BW of the MSA is inversely proportional to its quality factor Q and is given by

$$BW = \frac{VSWR - 1}{Q\sqrt{VSWR}} \qquad \ldots (3.1)$$

; where VSWR is defined in terms of the input reflection coefficient Γ as:

$$VSWR = \frac{1 + |\Gamma|}{1 - |\Gamma|} \qquad \ldots (3.2)$$

The Γ is a measure of reflected signal at the feed-point of the antenna. It is defined in terms of input impedance $\boldsymbol{Z_{in}}$ of the antenna and the characteristic impedance $\boldsymbol{Z_0}$ of the feed line as given below:

$$\Gamma = \frac{Z_{in} - Z_0}{Z_{in} + Z_0} \qquad \ldots (3.3)$$

The BW is usually specified as frequency range over which VSWR is less than 2 (which corresponds to a return loss of 9.5 dB or 11% reflected power). Sometimes for stringent applications, the VSWR requirement is specified to be less than 1.5 (which corresponds to a return loss of 14 dB or 4% reflected power).

The BW of a single-patch antenna increases with an increase in the substrate thickness and a decrease in ε_r of the substrate. The BW is approximately 15% for $\varepsilon_r = 2.2$ and $h = 0.1\ \lambda_0$.

The ε_r can be chosen close to 1 to obtain a broader BW. The larger thickness of the substrate gives rise to an increase in probe reactance for the coaxial feed and the excitation of surface waves, which reduces the efficiency η of the antenna.

The expressions for approximately calculating the percentage BW of the RMSA in terms of patch dimensions and substrate parameters is given by

$$\%BW = \frac{Ah}{\lambda_0 \sqrt{\varepsilon_r}} \sqrt{\frac{W}{L}} \qquad \ldots (3.4)$$

where,

A=180 for $\frac{h}{\lambda_0 \sqrt{\varepsilon_r}} \leq 0.045$

A=200 for $0.045 \leq \frac{h}{\lambda_0 \sqrt{\varepsilon_r}} \leq 0.075$

A=220 for $\frac{h}{\lambda_0 \sqrt{\varepsilon_r}} \geq 0.075$

; where W and L are the width and length of the RMSA. With an increase in W, BW increases. However, W should be taken less than to avoid excitation of higher order modes.

The BW can also be defined in terms of the antenna's radiation parameters. It is defined as the frequency range over which radiation parameters such as the gain, half-power beam-width (HPBW), and sidelobe levels are within the specified minimum and maximum limits. This definition is more complete as it also takes care of the input impedance mismatch, which also contributes to change in the gain.

The expression for approximately calculating the directivity D of the RMSA is given by

$$D \cong 0.2 + 6.6 + 10\log(1.6/\sqrt{\varepsilon_r})dB \qquad \ldots (3.5)$$

3.6 Rectangular MSA

An MSA in its simple form consists of a radiating patch on one side of a thin dielectric substrate backed by a ground plane. The radiating patch could be of any arbitrary shape, but it is generally taken as a regular shape for the ease of analysis and understanding of the antenna characteristics. The BW of the MSA is directly proportional to the substrate thickness h and inversely proportional to the square root of its dielectric constant ε_r. As a result, a thicker substrate with a low dielectric constant is generally used to obtain broad BW. One of the commonly used substrates for MSA is fiberglass-reinforced synthetic substrate, whose ε_r is typically between 2.1 to 2.6. This substrate has low dielectric loss (tanδ in the range of 0.0006 to 0.002) resulting in better efficiency η. For low-cost applications or for initial design and testing, inexpensive glass-epoxy substrate (ε_r in the range of 3.8 to 4.7) is used. Sometimes, air or foam substrate (ε_r = 1–1.1) is used to enhance the BW. Alternatively, suspended microstrip configuration can be used; this increases the total thickness and decreases the effective dielectric constant of the patch.

One of the simplest and widely used MSA configurations is the RMSA. Figure 3.3 shows the top and side views of a coaxial-fed RMSA along with the coordinate system. A rectangular patch is defined by its length L and width W. For a simple microstrip line, the width is much smaller than the wavelength. However, for the RMSA, the width is comparable to the wavelength to enhance the radiation from the edges. Since the substrate thickness is much smaller than the wavelength, the RMSA is considered to be a two-dimensional planar configuration for analysis.

For the fundamental TM_{10} mode, the length L should be slightly less than $\lambda/2$, where λ is the wavelength in the dielectric medium. Here, λ is equal to $\lambda_0/\sqrt{\varepsilon_e}$, where λ_0 is the free-space wavelength and ε_e is the effective dielectric constant of the patch. The value of ε_e is slightly less than ε_r, because the fringing fields around the periphery of the patch are not confined in the dielectric substrate but are also spread in the air as shown in Figure 3.4(a). However, for quick analysis or design, the following approximate formula

for εe could be used [1]:

$$\varepsilon_e = \frac{\varepsilon_r + 1}{2} + \frac{\varepsilon_r - 1}{2}\left[1 + \frac{10h}{W}\right]^{-1/2} \quad \ldots (3.6)$$

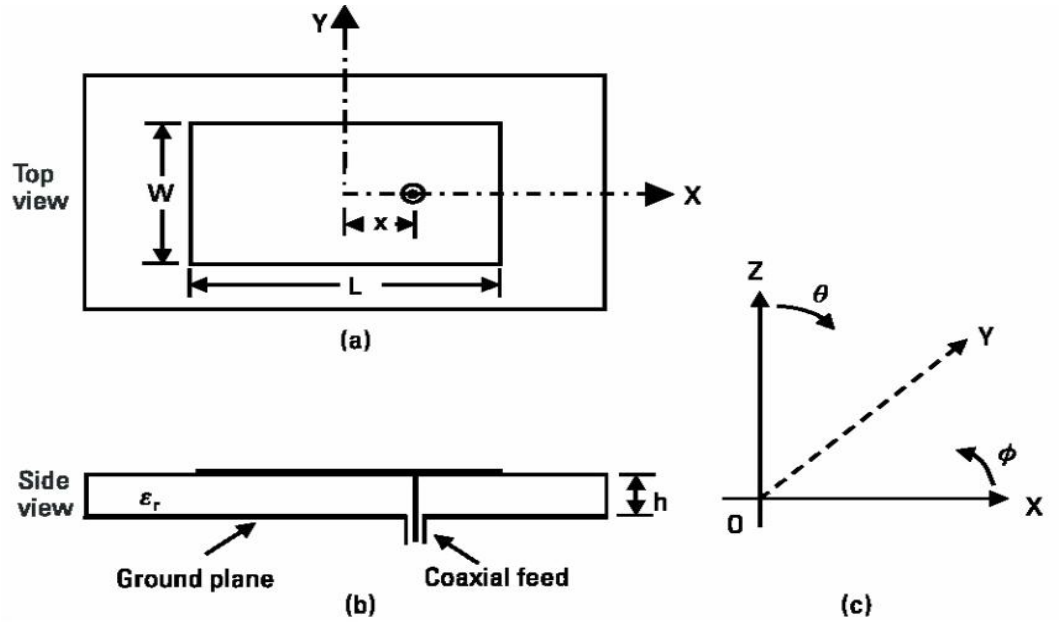

Figure 3.3 RMSA (a) Top view, (b) Side view, (c) co-ordinate system

The fundamental TM_{10} mode implies that the field varies one λ/2 cycle along the length, and there is no variation along the width of the patch. The variation of voltage V around the periphery and the current I along the length is shown in Figure 3.4(b). Along the width of the patch, the voltage is maximum and current is minimum due to the open end. It may be observed from Figure 3.4(a) that the vertical components of the electric field (E-field) at the two edges along the width are in opposite directions and hence cancel one another in the broadside direction, whereas the horizontal components are in same direction and hence combine in the broadside direction. Therefore, the edges along the width are termed as radiating edges. The fields due to the sinusoidal distribution along the length cancel in the broadside direction, and hence the edges along the length are known as non-radiating edges. The fringing fields along the width can be modeled as radiating slots as shown in Figure 3.4(c).

An RMSA operating at TM_{10} mode can be visualized as a transmission line, because the field is uniform along the width and varies sinusoidally along the length. The

fringing fields along the edges and radiation from the slots are modeled by their equivalent capacitance and radiation resistance, respectively as shown in Figure 3.4(d).

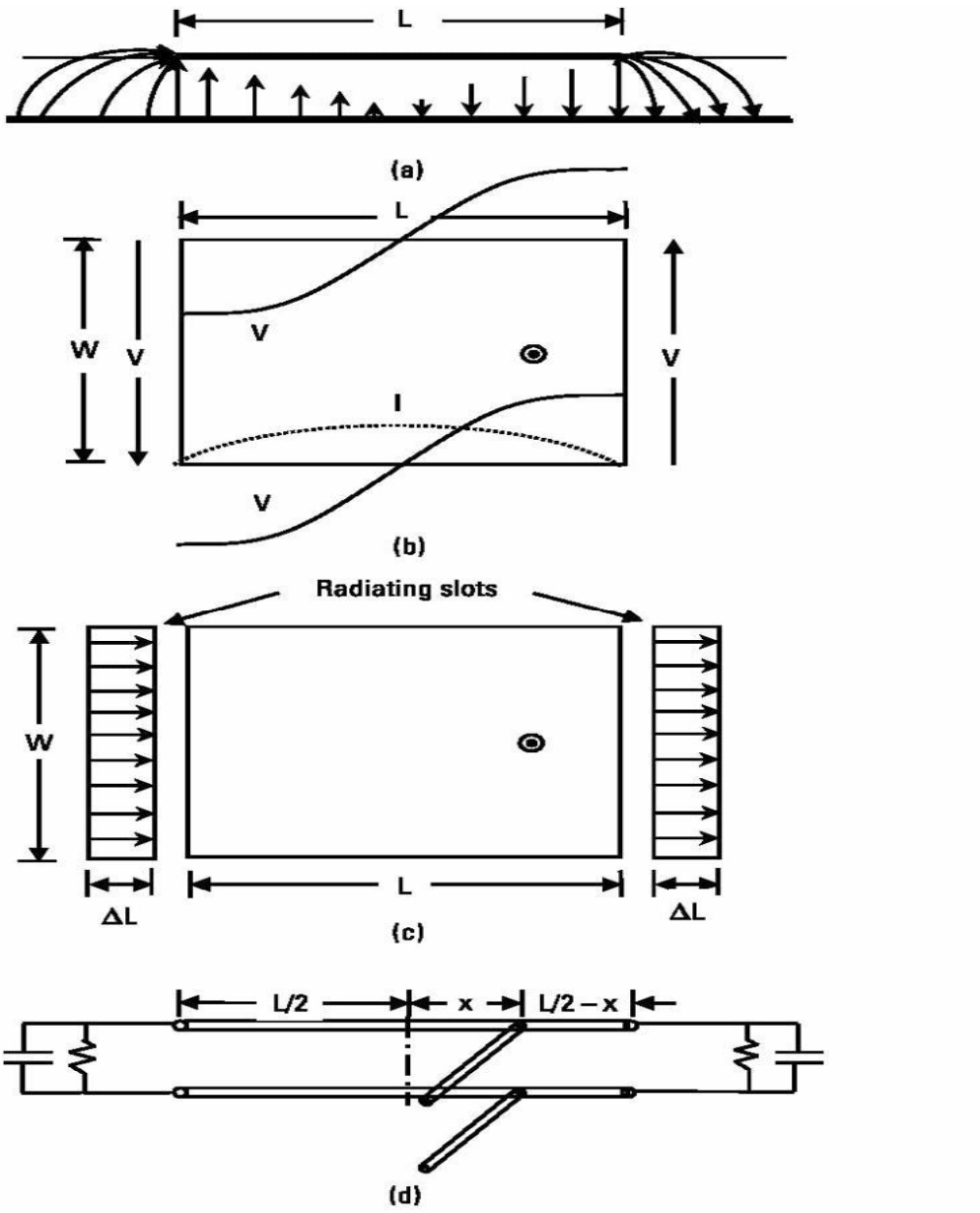

Figure 3.4 Fundamental TM_{10} mode of RMSA: (a) E-field distribution, (b) (___) voltage and (…) current variation, (c) two radiating slots and (d) equivalent transmission line model.

To account for the fringing fields, the dimensions around the periphery of the patch can be extended outwards. So the effective dimension Le and We are equal to:

$L_e = L + 2\Delta L$ … (3.7)

$W_e = W + 2\Delta W$ … (3.8)

The ΔL and ΔW are the extensions along the L and W respectively. For RMSA, generally W>>h, so for quick analysis and design, the extension in length may be approximately calculated by the following simple formula:

$$\Delta L = \frac{h}{\sqrt{\varepsilon_e}} \quad \text{… (3.9)}$$

Since the effectivelength of the patch is equal to λ/2, it can be calculated for a given resonance frequency f_0 as:

$$L_e = L + 2\Delta L = \frac{\lambda_0}{2\sqrt{\varepsilon_e}} = \frac{c}{2 f_0 \sqrt{\varepsilon_e}} \quad \text{… (3.10)}$$

Where c = $3x10^8$ meter/sec

To calculate ε_e, the value of W should be known. For an RMSA to be an efficient radiator, W should be taken equal to a half wavelength corresponding to the average of the two dielectric mediums (i.e., substrate and air) [1].

$$W = \frac{c}{2 f_0 \sqrt{\frac{\varepsilon_r + 1}{2}}} \quad \text{… (3.11)}$$

The width W of the patch can be taken smaller or larger than the value obtained using (3.11). If W is smaller, then the BW and gain will decrease. If W is larger, then the BW increases due to the increase in the radiated fields. The directivity also increases due to the increase in the aperture area as given in (3.5). However, if W is too large, then the higher order modes could get excited.

For the fundamental TM_{10} mode, since the voltage is maximum and the current is minimum at the edges, the input impedance of the RMSA varies from a zero value at its center to the maximum value at the radiating edges. To obtain impedance matching with the coaxial probe (generally a 50 Ω - feed line), the feed point should be placed at the location where the input impedance of the antenna matches the characteristic impedance of the feed.

CHAPTER 4

GENETIC ALGORITHM

4.1 Introduction

A genetic algorithm (GA) offers an alternative to traditional local search algorithms. It is an optimization algorithm inspired by the well-known biological processes of genetics and evolution. Genetics is the study of the inheritance and variation of biological traits. Manipulation of the forces behind genetics is found in breeding animals and genetic engineering. Evolution is closely intertwined with genetics. It results in genetic changes through natural selection, genetic drift, mutation, and migration. Genetics and evolution result in a population that is adapted to succeed in its environment. In other words, the population is optimized for its environment.

A combination of genetics and evolution is analogous to numerical optimization in that they both seek to find a good result within constraints on the variables. Input to an objective function is a chromosome. The output of the objective function is known as the cost when minimizing. Each chromosome consists of genes or individual variables. The genes take on certain alleles much as the variable has certain values. A group of chromosomes is known as a population. For our purposes, the population is a matrix with each row corresponding to a chromosome: It is the cost that determines the fitness of an individual in the population. A low cost implies a high fitness.

As you will see, GA operations work only with numbers. Thus, non-numerical values, such as a color or an opinion, must be assigned a number. Often, the numerical values assigned to genes are in binary format. Continuous values have an infinite number of possible combinations of input values, whereas binary values have a very large but finite number of possible combinations of input values. Binary representation is also common when there are a finite number of values for a variable, such as four values of permittivity for a dielectric substrate.

A basic GA is quite simple and powerful. The algorithm has the following steps:

1. Create an initial population.
2. Evaluate the fitness of each population member.
3. Invoke natural selection.
4. Select population members for mating.
5. Generate offspring.
6. Mutate selected members of the population.
7. Terminate run or go to step 2.

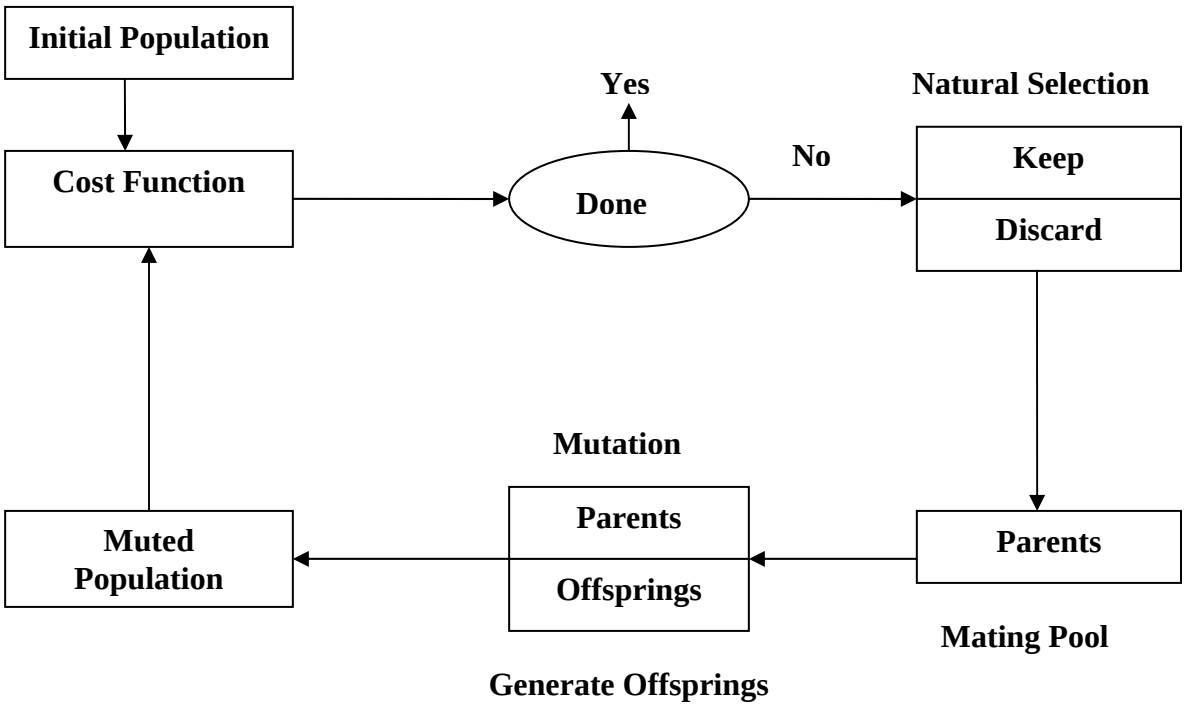

Figure 4.1 Flow chart of Genetic Algorithm

These steps are shown in the flow chart in Figure 4.1. Each of these steps is discussed in detail in the following sections.

4.2 Creating an Initial Population

The initial population is the starting matrix of chromosomes. Each row is a random "guess" at the optimum solution. Each variable is constrained to be between zero and one. Genes are the binary encoding of each problem variable, and all of the genes as

a string are referred to as a chromosome. A set of chromosomes is called a population. Each variable in the optimization problem must be coded as a gene, and all variables concatenated together form a chromosome. The sample chromosome shown in Figure 4.2 is composed of N parameters with each parameter containing 8 binary digits.

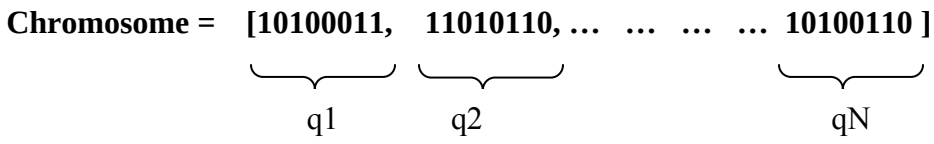

Figure 4.2 Chromosome with N parameters composed of 8 binary digits each

Each gene qn has a mapping from the chromosome space to the parameter space. It is important to fully understand the range and precision necessary for each variable so that the entire solution space can be explored and also to ensure that each gene, and thus each chromosome, generated by the GA is a realizable solution to the optimization problem.

4.3 Natural Selection (Evaluating Fitness)

Only the healthiest members of the population are allowed to survive to the next generation. The fitness function is the most important part of a genetic algorithm, as it is part of the algorithm that forms the connection to the physical problem being optimized. The fitness function must assign a number to each individual that is a measure of the goodness of the present individual in relation to the optimization goals. The success of the algorithm is dependent on how well the fitness function evaluates each solution in relation to the overall objectives of the optimization problem. The fitness function is generally the most time-intensive part of a genetic algorithm, so is also important when considering the time efficiency of the optimization algorithm.

4.4 Mate Selection

The most fit members of the population are assigned the highest probability of being selected for mating. The four most popular ways of choosing mates are population decimation, roulette wheel selection, tournament selection, and stochastic universal

sampling.

4.4.1 Population Decimation

In population decimation the individuals are ranked from highest to lowest based on their fitness. A minimal fitness is chosen as the cut-off and any individuals with a lower fitness than this threshold is removed from the population. The remaining individuals are randomly paired to produce offspring and create the next generation. The advantage of population decimation is the simplicity of its implementation. However, this simplicity is offset by the tendency to eliminate unique characteristics of the population thus decreasing the diversity of the sample population at a very early stage.

4.4.2 Roulette Wheel Selection

Roulette wheel selection assigns a selection probability to each individual in the population based on relative fitness values. Figure 4.3 shows how individuals are assigned a space on the wheel that is directly related to their relative fitness. The wheel is "spun" and the result of the spin selects the individual to use in the mating process. Individuals with high fitness values will be selected as parents more frequently than the less-fit individuals causing characteristics associated with higher fitness values to be represented more in subsequent generations. However, it can be seen that there is still a small probability that an individual with a low fitness value will be selected for the mating process, thus preserving their genetic information and maintaining a higher level of diversity.

The roulette wheel for a selection pool of four parents is shown in Figure 4.3. Chromosomes with low costs have a higher percent chance of being selected than do chromosomes with higher costs. In this case, the first or best chromosome has a 40% chance of being selected. As more parents are added, the percent chance of a chromosome being selected changes. For instance, Figure 4.4 shows a roulette wheel for eight parents in the mating pool. Now, the best chromosome has a 22% chance of being selected. The roulette wheel needs to be computed only once, since the number of parents in the mating pool remains constant from generation to generation.

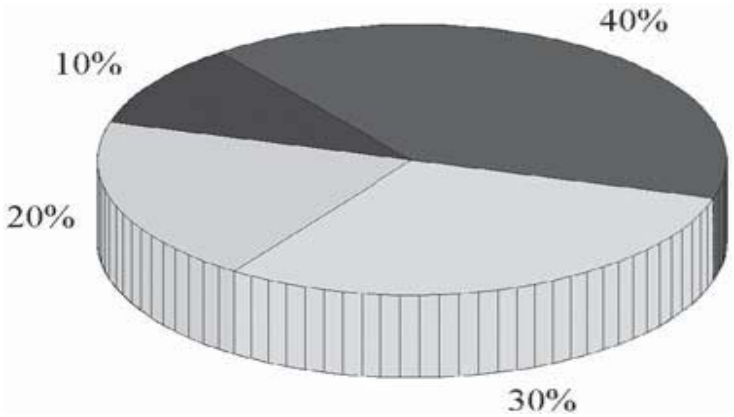

Figure 4.3 Four parents selection in Roulette wheel selection

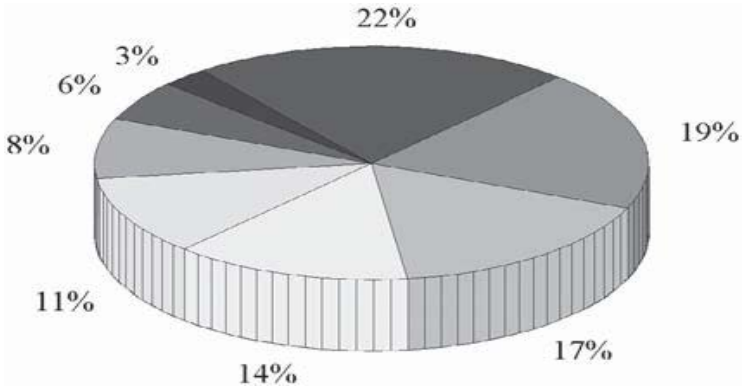

Figure 4.4 Eight parents selection in Roulette Wheel selection

4.4.3 Tournament Selection

In tournament selection, a sub-population of N individuals is chosen at random from the population and compete based on their fitness values. The individual with the highest fitness value wins the tournament and is selected as a parent in the mating pool. All the sub-population members are returned to the general population and the process repeats till the mating pool is full. Tournament selection acts much as roulette wheel selection, with the more fit individuals having a higher probability of selection while still maintaining the diversity of the population. The advantage of tournament selection is the absence of fitness ranking, which makes it a faster process than roulette wheel selection. Sort speed becomes an issue only with large population sizes. Figure 4.5 diagrams the tournament selection process when three chromosomes are selected for each tournament.

Rank order roulette wheel and tournament selection result in nearly the same probability of selection for the chromosomes.

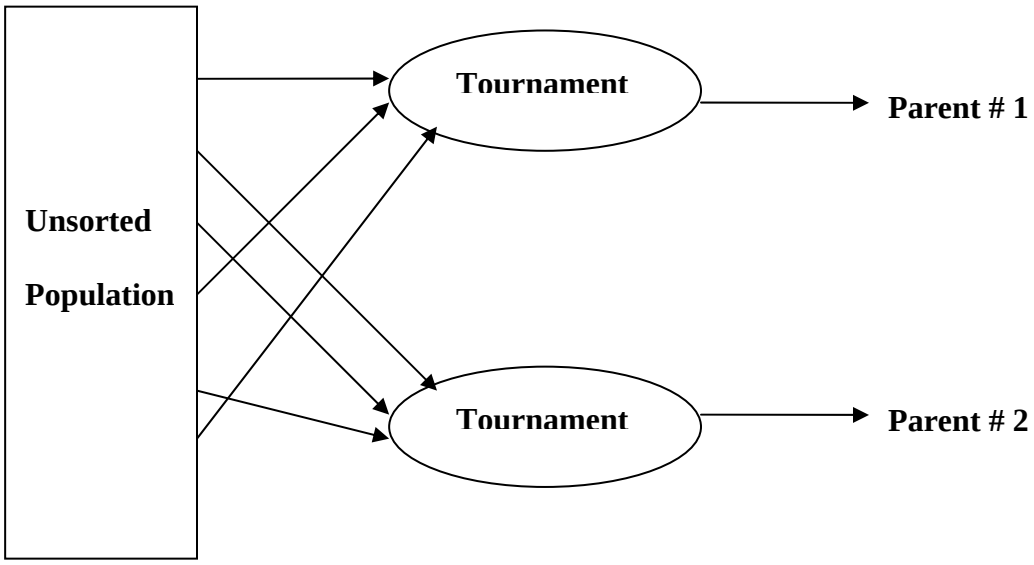

Figure 4.5 Tournament Selection

4.5 Generating Offspring

Offspring are generated from two parents through the process of crossover. There are many variations of crossover, but the most popular methods include uniform, single-point, and multiple-point crossover.

4.5.1 Single-Point Crossover

Single point crossover is the simplest. A random location in the parent's chromosome is selected and the portion preceding that location is copied from parent 1 to child 1 and from parent 2 to child 2. The portion of the chromosome following this point is copied from parent 1 to child 2 and from parent 2 to child 1, as shown in Figure 4.6.

Parent #1 1 0 1 0 0 0 1 1 **Child #1** 1 0 1 0 0 1 1 0

Parent #2 1 1 0 1 0 1 1 0 **Child #2** 1 1 0 1 0 0 1 1

Figure 4.6 Single Point Cross-over

4.5.2 Multi-Point Crossover

Multiple-point crossover is an extension of single point crossover, where more than one point is selected in the parent chromosome as shown in Figure 4.7.

Parent #1 1 0 1 0 0 0 1 1 **Child #1** 1 0 1 1 0 0 0 1

Parent #2 1 1 0 1 0 1 1 0 **Child #2** 1 1 0 0 0 1 1 0

Figure 4.7 Multi-Point Crossover

4.5.3 Uniform Crossover

Uniform crossover is accomplished through the use of a randomly generated mask that contains the same number of binary bits as the parent chromosomes. The numbers in the mask indicate whether the bit from parent 1 or parents 2 should be translated to each child. Figure 4.8 shows an example of uniform crossover, where a 0 in the mask indicates for child 1 that the bit should taken from parent 1 and a 1 indicates that the bit should be taken from parent 2. The opposite is true for child 2, where a 0 indicates that the bit should come from parent 2 and a 1 indicates the bit should be from parent 1. In Figure 4.8, all bits taken from parent 1 are noted with a dot, and those lacking dots are from parent 2.

Parent #1 1 0 1 0 0 0 1 1 **Child #1** 1 0 1 0 0 1 1 0

Mask : 1 0 0 1 0 0 1 1

Parent #2 1 1 0 1 0 1 1 0 **Child #2** 1 1 0 1 0 1 1 1

Figure 4.8 Uniform Crossover

4.6 Mutation

Mutations are random changes in chromosomes at the bit level and occur by changing a “1” to a “0” or a “0” to a “1”. Mutations are important as they allow the algorithm to search outside the current solution region and increase the likelihood that the genetic algorithm will explore the entire solution space.

4.7 Terminating the run

This generational process is repeated until a termination condition has been reached. Common terminating conditions are

- Set number of iterations.
- Set time reached.
- A cost that is lower than an acceptable minimum.
- Set number of cost function evaluations.
- A best solution has not changed after a set number of iterations.
- Operator termination.

These processes ultimately result in the next-generation population of chromosomes that is different from the initial generation. Generally the average fitness will have increased by this procedure for the population, since only the best chromosomes from the preceding generation are selected for breeding.

CHAPTER 5

PARAMETRIC STUDY OF RECTANGULAR MICROSTRIP ANTENNA AT 2.5 GHz FREQUENCY

5.1 Introduction:

For the fundamental TM_{10} mode, we apply 2.5 GHz as resonant frequency to design an RMSA. So, the wavelength of the resonant frequency is 0.12 m or 12 cm. The BW of the MSA is directly inversely proportional to the square root of its dielectric constant ε_r. As a result, a thicker substrate with a low dielectric constant is generally used to obtain broad BW. We select Rogers RT/duroid 5800 substrate with relative permittivity 2.2 and very low dielectric loss, tanδ with 0.001.

Used mode: TM_{10}
Resonant frequency, f_0 = 2.5 GHz,
Wavelength, λ_0 = 0.12 m
Relative Permittivity, ε_r =2.2
Line Impedance = 50 Ω
Polarization = Linear
Velocity of light, c = $3\times10^8 m/\sec$

5.2 Calculation of Substrate Height, h:

With the increase in h, the fringing fields from the edges increase, which increases the extension in length L and hence the effective length, thereby decreasing the resonance frequency. So, to calculate the height of the substrate we have to follow the below equation and our calculation.

$$\frac{h}{\lambda_0} \le \frac{0.3}{2\pi\sqrt{\varepsilon_r}} \qquad \ldots (5.1)$$

$$h \le \frac{0.3\lambda_0}{2\pi\sqrt{\varepsilon_r}}$$

$$h \le \frac{0.3 \times 0.12m}{2\pi\sqrt{2.2}}$$

$$h \le 0.38cm.$$

So, for broadbanding our RMSA design criteria, the height of the substrate should not be larger than 0.38 cm. We consider 0.38 cm to design the RMSA.

5.3 Calculation of Patch Width, W:

For the RMSA,the width is much smaller than the wavelength. If W is smaller, then the BW and gain will decrease. If W is larger, then the BW increases due to the increase in the radiated fields. The directivity also increases due to the increase in the aperture area. However, if W is too large, then the higher order modes could get excited. The following equation helps us to calculate our width of the RMSA.

$$W = \frac{c}{2 f_0 \sqrt{\frac{\varepsilon_r + 1}{2}}} \qquad \ldots (5.2)$$

$$W = \frac{3 \times 10^8 m/\sec}{2 \times 2.5 \times 10^9 \sqrt{\frac{2.2+1}{2}}}$$

$$W = 4.7cm \approx 4.5cm$$

Therefore, we take the width of the RMSA approximately 4.5 cm.

5.4 Calculation of Substrate's Effective Permittivity, ε_e :

The value of ε_e is slightly less than εr, because the fringing fields around the periphery of the patch are not confined in the dielectric substrate but are also spread in the air. For quick analysis or design of our RMSA, the following approximate formula for ε_e could be used:

$$\varepsilon_e = \frac{\varepsilon_r + 1}{2} + \frac{\varepsilon_r - 1}{2}\left[1 + \frac{10h}{W}\right]^{-1/2} \qquad \ldots (5.3)$$

$$\varepsilon_e = \frac{2.2+1}{2} + \frac{2.2-1}{2}\left[1 + \frac{10 \times 0.38cm}{4.7cm}\right]^{-1/2}$$

$\varepsilon_e = 2.05$

5.5 Calculation of Patch Length, L: for TM_{10} mode, m=1 and n=0

For the fundamental TM_{10} mode, the length L should be slightly less than λ/2, where λ is the wavelength in the dielectric medium. The following formula is very effective to calculate the length of the RMSA.

$$f_0 = \frac{c}{2\sqrt{\varepsilon_e}}\left[\left(\frac{m}{L}\right)^2 + \left(\frac{n}{W}\right)^2\right]^{1/2} \quad \ldots (5.4)$$

$$2.5\times10^9 = \frac{3\times10^8\, m/\sec}{2\sqrt{2.05}}\left[\left(\frac{1}{L}\right)^2 + \left(\frac{0}{W}\right)^2\right]^{1/2}$$

$$L = 4.1cm \approx 4cm$$

Therefore, we take the length of the RMSA approximately 4 cm.

5.6 Unoptimized MSA configuration:

So, from the above equations and calculations we have a RMSA configuration which is tabulated below:

TABLE 5.1: UNOPTIMIZED MSA CONFIGURATION

Parameter	**Value**
Height, h	0.38cm
Width, W	4.5cm
Length, L	4cm
Relative Permittivity, Rogers RT/duroid 5800	2.2
Feedpoint*	-0.6cm from center of Length
Feed radius*	0.07cm

* The values of feedpoint and feed radius has been taken from the parametric study of RMSA of "Compact and Broadband Microstrip Antenna" by Girish Kumar and K.P. Ray.

5.7 Unoptimized MSA Design in HFSS:

Designing a patch to resonant at a particular frequency involves only a few steps when using a simulation tool, such as Ansoft High Frequency System Simulator (HFSS). The four main design parameters for a microstrip patch antenna are the width and length of the patch, and the height and permittivity of the dielectric. The model for the patch antenna is created in HFSS, with the correct dielectric height, permittivity, and substrate dimensions. The patch antenna is then drawn on the substrate with the width and length dimensions of half a wavelength as mentioned previously. The patch will then be tuned to produce the exact input impedance, radiation patterns and gain that are needed for the design.

Here, in HFSS modeling 2.5 GHz resonance is examined. The substrate dimensions are 6 cm by 7 cm, with the thickness of 0.38 cm, a permittivity 2.2 and a loss tangent 0.001. In the figure 5.1,5.2 and 5.3, the substrate is based on the infinite ground plane on 6cm x 7cm platform. The patch dimensions are 4cm x 4.5cm and an air-box surrounding the antenna providing a radiation boundary is 6cm x 7cm x 3cm. The patch is fed by a lumped port of 0.07cm radius and centered at 0.6cm right away from the central x-axis of the patch with an impedance of 50 Ω.

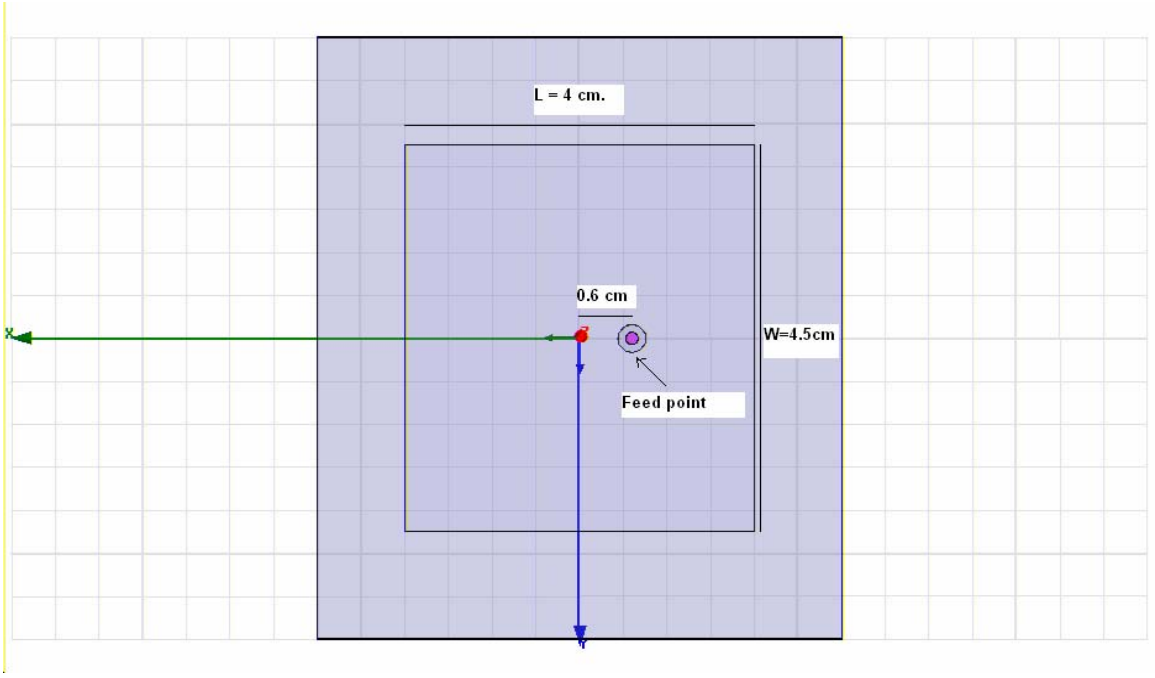

Figure 5.1 Top View of Unoptimized MSA

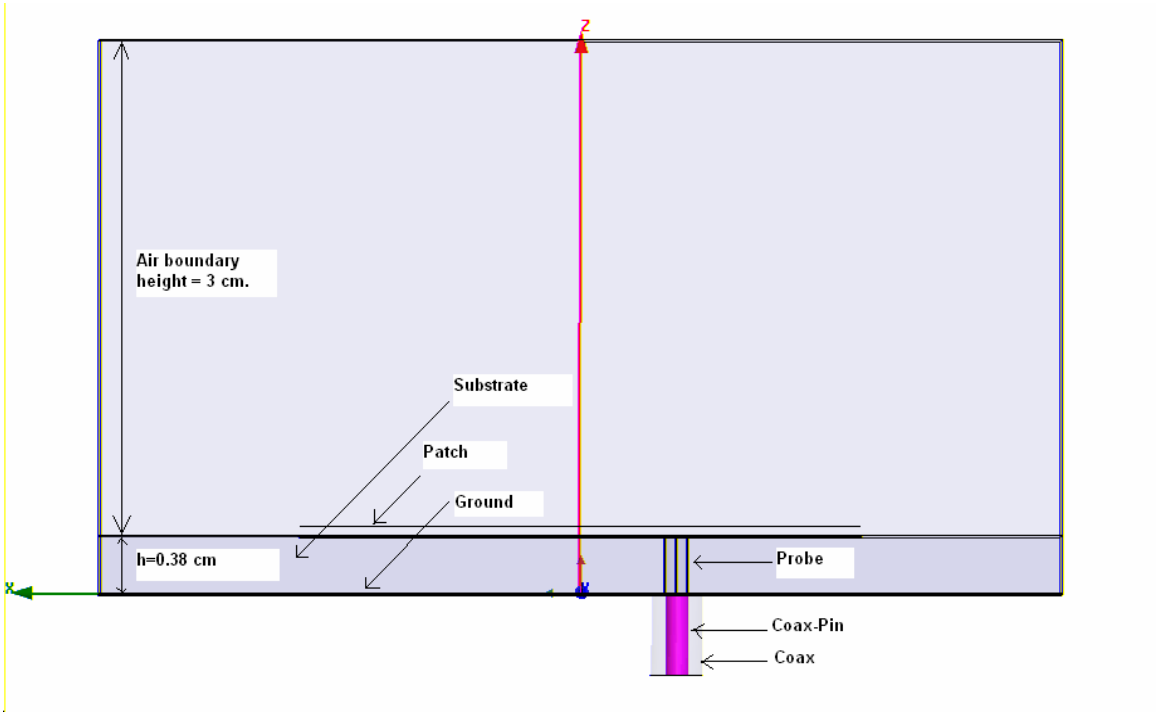

Figure 5.2 Side View of Unoptimized MSA

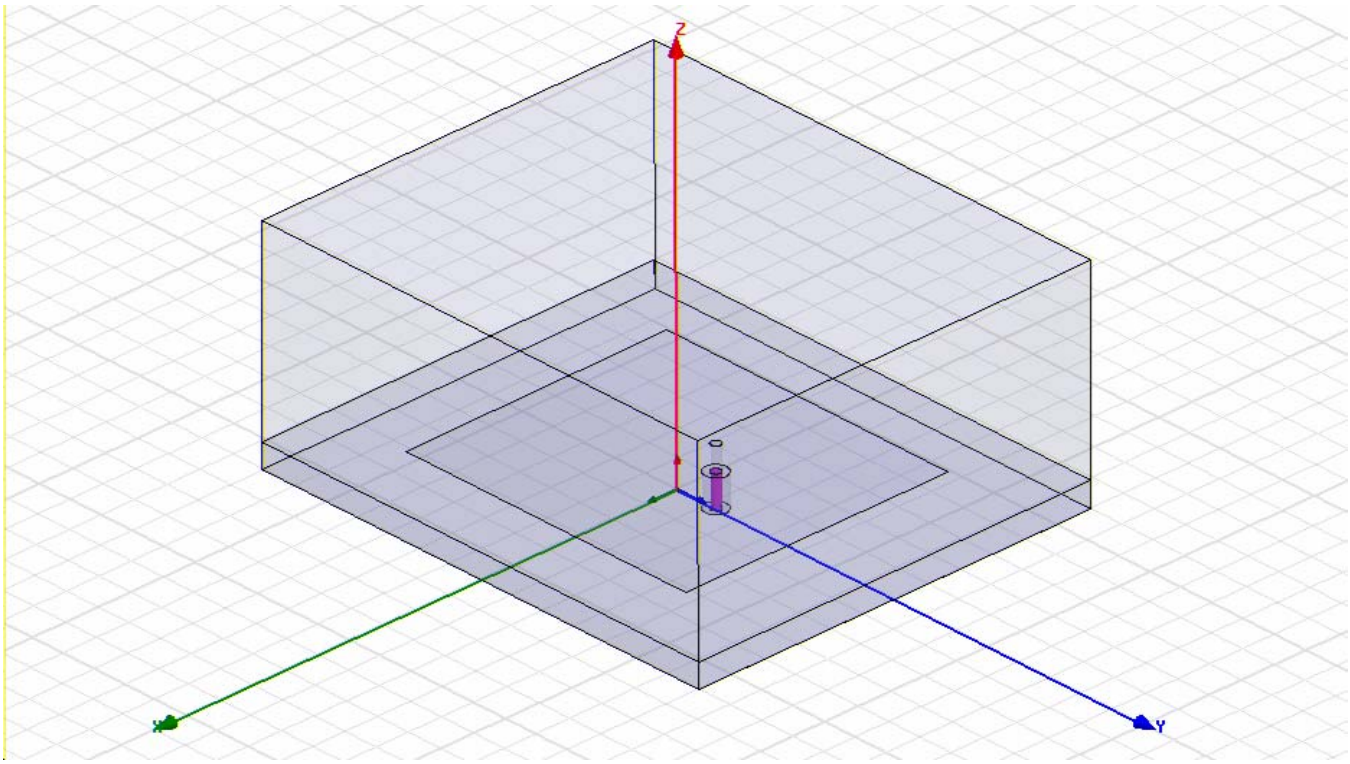

Figure 5.3 3D View of Unoptimized MSA

5.8 Output of Unoptimized MSA:

The S_{11} is plotted on the Smith Chart in figure 5.4, and the frequency where the impedance becomes purely resistive is the resonant frequency of the patch. Figure 5.8 shows the VSWR is 2.55 and the Q factor is 1.078. The impedance of the antenna is 0.678+j0.741. From frequency sweep, in figure 5.5, plotting the S_{11} versus frequency reveals the 2.21 GHz resonance at a return loss of -7.25dB. If we consider the return loss of -6dB we get 60MHz bandwidth from the patch antenna design. From the figure 5.6, 5.7 and 5.8 we get the gain and directivity of RMSA is 5.5 dB and 5.6 dB respectively.

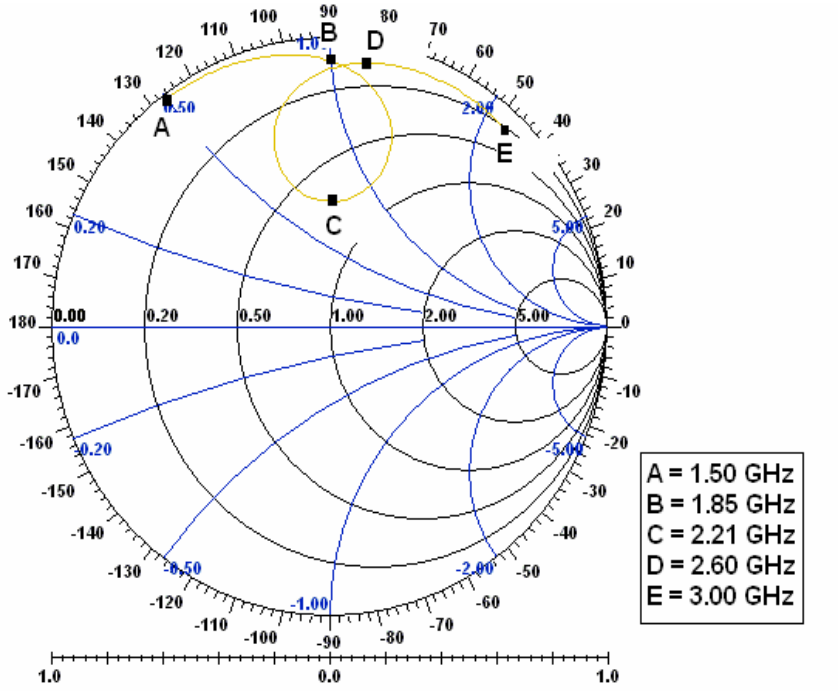

Figure 5.4 Smith Chart of Unoptimized MSA

TABLE 5.2. SMITH CHART RESULT FOR VARIOUS FREQUENCIES OF THE UN-OPTIMIZED RMSA

Frequency (GHz)	**1.5**	**1.85**	**2.21**	**2.6**	**3**
Reflection co-eff (Polar form)	$0.98 \angle 126.9^0$	$0.912 \angle 89.6^0$	$0.436 \angle 89.3^0$	$0.92 \angle 81.97^0$	$0.927 \angle 47.46^0$
Impedance plane	0.013+j0.5	0.092+j1	0.687+j0.741	0.095+j1.146	0.233+j2.255
Admittance plane	0.052-j2	.091-j0.99	0.674-j0.727	0.072 –j0.866	0.045-j0.439
Q factor	38.745	10.846	1.078	12.025	9.673
VSWR	96.895	21.737	2.55	24.328	26.295

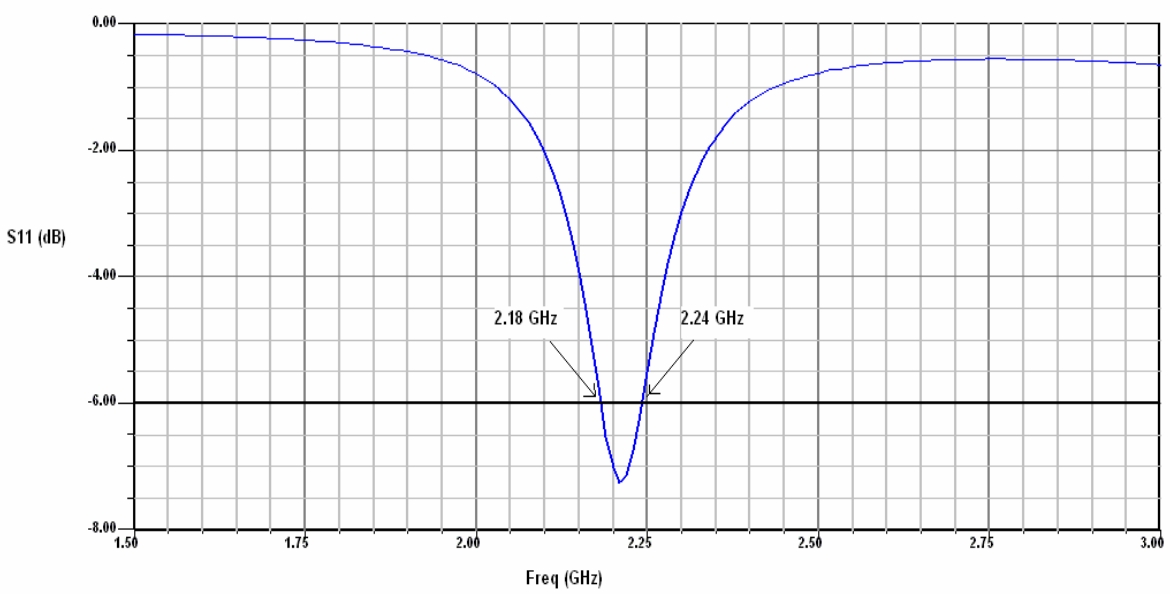

Figure 5.5 S_{11} – Freq Graph of Unoptimized MSA

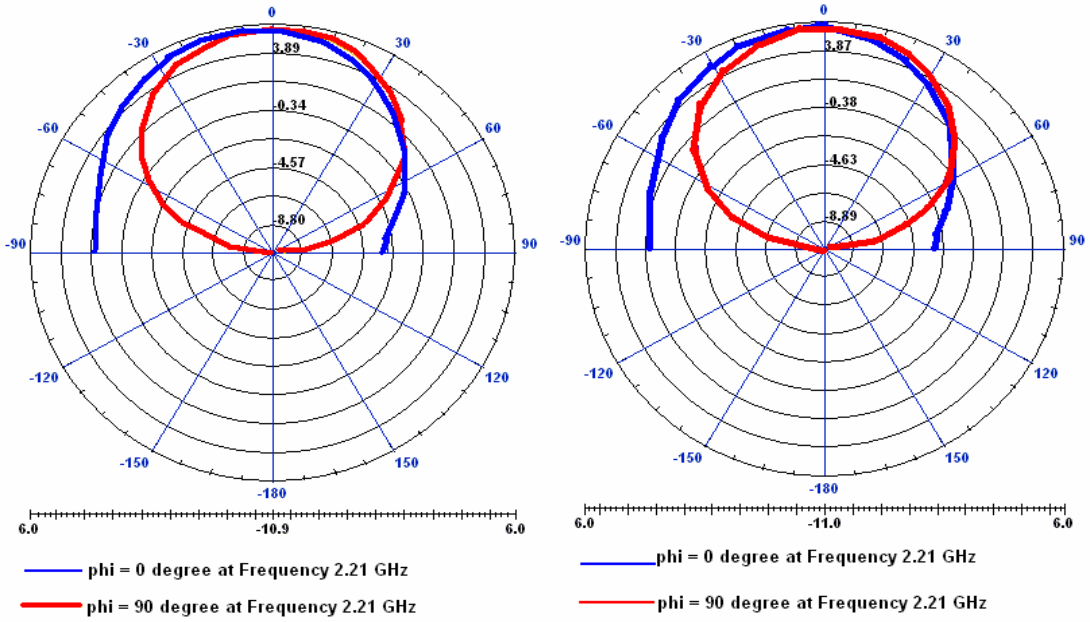

(a) (b)

Fig 5.6 (a)Directivity (Polar form) of Unoptimized MSA, (b) Gain (Polar form) of Unoptimized MSA

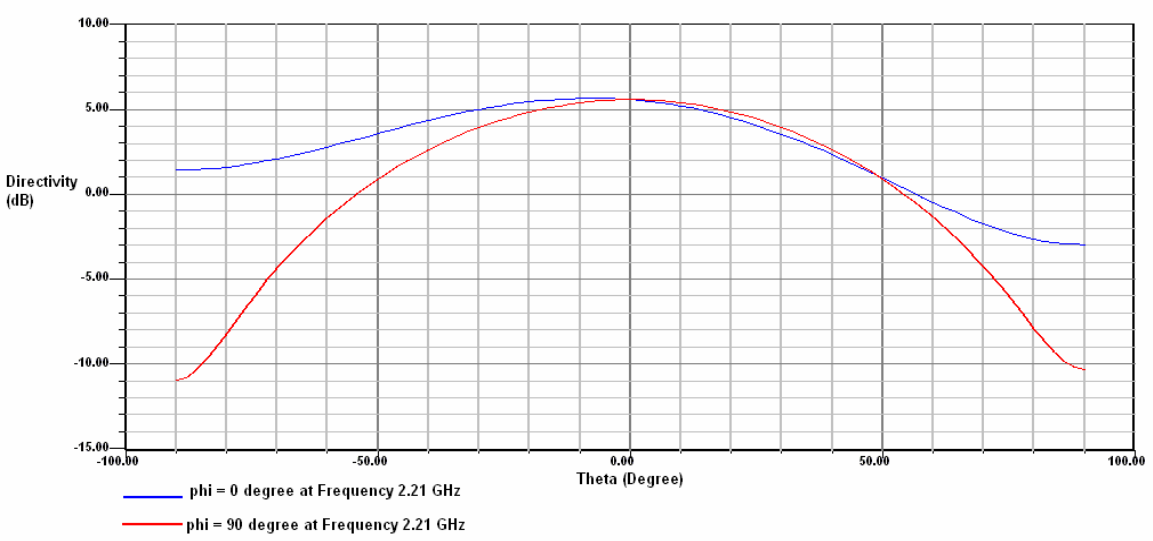

Figure 5.7 Directivity (Rectangular form) of Unoptimized MSA

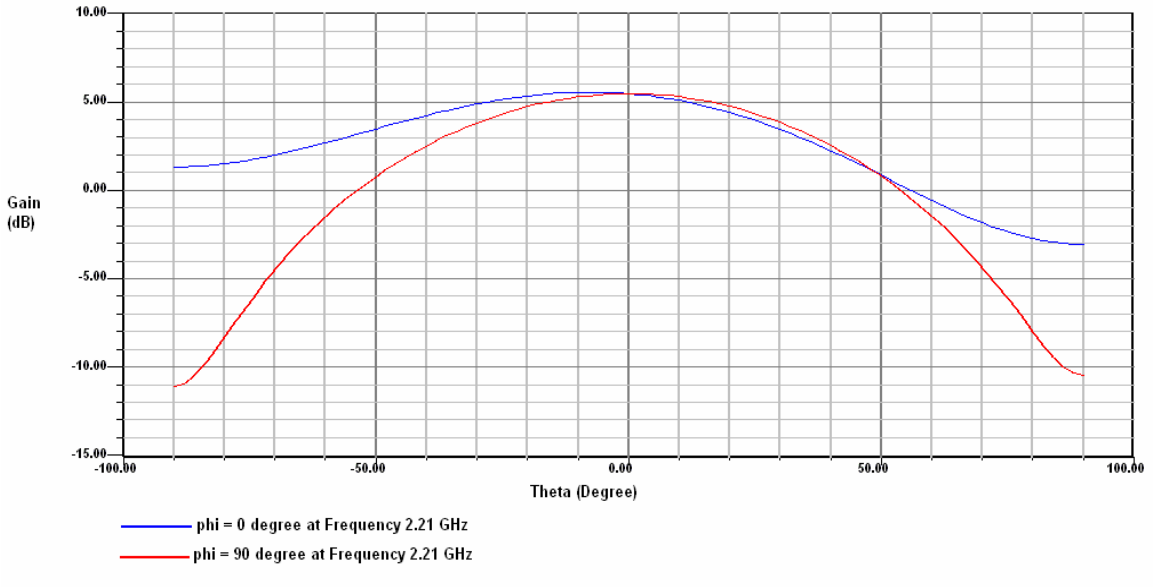

Figure 5.8 Gain (Rectangular form) of Unoptimized MSA

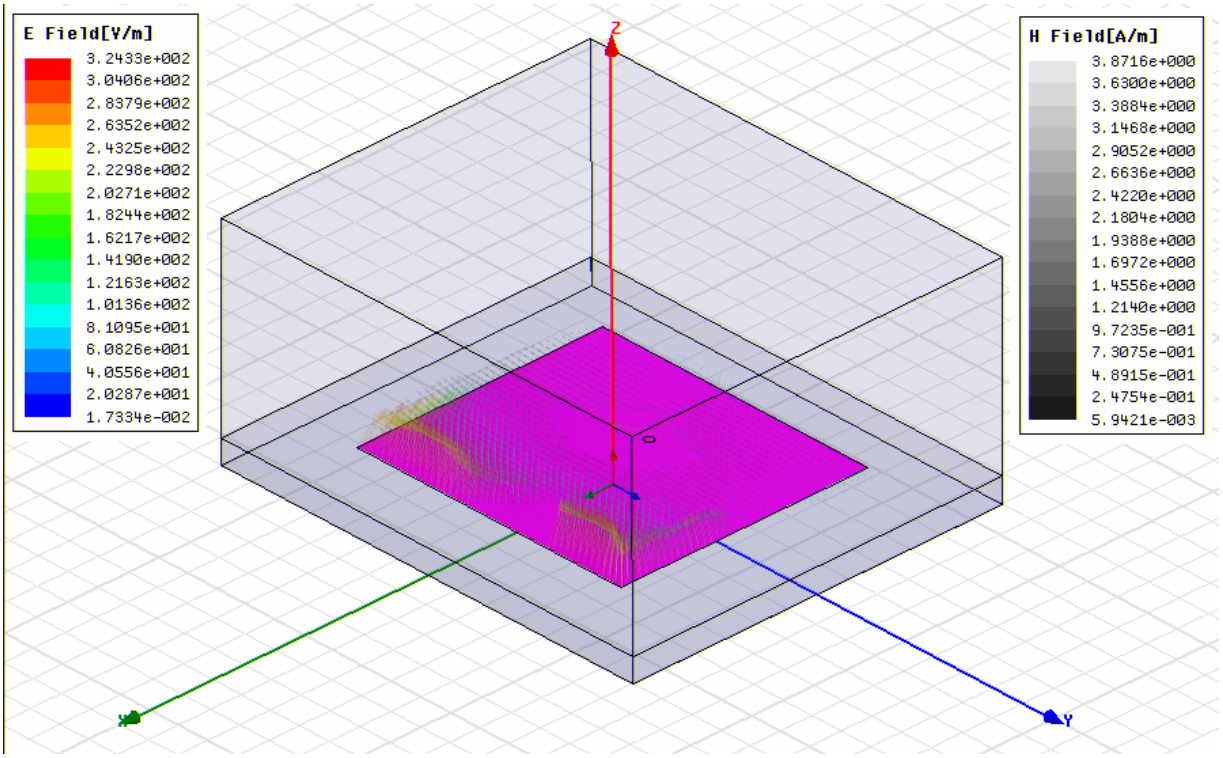

Figure 5.9 E-field and H-field direction and measurement of Unoptimized MSA

CHAPTER 6

GENETIC ALGORITHM IN MICROSTRIP ANTENNA

6.1 Introducing SuperNEC as Genetic Algorithm Solver

We use Genetic algorithm optimization using SuperNEC 2.9. SuperNEC is a Method of Moments electromagnetic (EM) simulation package for Windows or Linux platforms. The easy to use 3D input GUI, making use of multi-level assemblies, provides the easiest ever structure input and model creation tool. The output viewer provides the design engineer with all the necessary information for proper antenna analysis including features such as 3D & 2D pattern plots, smith chart plots with network analyzer style markers, Coupling plots, Efficiency plots etc. The SuperNEC solution engine includes optimized code for Intel processors, various fast solvers (including Dr Francis Canning's patented Simply Sparse method) and a parallel execution option for extremely large problems. Another essential design tool is the Genetic Algorithm optimizer included in SuperNEC.

6.2 GA Parameters in SuperNEC 2.9

This section briefly explains the parameters involved in a GA optimisation.

6.2.1 Selection Strategies

Selection strategies determine which chromosomes will take part in the evolution process (will be involved in the making up of the next generation in terms of mating with other chromosomes, or simply being inserted unchanged).

6.2.1.1 Population Decimation

In this strategy the chromosomes are ranked according to their fitness or cost values from highest to lowest. This is the recommended strategy to use as it leads to proper convergence and has been found in to produce the best solutions as compared to the other strategies.

6.2.1.2 Proportionate Selection

In this selection strategy the probability of a chromosome being selected is proportionate to the fitness of the chromosome as compared to the fitness of the total population. That is a chromosome with a 'good' fitness has a higher probability of being selected, than one that has a low fitness value. This strategy is also commonly referred to as 'roulette wheel' selection as it can be viewed as a roulette wheel containing all the chromosomes, with the chromosomes having a better fitness occupying a larger surface area of the wheel, and thus have a greater probability of being selected.

6.2.1.3 Tournament Selection

In tournament selection two individuals are randomly selected and then the one with the highest fitness 'wins'. This process continues until the required number of chromosomes has been reached. This method produces slightly better solutions as compared to Proportionate Selection, but does not perform nearly as well as Population Decimation.

6.2.2 Mating Schemes

While the selection strategies are involved with selecting which individuals will take part in the evolution process (be parents), the mating schemes select which two parent chromosomes will mate with one another. The mating schemes that exist include Best Mates-Worst, Adjacent Fitness pairing and Emperor Selective mating.

6.2.2.1 Best Mates-Worst

As the name suggest the chromosomes with the highest fitness mates with the chromosomes with the lowest fitness. Tests have shown that this method operates comparatively with Adjacent Fitness Pairing, which is the recommended mating scheme.

6.2.2.2 Adjacent Fitness Pairing

In this scheme the two individuals ranked the highest mate together, and then the next two highest ranked individuals mate together etc. This is the recommended mating scheme.

6.2.2.3 Emperor Selective Mating

In the Emperor selective mating scheme, the highest ranked individual mates with

the second highest, fourth highest, etc individuals, while the third, fifth, etc highest individuals remain unchanged.

6.2.3 Crossover Point

A crossover occurs when two parent chromosomes mate with one another. When this occurs the two parent chromosomes are both dissected at the same predefined crossover point. The two pieces from the first parent chromosome mate with the two complementary pieces from the second parent chromosome, to form two new chromosomes.

As mentioned above, the crossover point determines the point at which a chromosome will be dissected. Allowable inputs values for crossover point is $0 \leq$ crossover pt ≤ 1 where 0 indicates a crossover point that is determined randomly, and 1 indicates that no crossover will occur. For example a crossover point of 0.5 would indicate that the chromosomes would be cut in half. It is recommended that a random crossover point be used, as this has been shown to produce the best results.

6.2.4 Mutation

A mutation occurs in a chromosome with a small probability of Pmutation. When a mutation occurs in a chromosome, a random bit in the binary chromosome is inverted. For example a '1' will be changed to a '0' and vice versa. Mutations are very important as they allow solutions to be explored, which may have not previously been in the optimiser search space. A mutation rate of 0.15 (ie. 15%) has been found to be the optimum value in most cases.

6.2.5 Chromosomes and Generations

In the Genetic Algorithm each chromosome represents a specific antenna design/configuration. The number of chromosomes used in a Generation and the number of generations are both user-defined inputs. The number of chromosomes determines the number of antenna configurations that will be evaluated in each generation, and the number of generations determines how many iterations the GA optimiser will run through before coming to completion.

6.2.6 Success of the GA optimiser

The success of a Genetic Algorithm optimiser depends mostly on how your GA parameters are selected, and in particular the amount of generations and chromosomes used. In general the amount of generations determines if convergence will be obtained, and the amount of chromosomes used will determine how good the solution obtained at convergence will be. For example, lets say that you manage to obtain convergence after 20 generations, then further increasing the amount of generations will most likely not improve your best solution obtained, however it will also not take a significant amount of extra time to run, as the optimiser will be evaluating chromosomes already simulated in early generations, and thus need not re-simulate them. Another example, choosing to use 40 chromosomes as compared to 20 chromosomes for a specific problem, will most probably lead to convergence after more or less the same amount of generations, but may lead to an answer which is substantially better. On the other hand, choosing too many chromosomes will lead to more or less the same answer obtained by using slightly less chromosomes, but will lead to a large increase in running time of the optimiser.

6.2.7 Fitness Function/Costing function

The fitness/cost of a chromosome determines how 'good' a chromosome is, with a high fitness indicating a 'good' chromosome.

6.2.7.1 Built in Fitness/Cost functions

The built in fitness function used by the optimiser is as follows:

$$Fitness/Cost = \left(\frac{ActualGain}{\mathrm{Re}\, q.Gain} \right)^{gFactor} + \left(\frac{\mathrm{Re}\, q.VSWR}{ActualVSWR} \right)^{vFactor}$$

gFactor and vFactor allow the user to make the costing to depend more on Gain or VSWR or vice versa. The default and recommended values for gFactor and vFactor are 2 (the norm value).

If the requirements dictate that the antenna structure be optimised over a range of frequencies, three options are available namely: by calculating the fitness in the equation above for each frequency and then averaging the result, by using the worst ratio of actual gain to required gain and worst ratio of required VSWR to actual VSWR over the range

of frequencies or by limiting the ratios in the above equation to a maximum of 1 until all the requirements at all the frequencies are met (will only start getting very high fitness values once all requirements are met).

6.2.7.2 User Defined Fitness/Cost Functions

The user may decide to write his/her own cost functions and/or modify the existing costing functions for the following reasons. The built in cost functions may not be adequate for the specific application. The user may wish to use parameters other than Gain at one point and/or VSWR to calculate cost. The user may wish to calculate the fitness using gain found at more than one point (may wish to look at the entire radiation pattern for example. In order for the user to define his/her own costing function(s), the user must edit the gaconfig.ini file to allow the new costing functions to be made accessible via the GA Optimiser interface, and the user must edit the GA costing function m-file. The following is the costfunction definition line in the default configuration file:

costfunctions [Average_Cost,Worst_Cost,Multifreq_costing]

6.3 GA Parameter INPUT in SuperNEC 2.9

To optimize the previously calculated geometry of the patch antenna, we consider its substrate height, patch width and patch length. For this we use the GUI of the SuperNEC simulator. In Solver section, both patch length and width are initialized -1 and are bounded by minimum value 25mm and maximum 50mm with the resolution of 1mm x 1mm. The substrate height is also initialized -1 and is bounded by minimum value 3mm and maximum value 4mm. But the resolution is set here 0.1mm x 0.1mm. Feedposition is taken into axis co-ordinate system of [0.006m, 0.0001≈0m(as SuperNEC doesn't allow 0 input in this case)]

TABLE 6.1: BASIC PARAMETERS' BOUNDARY VALUES OF MSA FOR GA OPTIMIZATION

Parameter	Min	Max
Height, h	0.3 cm	0.4 cm
Width, W	2.5 cm	5.0 cm
Length, L	2.5 cm	5.0 cm

In SuperNEC, cost/fitness settings, we select 10dB gain as Required Gain and

gain factor (gFactor) of 2 and required VSWR is 1 and VSWR factor (vFactor) of 2. The cost calculation adopts ‘Average cost’ method for the output.

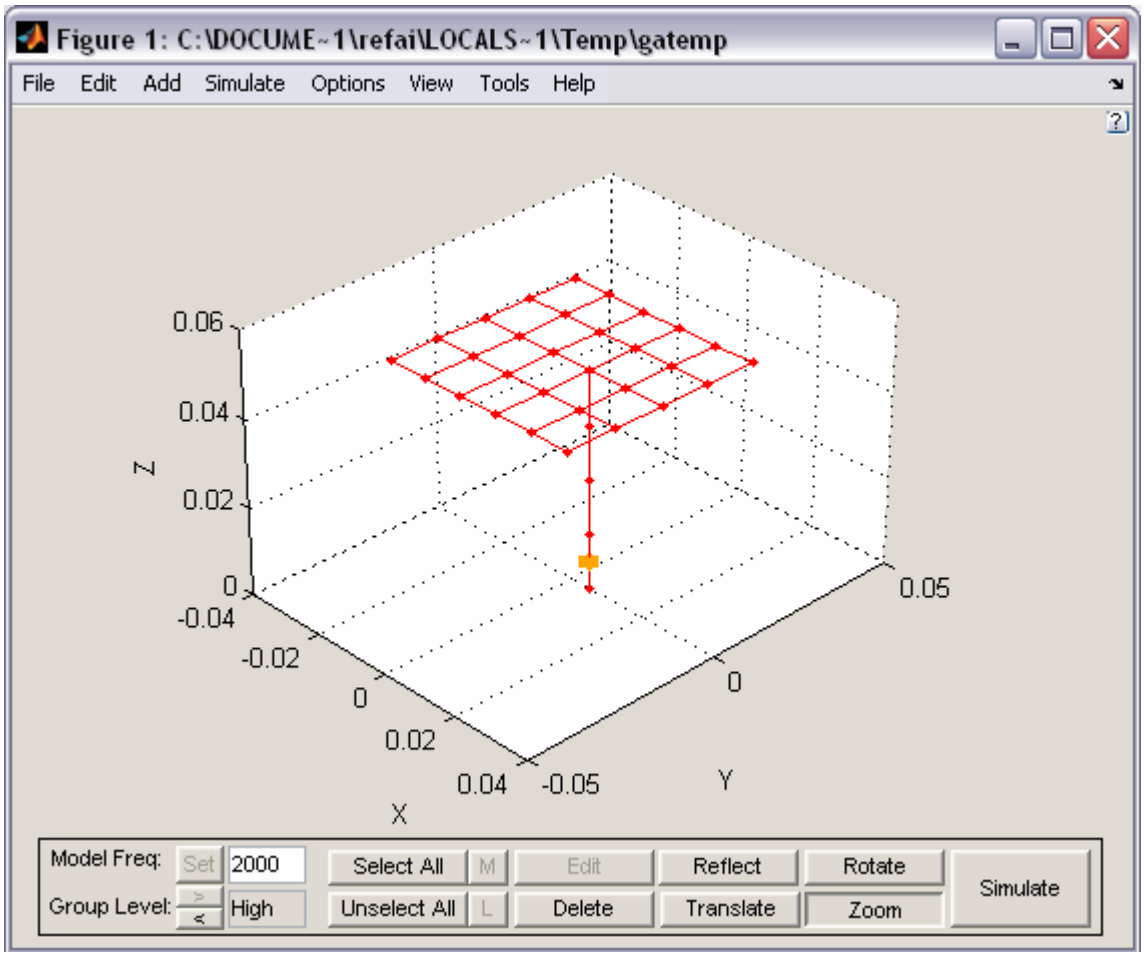

Figure 6.1 SuperNEC GA calculation GUI (Screen-shot)

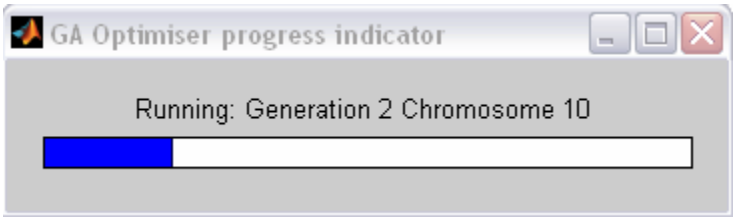

Figure 6.2 SuperNEC GA Optimizer progress indicator (Screen-shot)

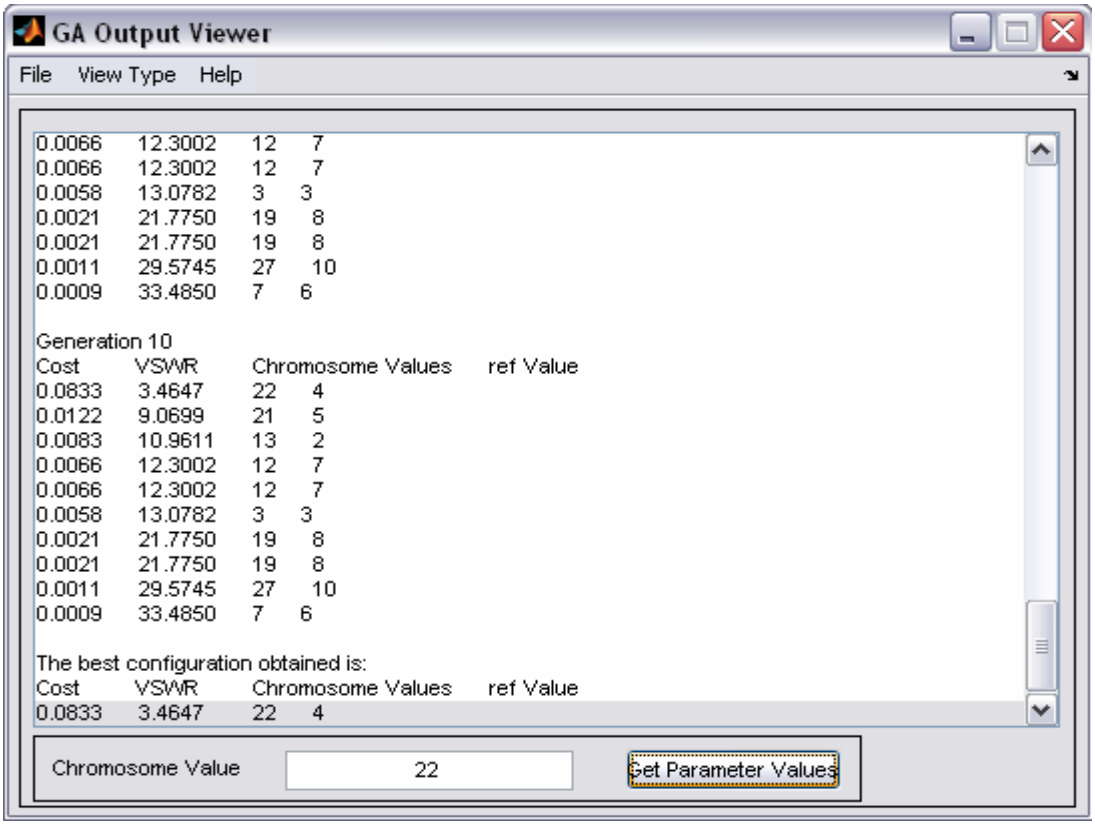

Figure 6.3 SuperNEC GA output viewer (Screen-shot)

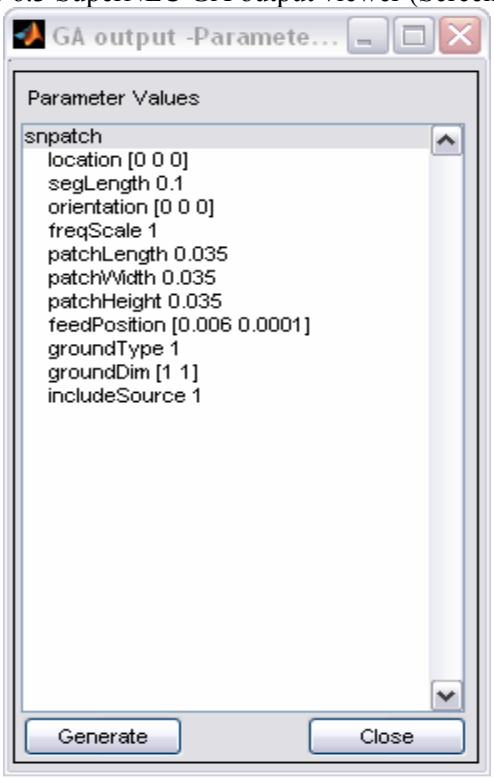

Figure 6.4 the best chromosome's MSA configuration output

In Genetic Algorithm setting section, for the selection of fittest population, we take 'Tournament Selection' and for mate we select 'Emperor Selection'. For generating offspring, we select 'Random Crssover Points' with a mutation rate of 0.25 (i.e.25%). In model settings, simulation frequency is 2500MHz (2.5GHz) with line impedance 50 Ω.

The Genetic Algorithm will run upto 10 generation creating 10 chromosomes in each generation and finally select the best fit chromosome from that.

As we use infinite ground plane in the previously simulated RMSA, we select 'NONE' ground as SuperNEC provide no infinite groundplane. Ofcourse, this is not vulnerable part cause we will verify the output of the SuperNEC's optimization by HFSS simulator.

*.gaf file:

```
asmb snpatch
location [0,0,0]
orientation [0,0,0]
patchLength -1 [25,50,1]
patchWidth -1 [25,50,1]
patchHeight -1 [3.0,4.0,0.1]
feedPosition [0.006,0.0001]
groundDim [1,1]
gnd [0,0.04,1,4]
gnd.secondary [0,1,10,0,0.04,4]
gnd.screen [0,8,2,0.005]
freq 2500
imp 50
sim.radpat {[0,1,1,0,0,0,1,90,45,0,0,0,0]}
ga.chromo 10
ga.gen 10
```

ga.type [3,10,0,1,0,0.25]

cost.gain 10 2

cost.vswr 1 2

cost.type 0

6.4 GA Optimized MSA configuration:

TABLE 6.2: GA OPTIMIZED MSA CONFIGURATION

Parameter	**Value**
Height, h	0.35cm
Width, W	3.5cm
Length, L	3.5cm
Relative Permittivity, Rogers RT/duroid 5800	2.2
Feedpoint	-0.6cm from center of Length
Feed radius	0.07cm

6.5 GA Optimized MSA Design in HFSS 9.2

After getting the optimized RMSA from genetic algorithm solver, in HFSS modeling 2.5 GHz resonance is examined again. The substrate dimensions are 6 cm by 7 cm, with the thickness of 0.35 cm, a permittivity 2.2 and a loss tangent 0.001. The substrate is based on the infinite ground plane on 6cm x 7cm platform. The patch dimensions are 3.5cm x 3.5cm and an air-box surrounding the antenna providing a radiation boundary is 6cm x 7cm x 3cm. The patch is fed by a lumped port of 0.07cm radius and centered at 0.6cm right away from the central x-axis of the patch with an impedance of 50 Ω.

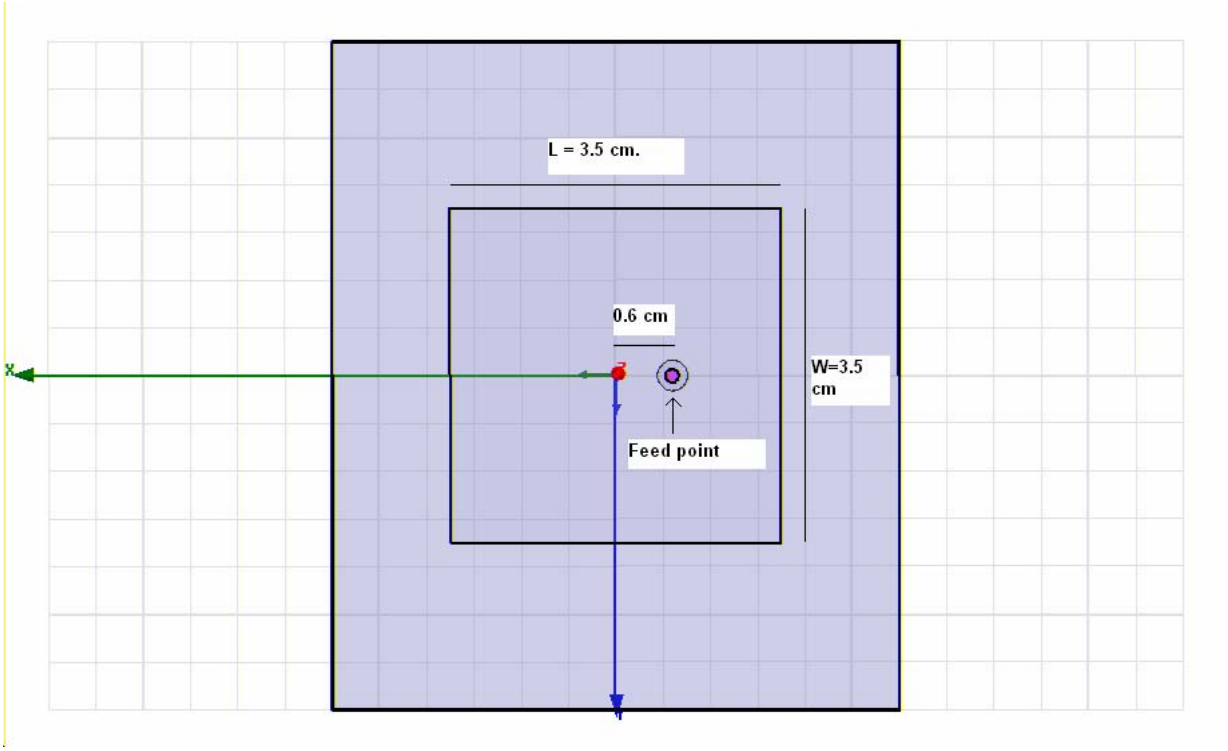

Figure 6.5 Top View of GA optimized MSA

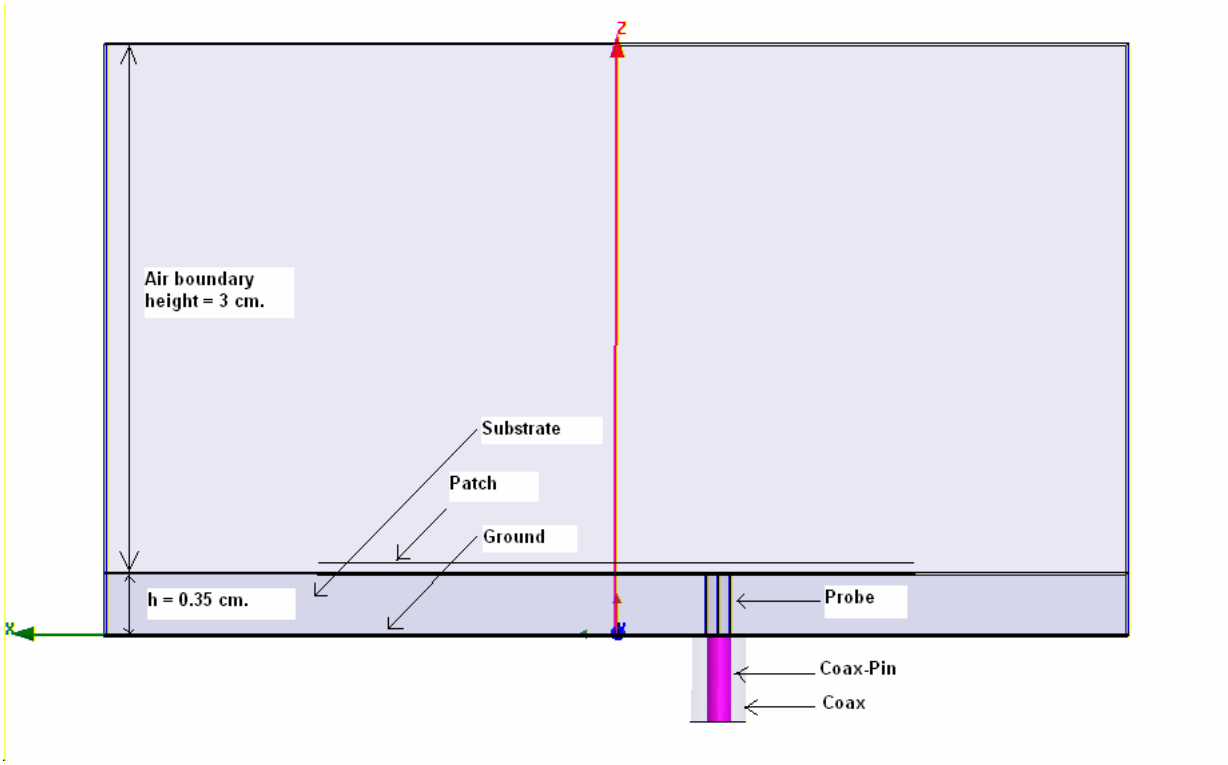

Figure 6.6 Side View of GA optimized MSA

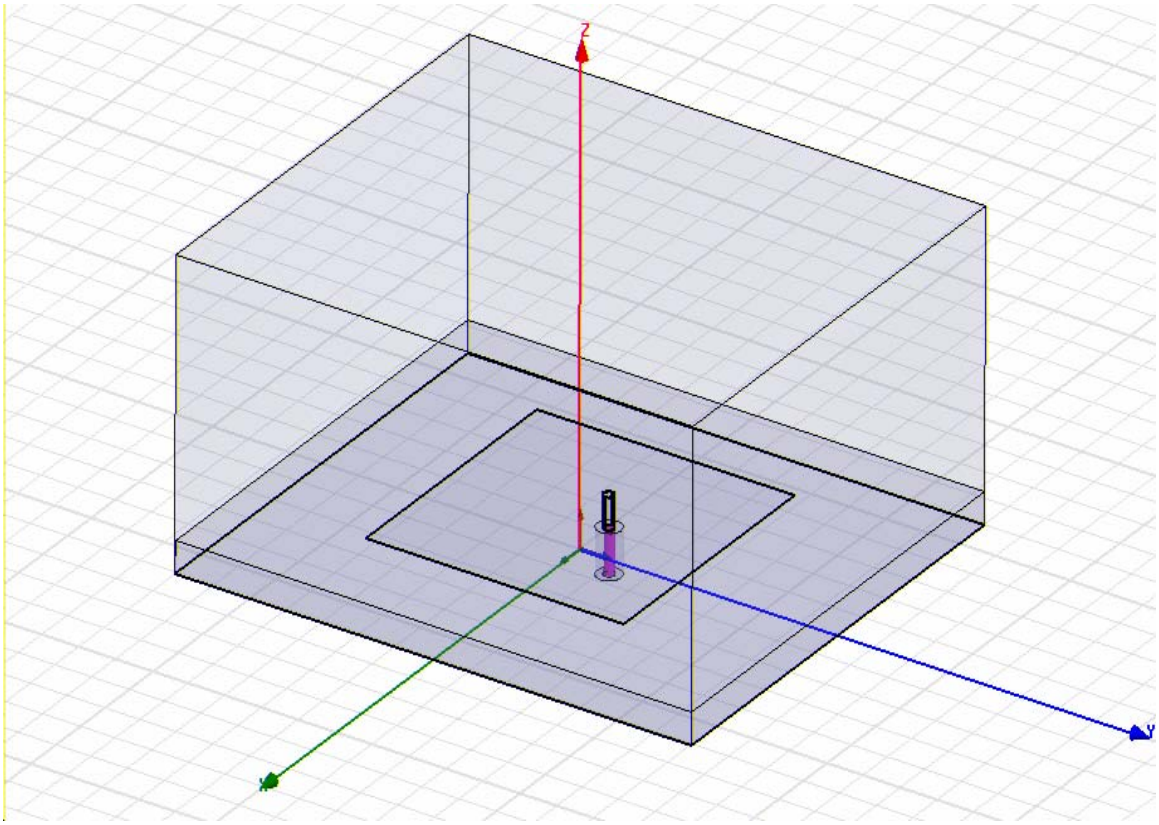

Fig 6.7 3D View of GA optimized MSA

6.6 OUTPUT of GA optimized MSA:

The S_{11} is plotted on the Smith Chart in figure 6.8, and the frequency where the impedance becomes purely resistive is the resonant frequency of the patch. Figure 6.8 shows the VSWR is 1.678 and the Q factor is 0.538. The impedance of the antenna is 0.836+j0.45. From frequency sweep, plotting the S_{11} versus frequency reveals the 2.42 GHz resonance at a return loss of -12.10dB. If we consider the return loss of -6dB, we get 100MHz bandwidth and if we consider the return loss of -10dB, we get 50MHz bandwidth from the patch antenna design. In figure 6.10, 6.11 and 6.12 the gain and directivity of the GA optimized RMSA is 6.25 dB and 6.1 dB respectively.

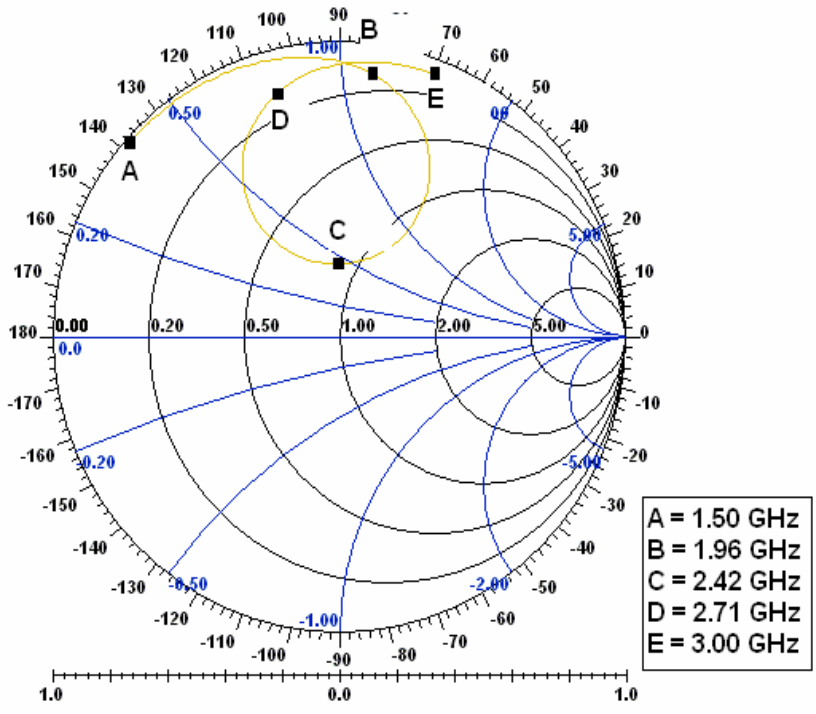

Figure 6.8 Smith Chart of GA optimized MSA

TABLE 6.3 SMITH CHART RESULT FOR VARIOUS FREQUENCIES OF THE GA OPTIMIZED RMSA

Frequency (GHz)	**1.5**	**1.96**	**2.42**	**2.71**	**3**
Reflection co-eff (Polar form)	$0.987 \angle 138^0$	$0.9 \angle 84.3^0$	$0.25 \angle 96.43^0$	$0.83 \angle 108.07^0$	$0.947 \angle 69.9^0$
Impedance plane	0.008+j0.384	0.11+j1.1	0.836+j0.45	0.141+j0.716	0.082+j1.426
Admittance plane	0.052-j2.604	.09-j0.9	0.929-j0.5	0.264 –j1.34	0.04-j0.7
Q factor	49.843	10.03	0.538	5.083	17.362
VSWR	148.96	20.21	1.678	10.786	36.988

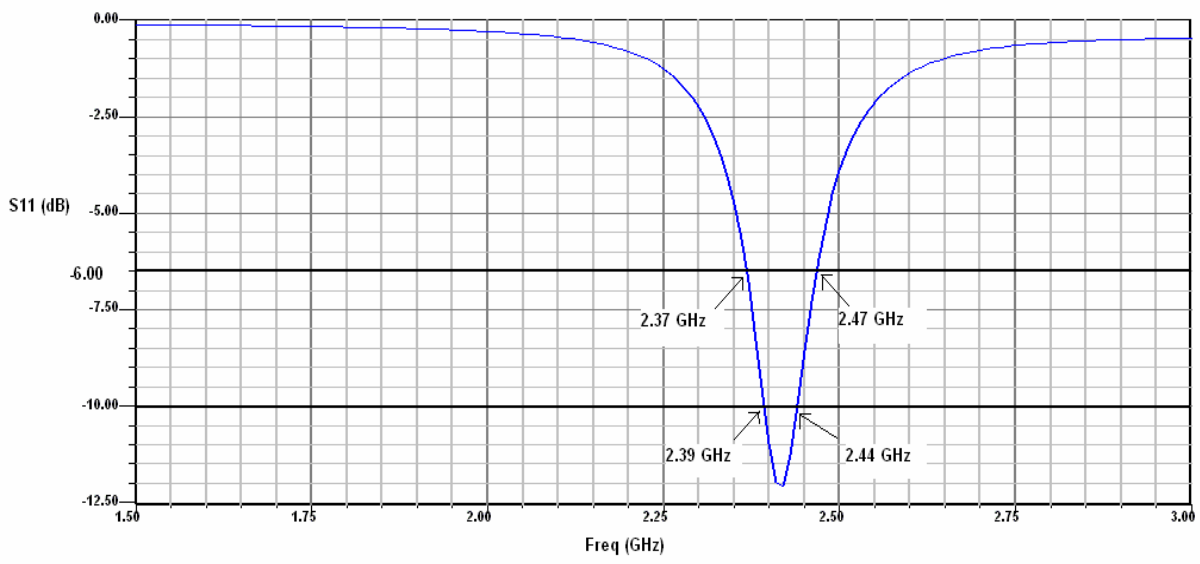

Figure 6.9 S_{11}-Freq graph of GA optimized MSA

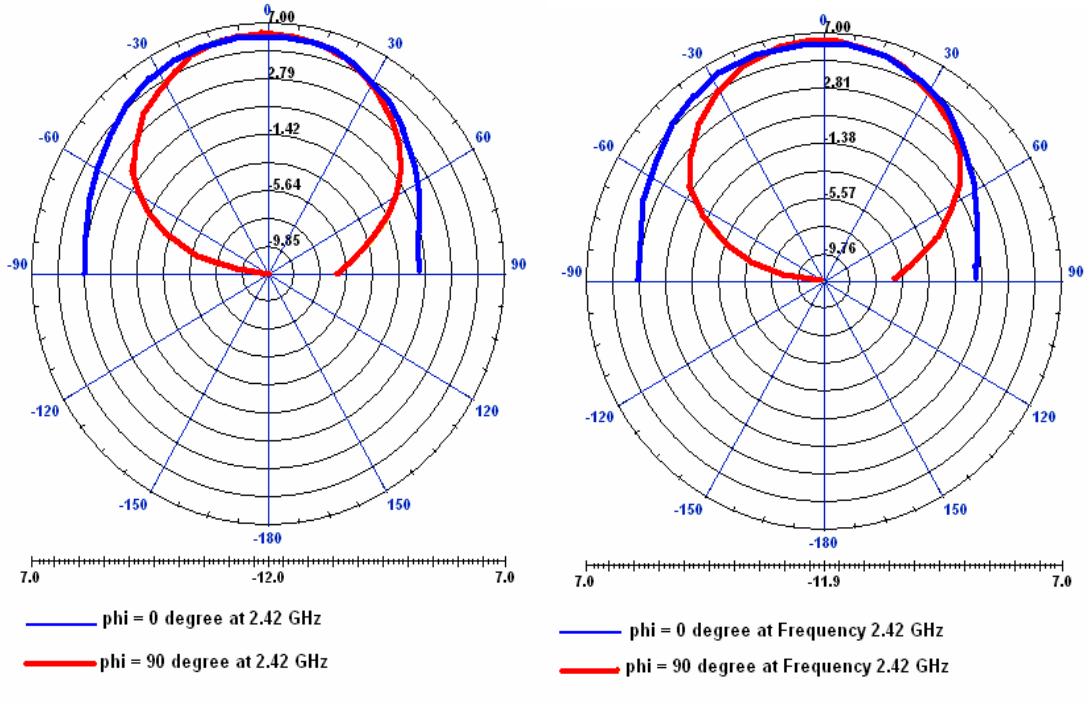

(a) (b)

Figure 6.10 (a) Directivity (Polar form) of GA optimized MSA, (b) Gain (Polar form) of GA optimized MSA

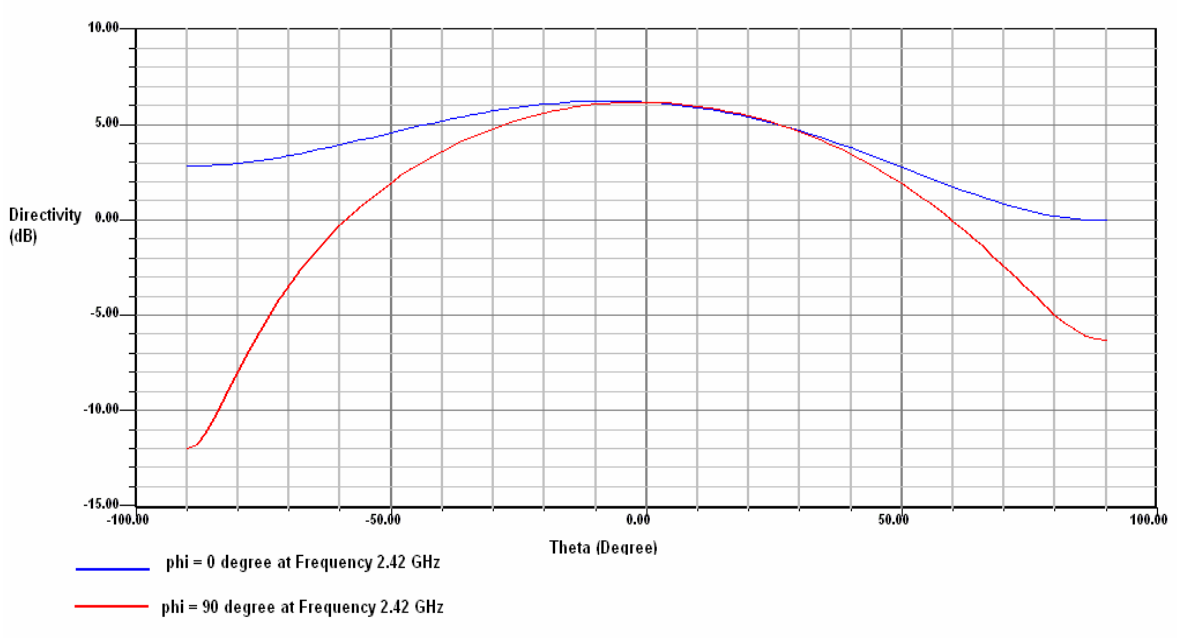

Figure 6.11 Directivity (Rectangular form) of GA optimized MSA

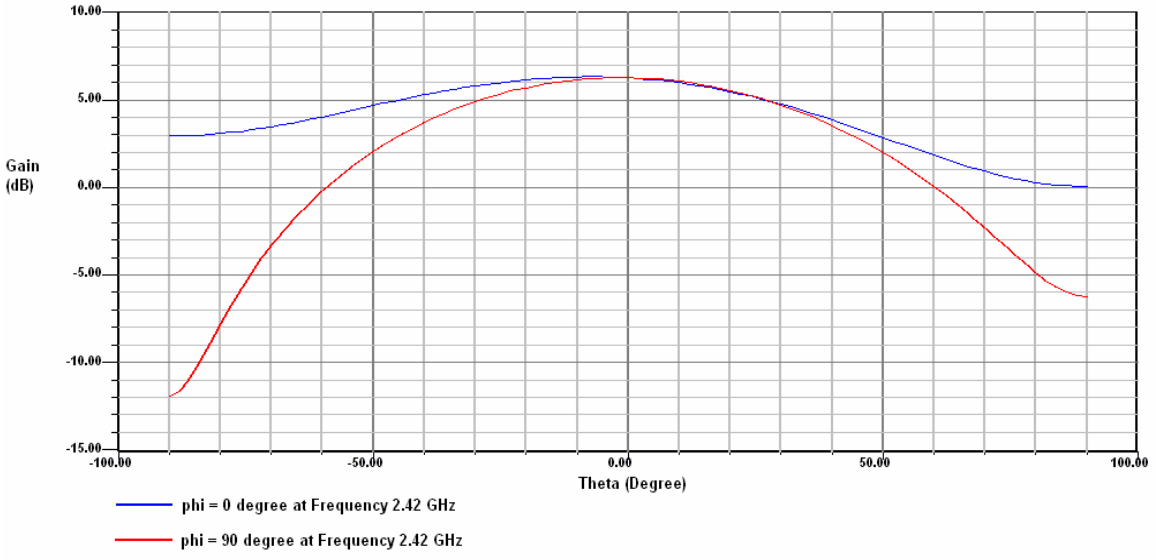

Figure 6.12 Gain (Rectangular form) of GA optimized MSA

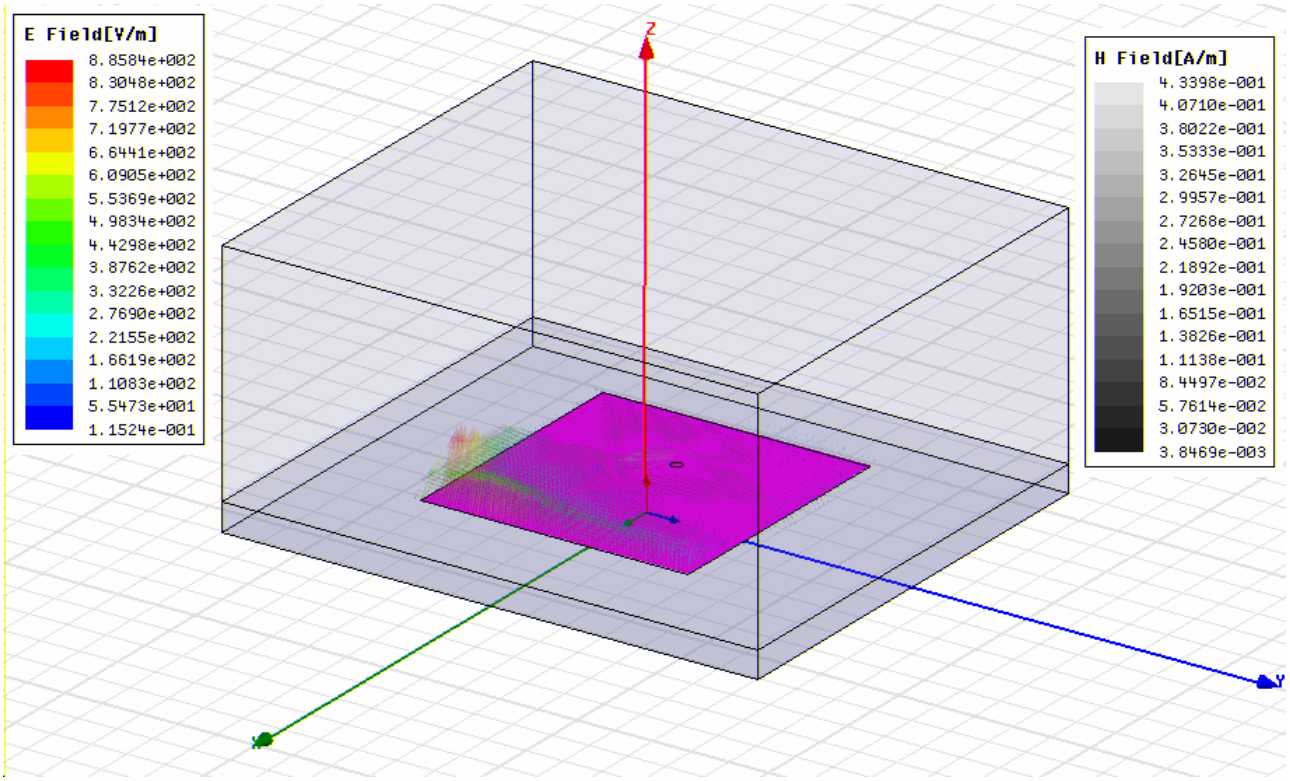

Figure 6.13 E-field and H-field direction and measurement of GA optimized MSA

CHAPTER 7

PARAMETRIC STUDY OF RECTANGULAR MICROSTRIP ANTENNA AT 7.5 GHz FREQUENCY

7.1 Introduction:

For the fundamental TM_{10} mode, we apply 7.5 GHz as resonant frequency to design an RMSA. So, the wavelength of the resonant frequency is 40 mm. As 10:1 dielctric (3.16:1 refractive index) ratio would satisfy the index requirement and form a broad bandgap, we select Rogers RT/duroid 6010 substrate with relative permittivity 10.2.

Used mode: TM_{10}
Resonant frequency, f_0 = 7.5 GHz,
Wavelength, λ_0 = 40 mm.
Relative Permittivity, ε_r =10.2
Line Impedance = 50 Ω
Polarization = Linear
Velocity of light, c = $3\times10^8 m/\sec$

7.2 Calculation of Substrate Height, h:

With the increase in h, the fringing fields from the edges increase, which increases the extension in length L and hence the effective length, thereby decreasing the resonance frequency. So, to calculate the height of the substrate we have to follow the below equation and our calculation.

$$\frac{h}{\lambda_0} \le \frac{0.3}{2\pi\sqrt{\varepsilon_r}} \qquad \ldots (7.1)$$

$$h \le \frac{0.3\lambda_0}{2\pi\sqrt{\varepsilon_r}}$$

$$h \le \frac{0.3\times0.12m}{2\pi\sqrt{2.2}}$$

$h \leq 0.6mm.$

So, for broadbanding our RMSA design criteria, the height of the substrate should not be larger than 0.6 mm. We consider 0.6 mm to design the RMSA.

7.3 Calculation of Patch Width, W:

For the RMSA,the width is much smaller than the wavelength. If W is smaller, then the BW and gain will decrease. If W is larger, then the BW increases due to the increase in the radiated fields. The directivity also increases due to the increase in the aperture area. However, if W is too large, then the higher order modes could get excited. The following equation helps us to calculate our width of the RMSA.

$$W = \frac{c}{2 f_0 \sqrt{\frac{\varepsilon_r + 1}{2}}} \qquad \ldots (7.2)$$

$$W = \frac{3 \times 10^8 m/\sec}{2 \times 2.5 \times 10^9 \sqrt{\frac{2.2+1}{2}}}$$

$$W = 8.489mm \approx 8.5mm$$

Therefore, we take the width of the RMSA approximately 8.5 mm.

7.4 Calculation of Substrate's Effective Permittivity, ε_e :

The value of εe is slightly less than εr, because the fringing fields around the periphery of the patch are not confined in the dielectric substrate but are also spread in the air. For quick analysis or design of our RMSA, the following approximate formula for εe could be used:

$$\varepsilon_e = \frac{\varepsilon_r + 1}{2} + \frac{\varepsilon_r - 1}{2}\left[1 + \frac{10h}{W}\right]^{-1/2} \qquad \ldots (7.3)$$

$$\varepsilon_e = \frac{2.2+1}{2} + \frac{2.2-1}{2}\left[1 + \frac{10 \times 0.38cm}{4.7cm}\right]^{-1/2}$$

$$\varepsilon_e = 9.122$$

7.5 Calculation of Patch Length, L: for TM_{10} mode, m=1 and n=0

For the fundamental TM_{10} mode, the length L should be slightly less than λ/2, where λ is the wavelength in the dielectric medium. The following formula is very effective to calculate the length of the RMSA.

$$f_0 = \frac{c}{2\sqrt{\varepsilon_e}}\left[\left(\frac{m}{L}\right)^2 + \left(\frac{n}{W}\right)^2\right]^{1/2} \qquad \ldots (7.4)$$

$$2.5\times10^9 = \frac{3\times10^8\, m/\sec}{2\sqrt{2.05}}\left[\left(\frac{1}{L}\right)^2 + \left(\frac{0}{W}\right)^2\right]^{1/2}$$

$$L = 6.622mm \approx 6.6mm$$

Therefore, we take the length of the RMSA approximately 6.6 cm.

7.6 Conventional MSA configuration:

So, from the above equations and calculations we have a RMSA configuration which is tabulated below:

TABLE 7.1 CONVENTIONAL MSA CONFIGURATION

Parameter	**Value**
Height, h	0.6 mm
Width, W	8.5 mm
Length, L	6.6 mm
Relative Permittivity, Rogers RT/duroid 6010	10.2
Feedline*	32.6 mm
Feed width*	2.6 mm

* The values of feedpoint and feed radius has been taken from the parametric study of RMSA of "Compact and Broadband Microstrip Antenna" by Girish Kumar and K.P. Ray.

7.7 Conventional MSA Design in HFSS:

Designing a patch to resonant at a particular frequency involves only a few steps when using a simulation tool, such as Ansoft High Frequency System Simulator (HFSS). The four main design parameters for a microstrip patch antenna are the width and length

of the patch, and the height and permittivity of the dielectric. The model for the patch antenna is created in HFSS, with the correct dielectric height, permittivity, and substrate dimensions. The patch antenna is then drawn on the substrate with the width and length dimensions of half a wavelength as mentioned previously. The patch will then be tuned to produce the exact input impedance, radiation patterns and gain that are needed for the design.

Here, in HFSS modeling 7.5 GHz resonance is examined. The substrate dimensions are 72 mm by 96 mm, with the thickness of 0.6 mm, a permittivity 10.2 and a loss tangent 0.0023. The substrate is based on the infinite ground plane on 72 mm x 96 mm platform. The patch dimensions are 6.6 mm x 8.5 mm and an air-box surrounding the antenna providing a radiation boundary is 72 mm x 96 mm x 10.6 mm. The patch is fed by a microstrip feed-line which is excited by a lumped port of 32.6 mm by 2.6 mm and directly unite to patch from its source with an impedance of 50 Ω. Both patch and the feed-line is made of 'pec' substrate with bulk conductivity 1e+030 Siemens/m.

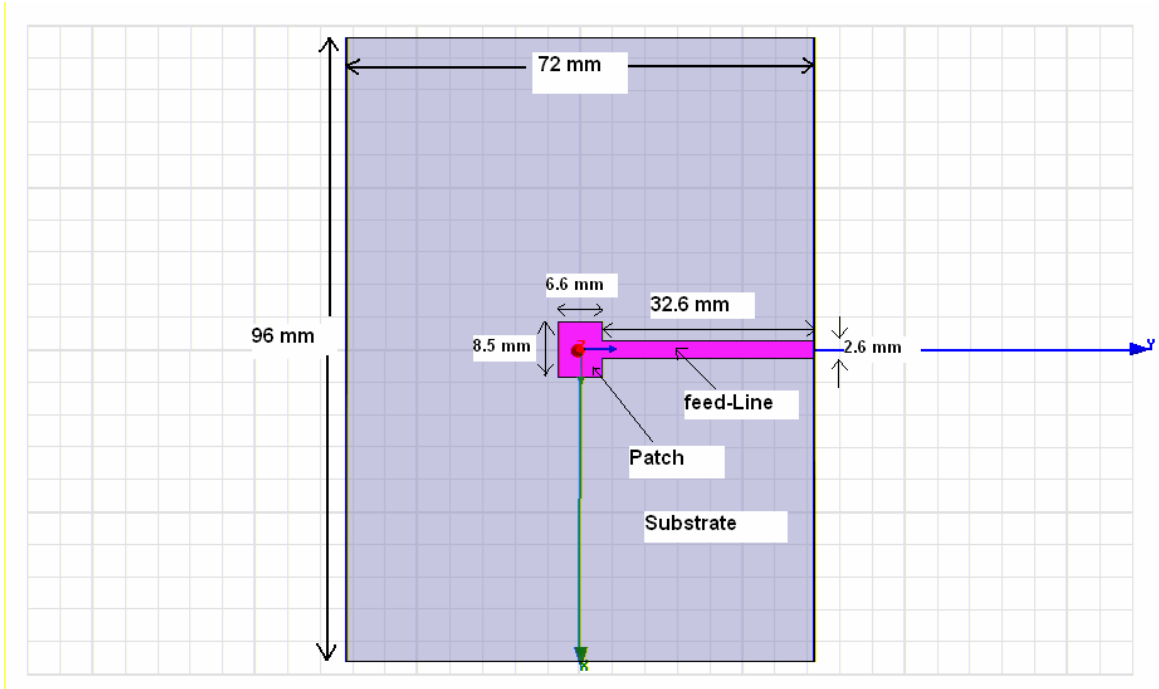

Figure 7.1 Top View of Conventional MSA

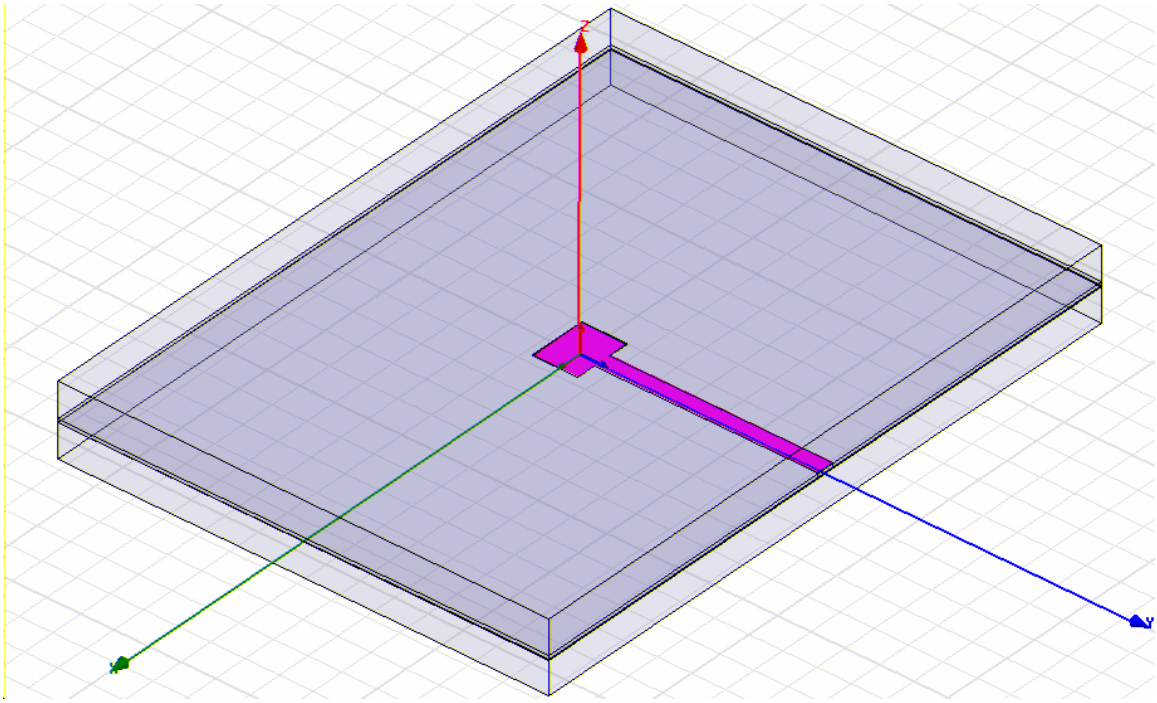

Figure 7.2 3D View of Conventional MSA

7.8 Output of Conventional MSA:

From frequency sweep, in Figure 7.3, plotting the S_{11} versus frequency reveals the 7.42 GHz resonance at a return loss of -11.75dB. If we consider the return loss of -6dB we get 190MHz bandwidth and if we consider the return loss of -10dB we get 80MHz bandwidth from the conventional patch antenna design.

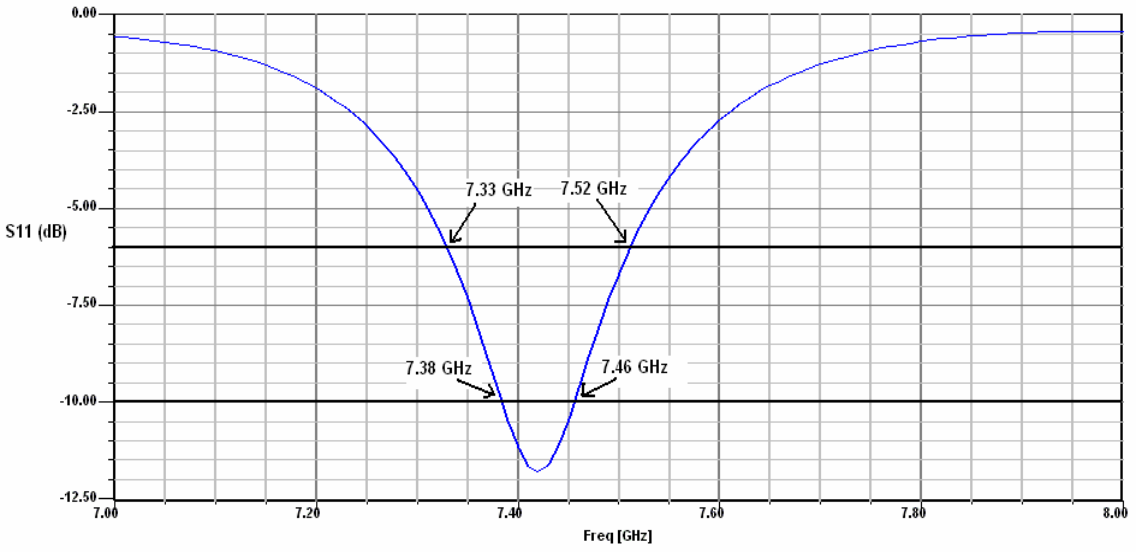

Figure 7.3 S_{11} – Freq Graph of Conventional MSA

The S_{11} is plotted on the Smith Chart in figure 7.4, and the frequency where the impedance becomes purely resistive is the resonant frequency of the patch. Figure 7.4 also shows the VSWR is 1.692 and the Q factor is 0.396. The impedance of the antenna is 1.318+j0.522. Table 7.1 shows the gradual change in S_{11} in polar form, impedance plane, admittance plane, Q factor and VSWR with respect to different frequencies.

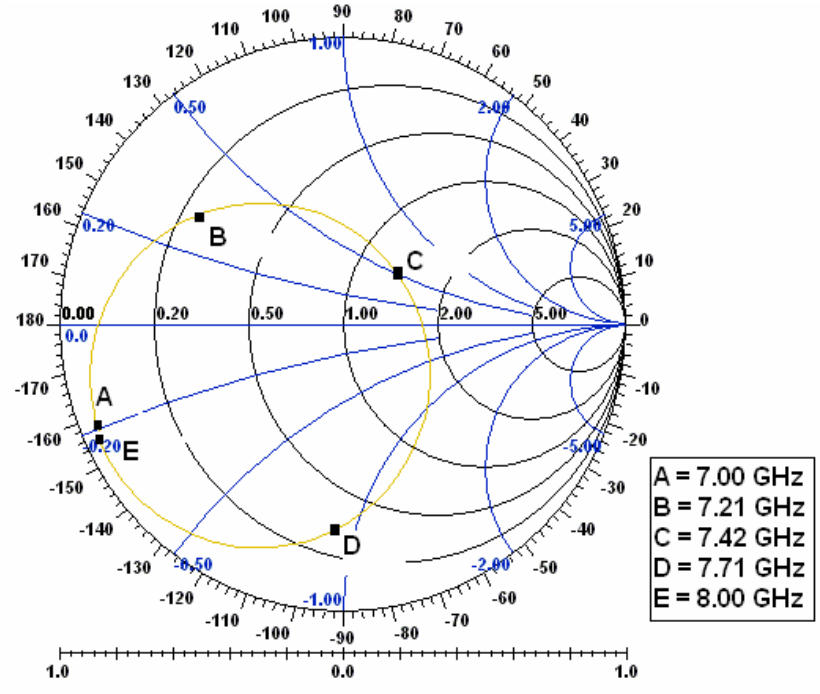

Figure 7.4 Smith Chart of Conventional RMSA

TABLE 7.1. SMITH CHART RESULT FOR VARIOUS FREQUENCIES OF THE CONVENTIONAL RMSA

Frequency (GHz)	**7**	**7.21**	**7.42**	**7.71**	**8**
Reflection co-eff (Polar form)	0.93 ∠ -158.1^0	0.65 ∠ 145.1^0	0.26 ∠ 45^0	0.7 ∠ -91.84^0	0.95 ∠ -156^0
Impedance plane	0.038-J0.19	0.228+j0.3	1.396+j0.522	0.33-j0.911	0.027-j0.212
Admittance plane	0.977+j4.978	1.61-j2.11	0.65-j0.257	0.353+j0.968	6.59+j4.634
Q factor	5.094	1.314	0.396	2.741	7.858
VSWR	27.323	4.804	1.707	5.662	38.676

It is noticed that in Figure-7.5,7.6 and 7.7 E-plane (Red) cuts for conventional

antennas are asymmetrical and the broader compared with the H-plane (Blue) cuts. There are also more peaks in E-plane cuts due to the radiation from the feedline. Both gain and directivity of the conventional RMSA is 21 dBi .

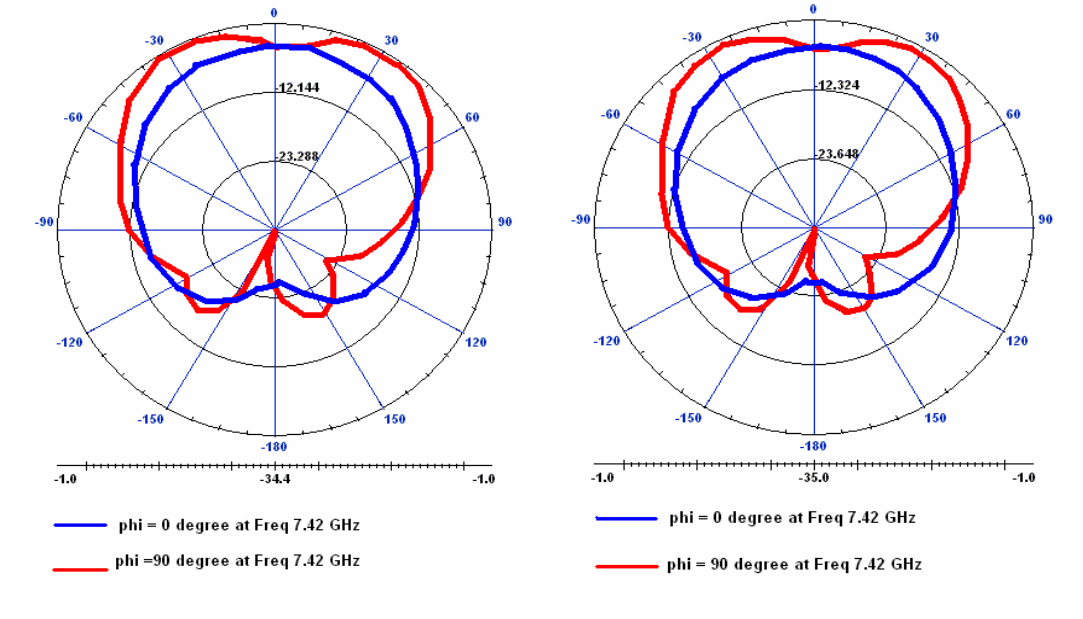

(a) (b)

Figure 7.5 (a) Directivity (H-plane in blue and E-plane in red) of conventional RMSA at 7.42 GHz (b) Gain (H-plane in blue and E-plane in red) of conventional RMSA at 7.42 GHz

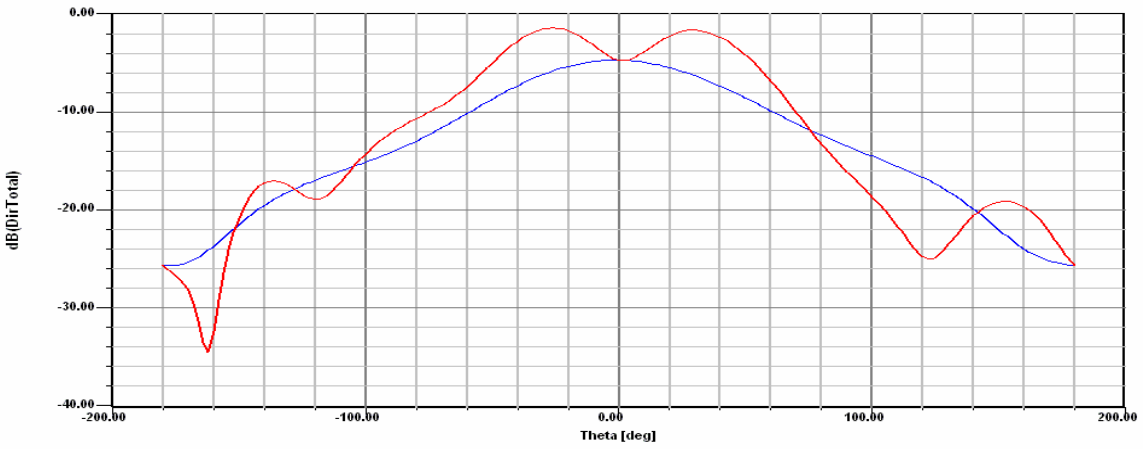

Figure 7.6 Directivity (H-plane in blue and E-plane in red) of conventional RMSA at 7.42 GHz

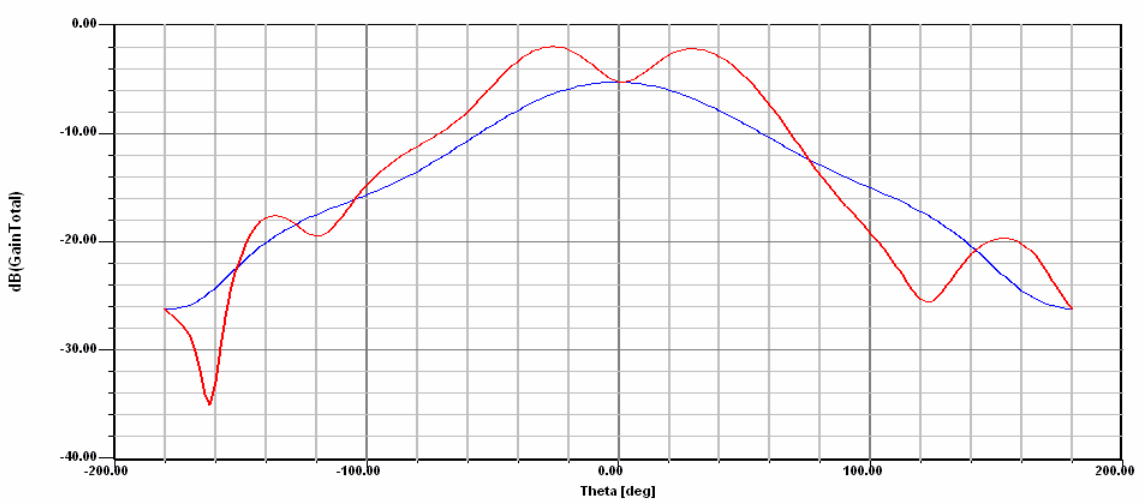

Figure 7.7 Gain (H-plane in blue and E-plane in red) of conventional RMSA at 7.42 GHz

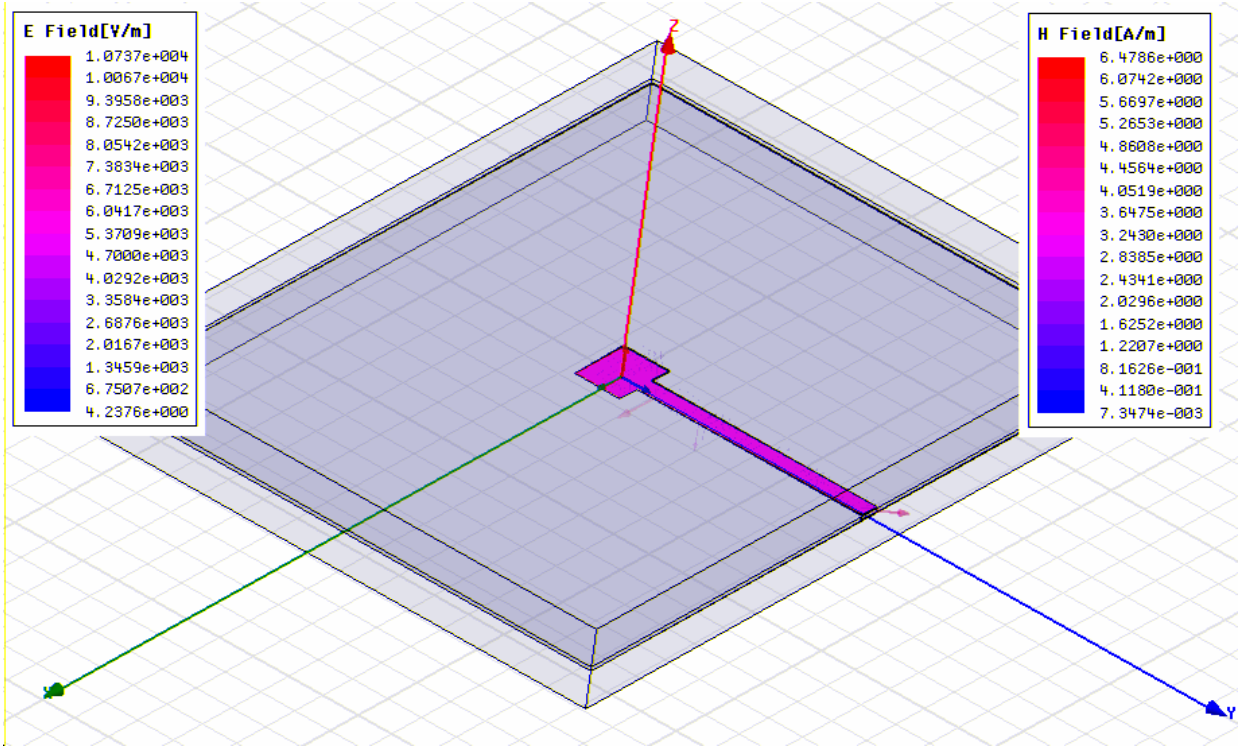

Figure 7.8 E-field and H-field direction and measurement of Conventional RMSA

CHAPTER 8

PHOTONIC BANDGAP SUBSTRATES AND MICROSTRIP PATCH ANTENNA

8.1 Introduction

The birth of the photonic band gap structure has triggered many novel antennas applications. Two commonly employed features are suppressing unwanted substrate modes and acting as an artificial magnetic ground plane. Today, many antennas are required to be small and broadband. Conventionally, in order to achieve small size and broadband operation patch antenna are fabricated on a thick piece of high permittivity substrate. There are two major disadvantages in this, firstly, the higher the relative permittivity of a material the more costly it would be. Second, unwanted substrate modes begin to form and propagate towards the edges of the substrate, which have a deleterious effect on the antenna radiation pattern. One can expect an increase in back radiation level, distortion of the main lobe and side lobes appearing.

In the 1990s, researches suggested the introduction of a photonic band gap structure into the printed antenna substrate, which saw the capability of removing unwanted substrate modes. This PBG substrate consists of the periodic arrangement of air-columns. The effectiveness of the perforated structure relies on the high refractive index contrast between the air-columns and the relative permittivity of the dielectric material and the type of the lattice to use. For broadband and small volume mobile communication applications, the honeycomb-lattice was shown to be of good potential.

8.2 Formation of surface wave (surface plasmon)

As a patch antenna radiates, a portion of the total available power for direct radiation becomes trapped along the surfaces of the substrate. This trapped electromagnetic energy leads to the development of surface waves. In fact, the ratio of power that radiates into the substrate compared to the power that radiates into air is

approximately $(\varepsilon^{3/2}:1)^{5}$. This is governed by the rules of total internal reflection, which state that any field line radiated into the substrate at angles greater than the critical angle ($\theta_c = \sin^{-1}(\varepsilon^{-1/2})$) are totally internally reflected at the top and bottom surfaces. This is illustrated in Figure 3.1. Therefore, for a substrate with dielectric constant $\varepsilon = 10.2$, nearly 1/3 of the total radiated power is trapped in the substrate with critical angle of roughly 18.2 degrees.[18]

Surface wave effects can be eliminated by using cavities or stacked substrate techniques. However, this has the fundamental drawback of increasing the weight, thickness, and complexity of the microstrip antenna, thus negating many of the advantages of using microstrip antennas. These complications and others prevent microstrip antennas from becoming the standard in the microwave telecommunications community.

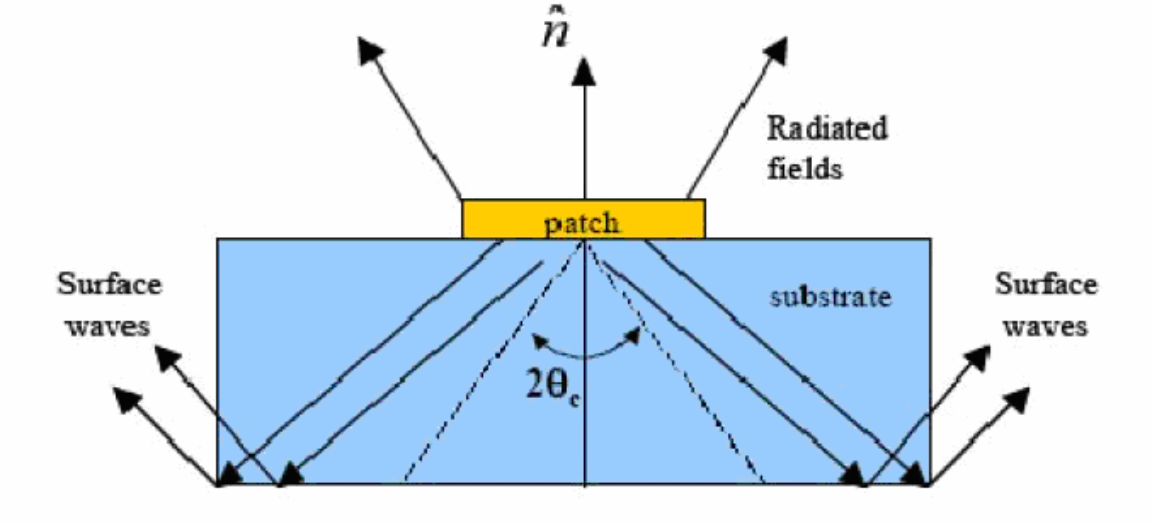

Figure 8.1 Field lines radiating from a patch antenna; illustrates the formation of surface waves

8.3 Photonic Band Gap Structure

The first PBG structure conceptualized and manufactured was in 1991 by Eli Yablonovitch, then at Bell Communications Research in New Jersey. Yablonovitch fabricated the crystal structure by mechanically drilling holes a millimeter in diameter into a high dielectric constant material as shown in Figure 3.2. This patterned material, which became known as "Yablonovitch" prevented incident microwave signals from propagating in any direction along a unit sphere – in other words, it exhibited a 3-D band

gap. This structure has become the cornerstone for much of the researcher in this area with applications still in use today.

In most communication applications, however, the use of Yablonovitch is not practical. The three dimensional nature of the band gap rejects incident energy from all directions around a unit sphere, making it better suited as a high efficiency reflector or mirror. Instead, in a 2-D photonic crystal, the band gap exists only within a plane, thereby allowing propagation along one axis of the crystal. This is the ideal scenario for microstrip antenna designs, since the "rejection plane" could be in the plane of the patch to prevent surface wave's formation. An example of a 2-D photonic crystal is a triangular lattice, as shown in figure 8.3.

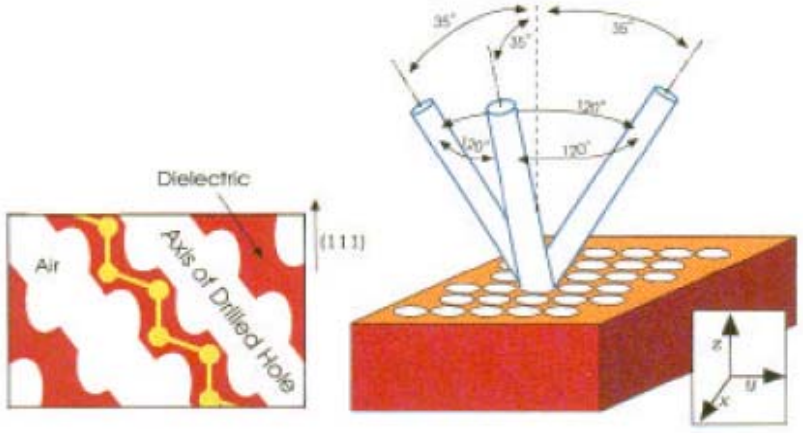

Figure 8.2 Technique used to fabricate the first 3D PBG structure, the Yablonovite

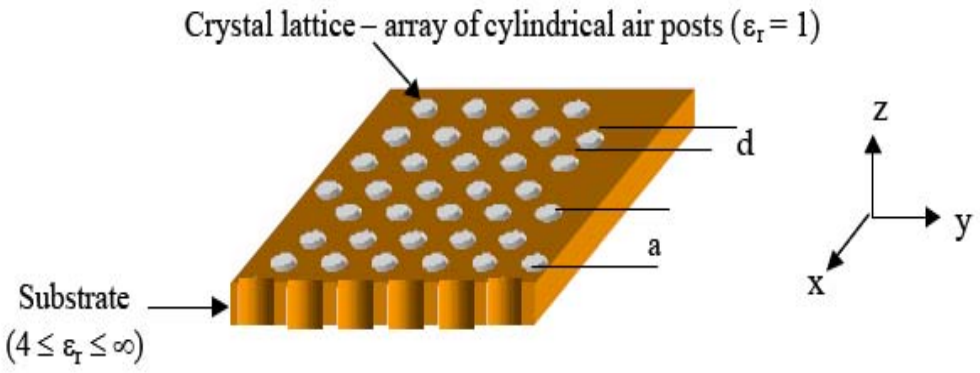

Figure 8.3 2D photonic crystal structure patterned with a triangular crystal lattice: the crystal lattice is a cylindrical air posts in a high dielectric substrates

A photonic crystal essential behaves much like a band-stop filter, rejecting the

propagation of energy over a fixed band of frequencies. However, once a defect is introduced such that it disrupts the periodicity in the crystal, an area to localize or "trap" electromagnetic energy is established. In this region, a pass-band response is created. This ability to confine and guide electromagnetic energy has several practical applications at microwave frequencies as filters, couplers, and especially antennas.

This rather simple concept of placing defects in a photonic crystal structure introduces a new methodology in the design of microstrip (patch) antennas. The idea is to design a patch antenna on a 2D photonic crystal substrate, where the patch becomes the "defect" in the crystal structure, as shown in figure 8.4. In this case, crystal arrays of cylindrical air holes are patterned into the dielectric substrate of the patch antenna. By not patterning the area under the patch, a defect is established in the photonic crystal, localizing the EM fields. Surface waves along the XY plane of the patch (Figure 8.4) are forbidden from forming due to the periodicity of the photonic crystal in that plane. This prevention of surface waves improves operational bandwidth and directivity, all while reducing side lobes and coupling, which commonly concerns in microstrip antenna designs.

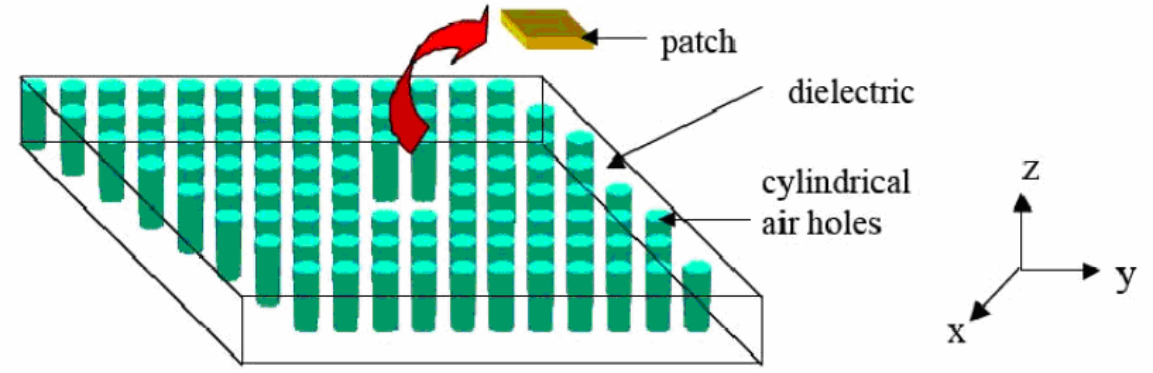

Figure 8.4 Illustration of a patch designed on a photonic crystal substrate

Although "photonic" refers to light, the principle of "band gap" applies to electromagnetic waves of all wavelengths. Consequently, there is a controversy in the microwave community about the use of the term "Photonic", and the name Electromagnetic band gap (EBG) material or Electromagnetic crystal is being proposed.

8.4 Unit cell of Photonic Crystals

As stated in the American Heritage Dictionary, a crystal is "a homogenous solid formed by a repeating, 3-D pattern of atoms, molecules or shapes, having fixed distances between constituent parts". This replicating pattern is reffered to as the unit cell of a crystal. Figure illustrates the unit cell for the triangular crystal lattice. The unit cell contains all the pertinent information of the crystal such as the crystal geometry (shape, thickness etc.), material properties (dielectric or magnetic), and the lattice spacing (shown as the dimension, lattice constant, 'a' in the figure) of each individual atom or molecule. It is this replicating unit cell that provides the periodicity in the crystal and controls the location and extent of the bandgap.

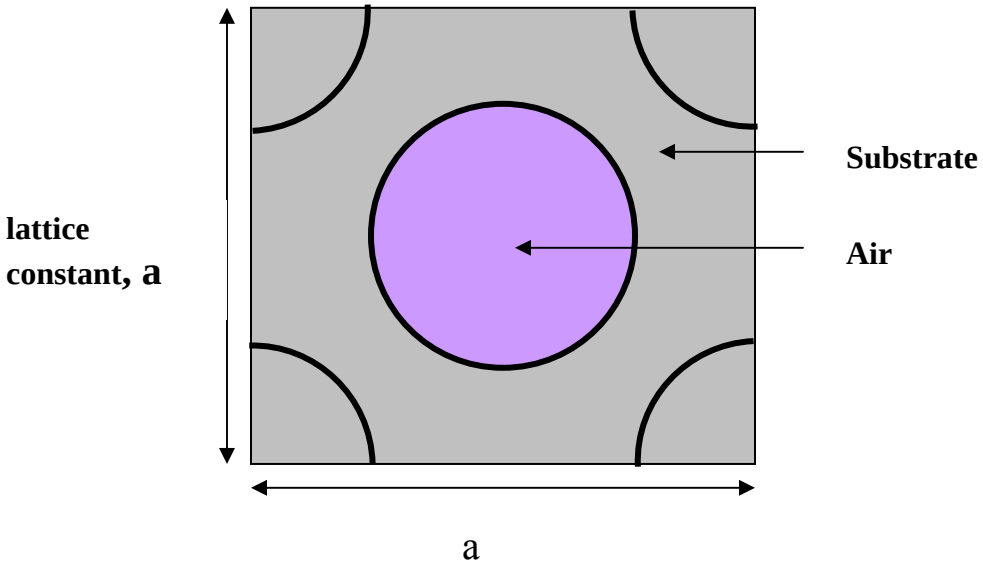

Figure 8.5 Top view of the unit cell of triangular crystal lattice

8.5 The Bandgap

As a first order approximation, a bandgap is obtainable in a high dielectric material with integrated photonic crystals when an incident electromagnetic field propagates with a guide-wavelength approximately equal to the lattice spacing of the crystal [30]. This rough approximation locates the center of the bandgap, which can be higher than ±10% of the center frequency for high index materials.

Indeed, the formation of the bandgap is dependent on the periodicity of the crystal, but it is also heavily dependent on the refractive index (dielectric constant) ratios between the base material (the substrate) and the impurities that form the crystal. Typically, the refractive index ratio must be atleast 2:1 (substrate-to-impurity) ratio for the bandgap to exist [29]. For the 2-D triangular structure, the broadest bandgap is obtainable when the impurities (the cylindrical post) are of air (ε_r =1), while the base material is a high dielectric constant (for example, ε_r =10). A 10:1 dielctric (3.16:1 refractive index) ratio would satisfy the index requirement and form a broad bandgap, with proper crystal spacings. This explains the need for a high dielectric substrate for a patch antennas designed on a photonic crystal substrate.

8.6 Translight 3.01b (Bandgap Analysis Software)

Numerical evaluation of the location and extent of the bandgap is performed using software called Translight©, a shareware graphic-user interface (GUI) distributed through the Department of Electronics & Electrical Engineering at the University of Glasgow. It was developed by Dr. Andrew L. Reynolds of the same department of the University of Glasgow. The code uses user definable “building blocks” or the unit cells, which are cascade in any direction to form photonic crystals. The software computes the reflection and transmission coefficients as electromagnetic signals are applied, at multiple angles of incidence, to the photonic crystal and output the size of the crystal. Figure 8.6, 8.7 and 8.8 illustrates the input windows of Translight 3.01b.

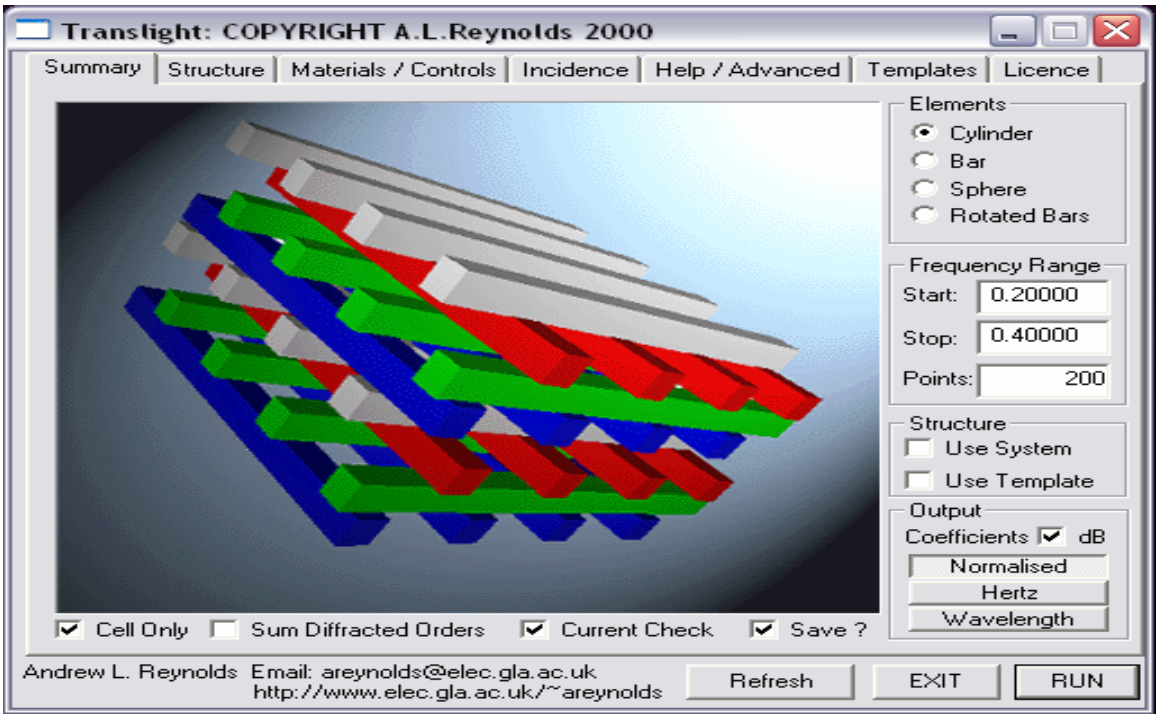

Figure 8.6 Translight Input Summary

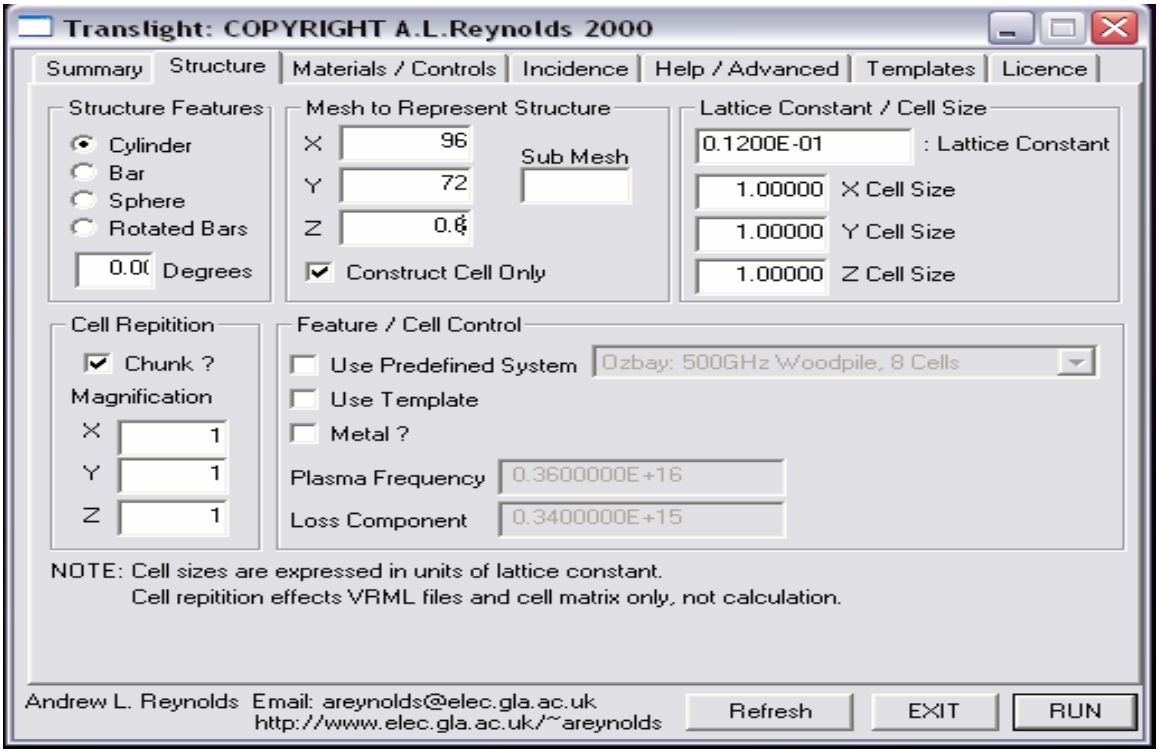

Figure 8.7 Translight Input Structure

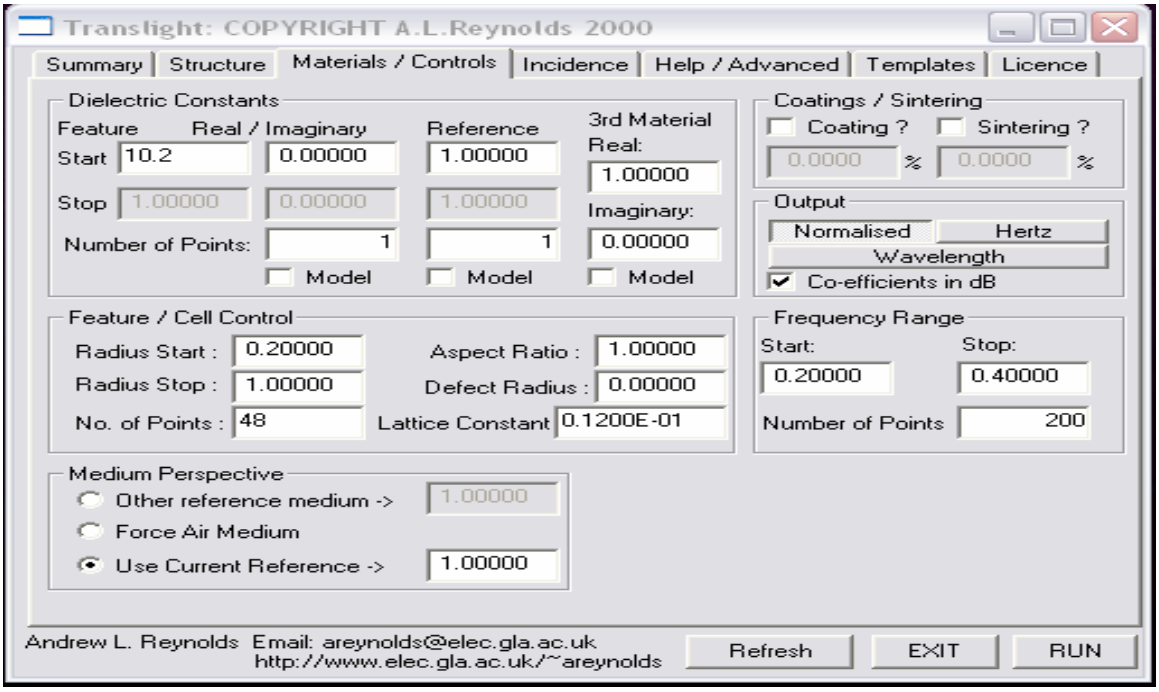

Figure 8.8 Translight Material Input

8.7 MSA on PBG Structure Design in HFSS

Here a microstrip patch antenna is designed on a 2-D single-period PBG structure. The PBG layer is sandwiched between the patch and the ground plane, as shown in Figure 3.5. The patch antennas on the single period PBG structure were evaluated using the HFSS. The conventional patch antenna, which is designed for comparison with the proposed patch antenna on the sandwiched single-period PBG, is shown in Figure 3.5(a). Here, in HFSS modeling 7.5 GHz resonance is examined. The substrate dimensions are 72 mm by 96 mm, with the thickness of 0.6 mm, a permittivity 10.2 and a loss tangent 0.0023. The substrate is based on the infinite ground plane on 72 mm x 96 mm platform. The patch dimensions are 6.6 mm x 8.5 mm and an air-box surrounding the antenna providing a radiation boundary is 72 mm x 96 mm x 10.6 mm. The patch is fed by a microstrip feed-line which is excited by a lumped port of 32.6 mm by 2.6 mm and directly unite to patch from its source with an impedance of 50 Ω. Both patch and the feed-line is made of ‘pec’ substrate with bulk conductivity 1e+030 Siemens/m. From the Translight 3.01b software we get the size of the cylindrical crystal is stated below:

Lattice Constant, a = 12 mm

Crystal diameter, d = 6 mm

Crystal height = 0.59 mm

Number of the crystal = (8 x 6 =) 48

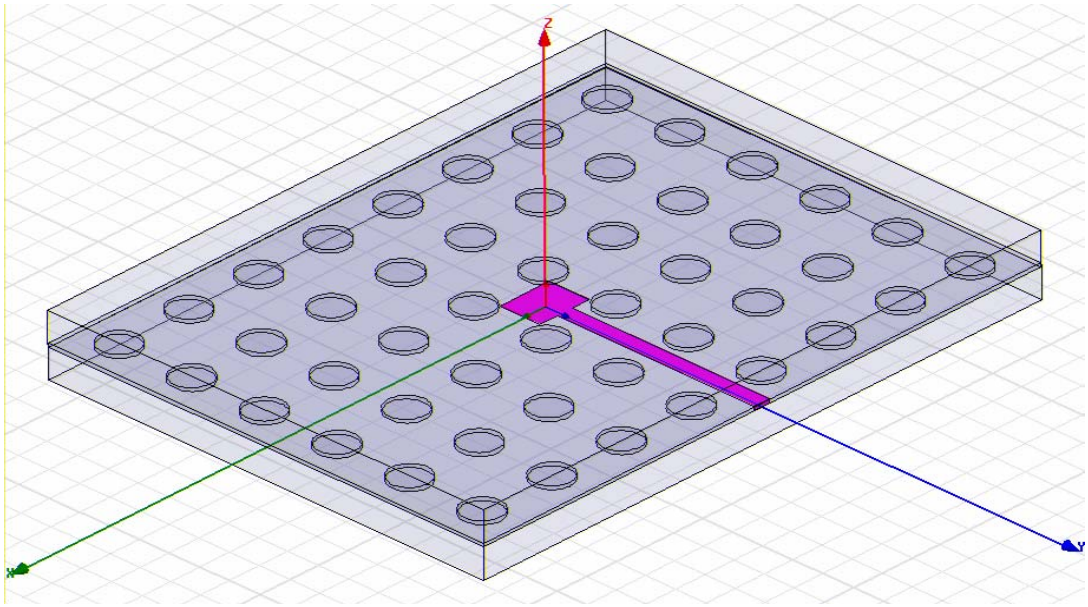

Figure 8.9 3D View of PBG structured MSA

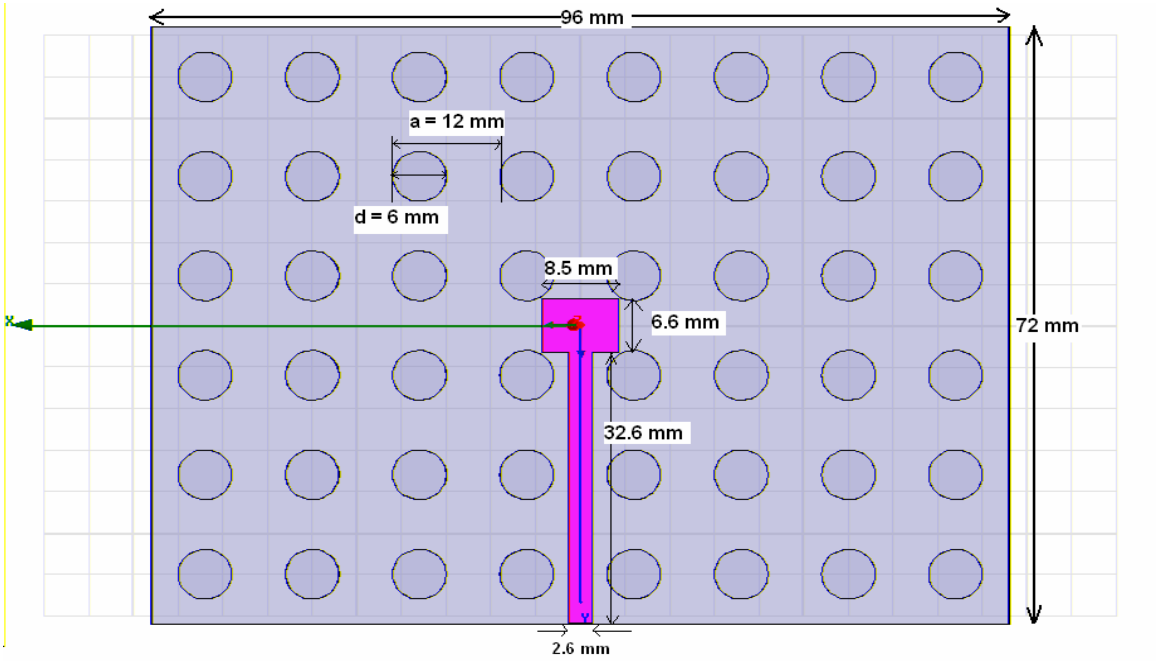

Figure 8.10 Top View of PBG structured MSA

8.8 Output of PBG structured MSA:

From frequency sweep, in Figure-7.3, plotting the S11 versus frequency reveals the 7.20 GHz resonance at a return loss of -27dB. If we consider the return loss of -6dB we get 220MHz bandwidth and if we consider the return loss of -10dB we get 140MHz bandwidth and if we consider the return loss of -20dB we get 40MHz bandwidth from the PBG structured patch antenna design.

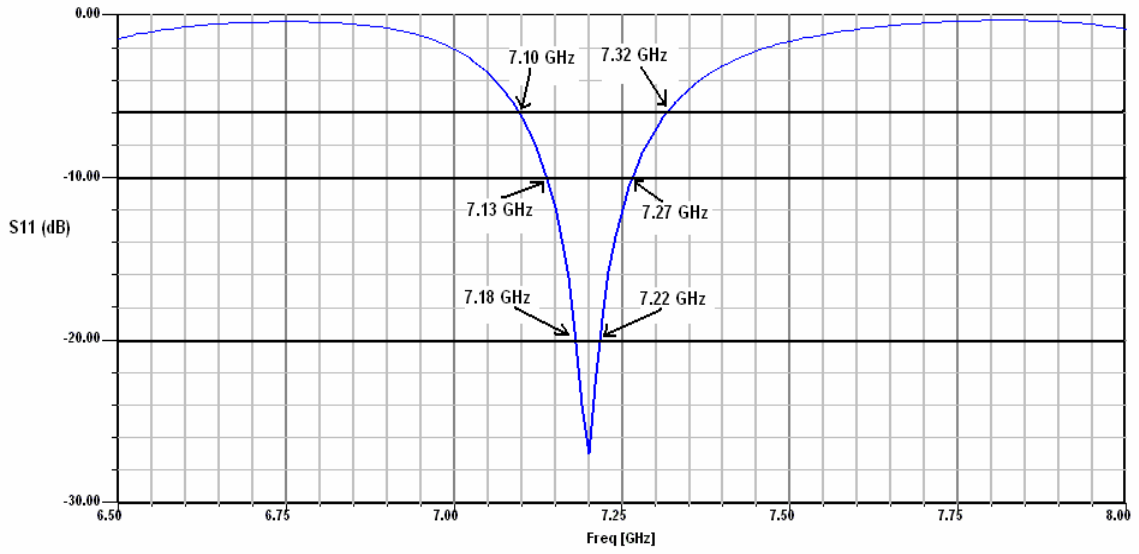

Figure 8.11 S_{11} – Freq Graph of PBG structured MSA

The S_{11} is plotted on the Smith Chart in figure 8.12, and the frequency where the impedance becomes purely resistive is the resonant frequency of the patch. Figure8.12 also shows the VSWR is 1.093 and the Q factor is 0.011. The impedance of the antenna is 1.092+j0.012. Table 7.1 shows the gradual change in S_{11} in polar form, impedance plane, admittance plane, Q factor and VSWR with respect to different frequencies.

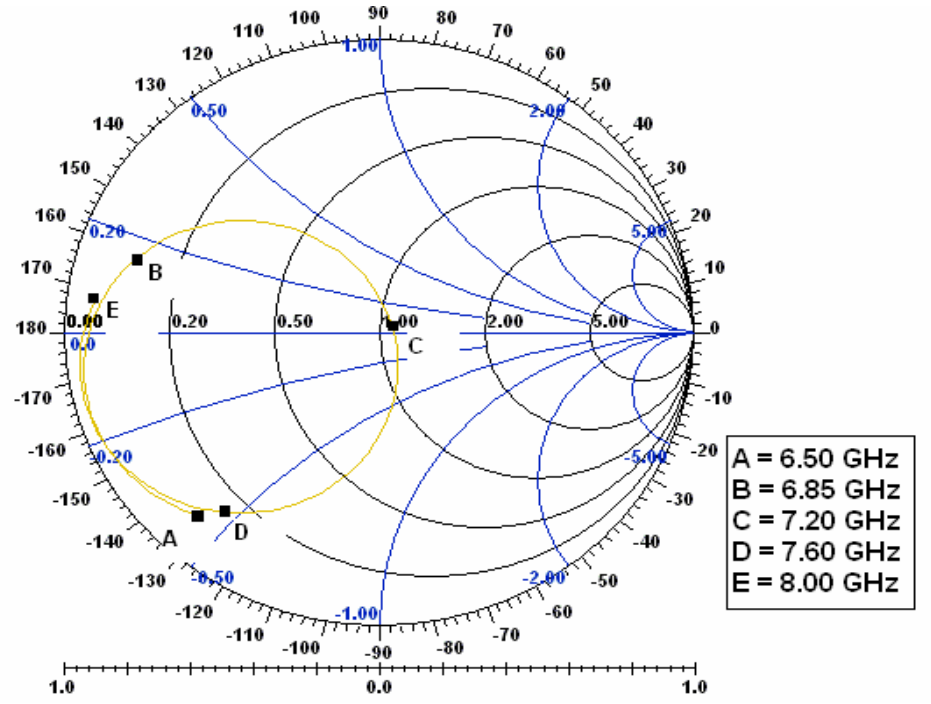

Figure 8.12 Smith Chart of PBG structured MSA

TABLE 8.1. SMITH CHART RESULT FOR VARIOUS FREQUENCIES OF THE PBG STRUCTURED MSA

Frequency (GHz)	**6.5**	**6.85**	**7.2**	**7.6**	**8**
Reflection co-eff (Polar form)	$0.85 \angle -132.9^0$	$0.825 \angle 163^0$	$0.045 \angle 6.9^0$	$0.79 \angle -129.5^0$	$0.91 \angle 172.59^0$
Impedance plane	0.101-j0.43	0.098+j0.148	1.092+j0.012	0.142-j0.463	0.045+j0.064
Admittance plane	0.516+j2.206	3.122-j4.706	0.915-j0.01	0.605+j1.973	7.307-j10.439
Q factor	4.275	1.507	0.011	3.262	1.428
VSWR	11.798	10.439	1.093	8.578	22.311

It is noticed that in Figure-8.11, 8.12 and 8.13 E-plane (Red) cuts for PBG structured antennas are asymmetrical and the broader compared with the H-plane (Blue) cuts. There are also more peaks in E-plane cuts due to the radiation from the feedline. The gain and the directivity of the PBG structured MSA is 21.5 dBi and 21 dBi respectively.

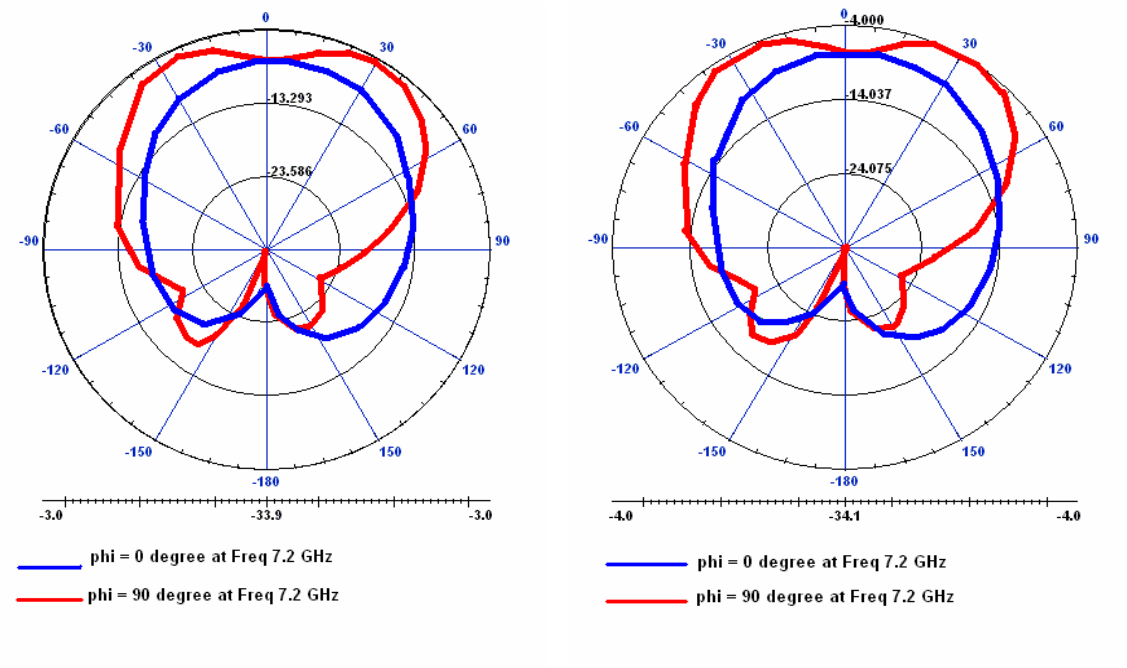

Figure 8.11 (a) Directivity (H-plane in blue and E-plane in red) of PBG structured MSA at 7.2 GHz (b) Gain (H-plane in blue and E-plane in red) of PBG structured MSA at 7.2 GHz

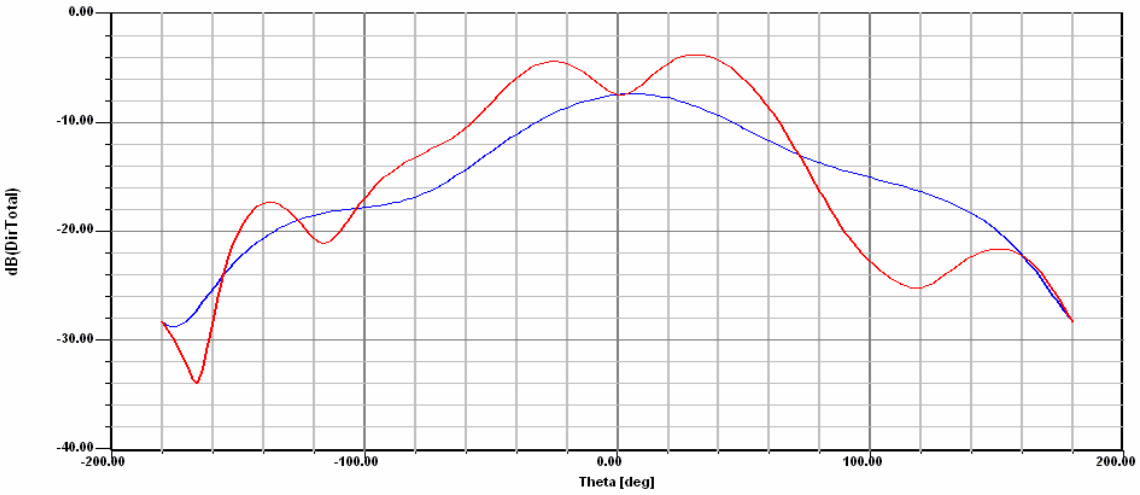

Figure 8.12 Directivity (H-plane in blue and E-plane in red) of PBG structured MSA at 7.2 GHz

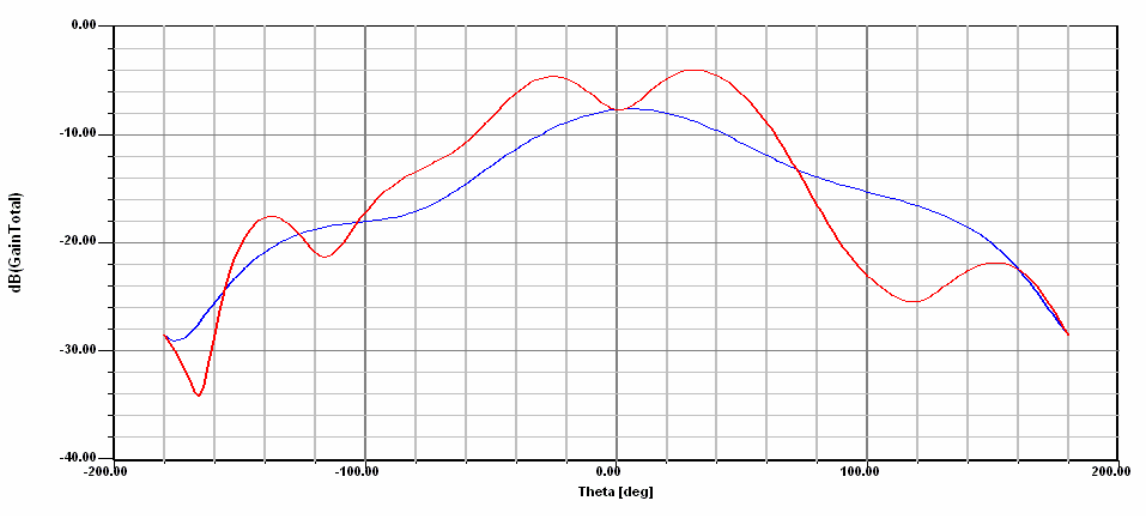

Figure 8.13 Gain (H-plane in blue and E-plane in red) of PBG structured MSA at 7.2 GHz

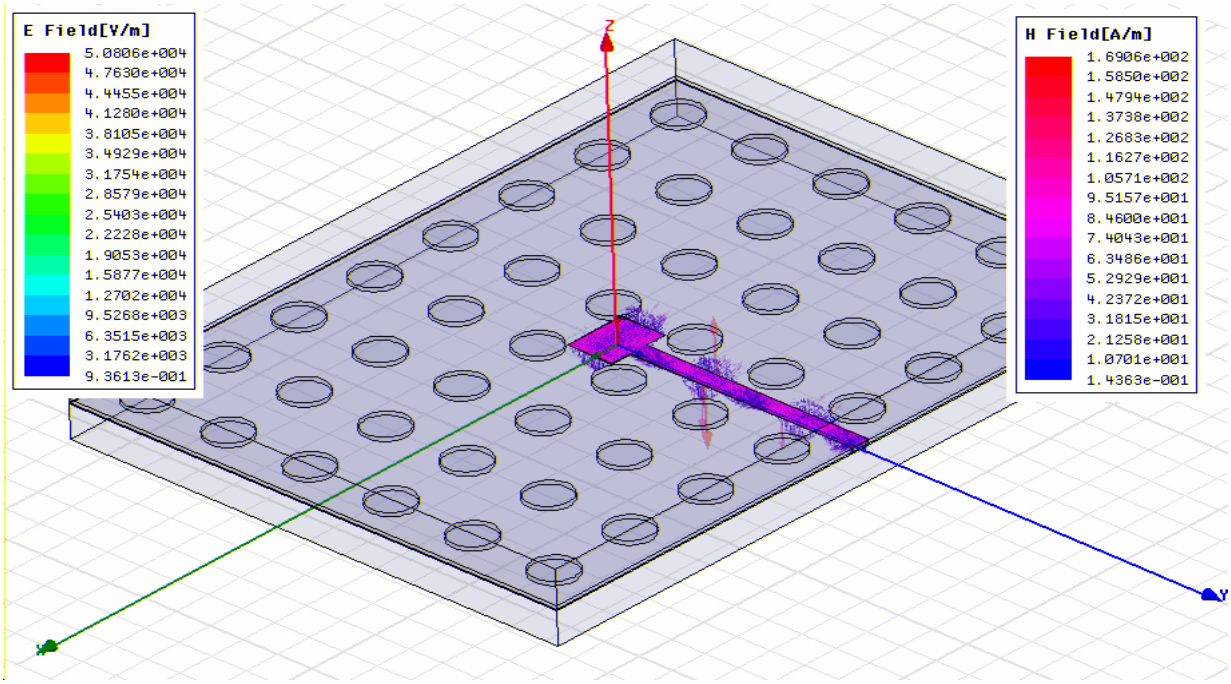

Figure 8.14 E-field and H-field direction and measurement of PBG structured MSA

CHAPTER 9

RESULT ANALYSIS AND DISCUSSION

9.1 Result Analysis and Comparison of GA optimized RMSA

Before start the thesis work result analysis and comparison between GA optimized RMSA and unoptimized RMSA, here is a brief discussion of comparing result analysis which motivate this thesis work successful. In 2005, Gareth Louis Shaw, MSc student of University of the Witwatersrand Johannesburg, South Africa did his research work in GA application in RMSA. He used 2.5 GHz frequency and output is at S_{11}<-6dB 13.2% enhanced bandwidth to unoptimized RMSA and gain is 6.1 dBi with the patch antenna size reduction of 10% [31]. Using the same frequency, in my research work the output is at S_{11}<-6dB is 66.66% enhanced bandwidth and gain is 18.2 dBi with the patch size reduction of 30.55%. The details result is shown in table 9.3.

TABLE 9.1 UNOPTIMIZED MSA CONFIGURATION

Parameter	**Value**
Height, h	0.38cm
Width, W	4.5cm
Length, L	4cm
Relative Permittivity, Rogers RT/duroid 5800	2.2
Feedpoint*	-0.6cm from center of Length
Feed radius*	0.07cm

TABLE 9.2 GA OPTIMIZED MSA CONFIGURATION

Parameter	**Value**
Height, h	0.35cm
Width, W	3.5cm
Length, L	3.5cm
Relative Permittivity, Rogers RT/duroid 5800	2.2
Feedpoint	-0.6cm from center of Length
Feed radius	0.07cm

TABLE 9.3 OUTPUT COMPARISON OF GA OPTIMIZED RMSA AND UNOPTIMIZED RMSA

	Unoptimized at 2.21 GHz	**GA optimized at 2.42 GHz**
BW, S11<-6dB	(2.24-2.18) GHz = 60 MHz	(2.47-2.37)GHz = 100 MHz
BW, S11<-10dB	N/A	(2.44-2.37) GHz = 50 MHz
Directivity	16.8 dBi	18 dBi
Gain	16.5 dBi	18.2 dBi
Q factor	1.078	0.538
VSWR	2.55	1.678
RX (Normalized)	0.687 + j 0.741	0.836 + j 0.45
GB (Normalized)	0.673 – j 0.726	0.928 – j 0.5

Result Analysis:

BW Enhancement, at $\mathbf{S_{11}}$**<-6dB** is **66.66%** and at $\mathbf{S_{11}}$**<-10dB** the GA optimized MSA has **50 MHz** while unoptimized MSA doesn't have that.
Directivity enhancement is **8.93%**
Gain enhancement is **13.64%**
Q factor lowering is **50.1%**
VSWR **1.678** achievement shows a very good impedance matching.

9.2 Result Analysis and Comparison of PBG structured MSA

In 2007, Ainor Khaliah, MSc student of University Technology of Malaysia, did his research work in PBG structured MSA at 7.5 GHz frequency. There his antenna configuration is almost same except the feedline width of 0.6 mm and airhole height and substrate height of 2.5 mm. At S_{11}<-10dB the output is 1.25% bandwidth enhancement than the conventional patch antenna design [32]. Whereas with a 2.6 mm feedline width and 0.6 substrate and airhole height, my thesis result output bandwidth is 75% enhanced than the conventional patch antenna. In table 9.5 the result comparison between conventional and PBG structured MSA is illustrated.

TABLE 9.4 CONVENTIONAL MSA CONFIGURATION

Parameter	**Value**
Height, h	0.6 mm
Width, W	8.5 mm
Length, L	6.6 mm
Relative Permittivity, Rogers RT/duroid 6010	10.2
Feedline	32.6 mm
Feed width	2.6 mm

TABLE 9.5 OUTPUT COMPARISON OF CONVENTIONAL AND PBG STRUCTURED MSA

	Without PBG at 7.42 GHz	**PBG at 7.20 GHz**
BW, S11<-6dB	(7.52-7.33) GHz = 190 MHz	(7.32-7.10) GHz = 220 MHz
BW, S11<-10dB	(7.46-7.38) GHz = 80 MHz	(7.27-7.13) GHz = 140 MHz
BW, S11<-20dB	N/A	(7.22-7.18) GHz = 40 MHz
Directivity	21 dBi	21 dBi
Gain	21 dBi	21.5 dBi
Q factor	0.396	0.011
VSWR	1.692	1.093
RX	1.318 + j 0.522	1.092 + j 0.012

Result Analysis:

BW Enhancement, at **S11<-6dB** is **15.8%** and at **S11<-10dB** is **75%** and at **S11<-20dB** the PBG structured MSA has 4**0 MHz** while without PBG MSA doesn't have that.
Directivity enhancement is **0%**
Gain enhancement is **2.38%**
Q factor lowering is **97.22%**
VSWR **1.692 and 1.093** achievement shows both MSA has a very good impedance matching.

CHAPTER 10

CONCLUSION AND FUTURE WORK

A Genetic Algorithm is successfully applied to a Rectangular Patch Antenna design to enhance the bandwidth with a size reduction of the patch. Patch size reduction upto 30.55% is achieved with the broadband and radiation pattern enhancement. Various other fundamental parameters of MSA is optimized and positively gained. On the otherhand, a novel concept in the development of wideband MSA using PBG structure is introduced and applied. The effort reduces the surface waves which increases bandwidth and lowering VSWR and Q factor.

The following are proposed extensions to the present work concerning wideband patch antenna design:

1. Use Genetic Algorithm to achieve wideband and size reduction in dual-band capabilities and array antenna design.
2. Apply Particle Swarm Optimization (PSO) in MSA.
3. Use different types of Photonic Crystal into the substrate under the patch in MSA.
4. Apply Electromagnetic Band Gap (EBG) structure in MSA design and analysis its effectiveness in bandwidth and directivity enhancement.
5. All the work will be practically implemented and output measured in the Microwave Laboratory.

References:

[1] R. Garg, P. Bhartia, I. Bahl and A. Ittipiboon, “Microstrip Antenna Design Handbook”, Artech House, 2001.

[2] Randy L. Haupt, “Genetic Algorithm in Electromagnetics”, John Wiley and Sons Inc.

[3] Pinaki Mukherjee, Bhaskar Gupta (Jadavpur University, India), “Genetic Algorithm Based Design Optimization of Aperture-Coupled Rectangular Microstrip Antenna”.

[4] Y. W. Jang, " Characteristics of a large bandwidth rectangular microstrip-fed inserted triangular patch in a circular slot antenna", Microwave Journal, vol.45, no.5, pp.288-298, May, 2002.

[5] Yahya Rahmat Samii and J. Michael Johnson (UC-Los Angeles), “Genetic Algorithm in Engineering Electromagnetics”, IEEE Antenna and Propagation Magazine, August-1997.

[6] Y. Horii, and M. Tsutsumi, "Harmonic control by photonic bandgap on microstrip patch antennas," IEEE Microwave and Guided Wave Lett. , vol. 9, No.1, pp. 13-15, Jan.1999.

[7] Y. E. Erdemli, K. Sertel, R. A. Gilbert, D. E. Wright, and J. L. Volakis, "Frequency selective surface to enhance performance of broad-band reconfigurable arrays," IEEE Trans. Antennas Propagat., Vol. 50, No. 12, PP.1716-1724, December 2002.

[8] Jani Ollikainen, “Design and Implemenntation Technique of Wideband Mobile Communications Antennas”, Helsinki University of Technology, Finland.

[9] Amer Md. Alsawadi, “Wideband Microstrip Antenna Optimization”, New Jersy Institute of Technology, USA.

[10] Alexander Kuchar, “Aperture-Coupled Microstrip Patch Antenna Array”, Wein University of Technology, Austria.

[11] F. Carrez, J. Vindevoghel, “Study and Design of Compact Wideband Microstrip Antennas”, 10th International Conference on Antenna Propagation, April-1997.

[12] Wang Yazhon, Su Donglin, Xiao Yong Xuan (Beijing University of Aeronautics and Astronautics, China), "Broadband Circularly Polarized Square Microstrip Antenna", 7th International Symposium on Antennas, Propagation & EM Theory, 2006.

[13] B. Lee and F.I. Harackiewicz, "Miniature Microstrip Antenna with a Partially Filled High-Permittivity Substrate," IEEE Trans. Antenna Propagation, vol. 50, pp. 11601162, Aug. 2002.

[14] W. S. Chen, C. K. Wu, and K. L. Wong, "Novel compact circularly polarized square microstrip antenna," IEEE Trans. Antennas and Propagat., vol. 49, pp. 340-342, March 2001.

[15] R. Mittra, J. Bringuier, M. Abdel-Mageed, K. Rajab, and J. I. Gonzalez, "Some Novel Techniques for Size Reduction of Microstrip Patch Antennas," Microwave Conference, Dec. 2005.

[16] M. Sanad, "Effect of the shorting posts on short circuit microstrip antennas," in Proc. IEEE Antennas Propagat. Symp. Dig., 1994, vol. 2, pp. 794-797.

[17] A. K. Skrivervik, J.-F. Zurcher, O. Staub, and J. R. Mosig, "PCS antenna design: the challenge of miniaturization," IEEE Antennas Propagat. Mag., vol. 43, pp. 12-27, Aug. 2001.

[18] C.Y. Huang, J.Y. Wu, C.F. Yang, and K. L. Wong, "Gain-enhanced compact broadband microstrip antenna," Electronic Letters., vol. 34, pp. 138-139, Jan. 1998.

[19] T. W. Chiou and K. L. Wong, "Designs of compact microstrip antennas with a slotted ground plane," in Int. Symp. Antennas and Propagation, vol. 2, 2001, pp. 732–735.

[20] J. Robinson and Y. Rahmat-Samii, "Particle swarm optimization in electromagnetics," IEEE Trans. Antennas Propag., vol. 52, no. 2, pp. 397–407, Feb. 2004.

[21] J. Kennedy and R. Eberhart, "Particle swarm optimization," in Proc. 1995 Int. Conf. Neural Networks, vol. IV, Perth, Australia, 1995, pp. 1942–1948.

[22] D. Gies, "Particle swarm optimization: Applications in electromagnetic design," M. S., Univ. California, Los Angeles, 2004.

[23] N. Jin and Y. Rahmat-Samii, “Parallel Particle Swarm Optimization and Finite-Difference Time-Domain (PSO/FDTD) Algorithm for Multiband and Wide-Band Patch Antenna Designs,” IEEE Trans. Antennas Propag., vol. 53, no. 11, pp. 34593468, Nov. 2005.

[24] A. Ray Chowdhury, B. Gupta, and R. Bhattacharjee, “Bandwidth improvement of microstrip antennas through a genetic-algorithm-based design of a feed network,” Micro. Opt. Technol. Lett. 27(4):273-275 (Nov. 2000).

[25] O. Ozgun, S. Mutlu, M.I. Aksun, and L. Alatan, “Design of Dual-Frequency Probe-Fed Microstrip Antenna With Genetic Algorithm,” IEEE Trans. Antennas Propagat., Aug. 2003.

[26] F. J. Villegas, T. Cwik, Y. Rahmat-Samii, and M. Manteghi, “A Parallel Electromagnetic Genetic-Algorithm Optimization (EGO) Application for Patch Antenna Design,” IEEE Trans. Antennas Propagation, vol. 52, no. 9, pp. 24242435, Sept. 2004.

[27] N. Herscovici, M. F. Osorio, and C. Peixeiro, “Miniaturization of Rectangular Microstrip Patches Using Genetic Algorithms,” IEEE Antennas and Wireless Propagation Letters, vol. 1, pp 94-97, Jan. 2002.

[28] Agi and Malloy, "Integration of a Microstrip Patch Antenna with a Two-Dimensional Photonic Crystal Substrate," Electromagnetics, vol. 19, 1999.

[29] Parker and Charlton, "Photonic Crystals," Physics World, 2000.

[30] Radisic and Qian, “Novel 2-D Photonic Bandgap Structure for Microstrip Lines.” IEEE Microwave and Guided Wave Letters, vol. 8, 1998.

[31] Gareth Louis Shaw, “Patch Antenna Design”, Faculty of Engineering and the Built Environment, University of the Witwatersrand, Johannesburg, April 2005.

[32] Ainor Khaliah, “ELECTROMAGNETIC BAND GAP (EBG) FOR MICROSTRIP ANTENNA DESIGN”, Faculty of Electrical Engineering Universiti Teknologi Malaysia, May 2007